AEC Category: HEALTH AND SAFETY

CEX-63.3

CIVIL EFFECTS STUDY

BARRIER ATTENUATION OF AIR-SCATTERED GAMMA RADIATION

Z. G. Burson and R. L. Summers

Issuance Date: June 18, 1965

CIVIL EFFECTS TEST OPERATIONS
U.S. ATOMIC ENERGY COMMISSION

LEGAL NOTICE

Printed in USA. Price $1.00. Available from the Clearinghouse for Federal Scientific and Technical Information, National Bureau of Standards, U. S. Department of Commerce, Springfield, Va.

USAEC Division of Technical Information Extension, Oak Ridge, Tennessee

DISCLAIMER

BARRIER ATTENUATION OF AIR-SCATTERED GAMMA RADIATION

By
Z. G. Burson
and
R. L. Summers

Approved by: L. J. DEAL, Chief
Civil Effects Branch

Edgerton, Germeshausen & Grier, Inc.
Las Vegas, Nevada
December 1964

NOTICE

This report is published in the interest of providing information which may prove of value to the reader in his study of effects data derived principally from nuclear weapons tests and from experiments designed to duplicate various characteristics of nuclear weapons.

This document is based on information available at the time of preparation which may have subsequently been expanded and re-evaluated. Also, in preparing this report for publication, some classified material may have been removed. Users are cautioned to avoid interpretations and conclusions based on unknown or incomplete data.

ABSTRACT

An experimental study was conducted to determine the attenuation provided by vertical and horizontal barriers exposed only to skyshine radiation from cobalt-60 and cesium-137 sources. Materials of steel, aluminum, concrete, and wood were used as barriers.

A sealed radioactive source was pumped at a uniform speed through a long length of flexible tubing to simulate a ring source. Point-source measurements were made by stopping the source at a given location. Dose measurements were made with ionization chamber detectors.

Measurements of the attenuation provided by a vertical barrier were made in a bunker where three sides and the top were of sandbags or lead; the fourth side was the barrier of interest for each experiment. The simulated ring source was set at a 100-ft radius. Just inside the 100-ft radius line surrounding the bunker, the ground was shaped to rise up a slight ramp to create a circular-shaped plateau. The angle of the ramp was designed to insure that direct radiation would pass between 1 and 2 ft above the top of the barriers - only air-scattered radiation reached the barriers.

Measurements of the attenuation provided by a horizontal barrier were made using detectors placed in a round hole in the ground, topped by the barrier material at ground level. A cobalt-60 point source was placed 100 ft from the hole. Sandbags or lead bricks were placed on the ground about 6 ft in front of the hole. The height of the lead bricks was the same height as the top of the shield. This assured that the shield was exposed only to air-scattered radiation.

Additional measurements at this same location were made to determine: (1) the skyshine dose rate as a function of distance from a cobalt-60 source placed on an air-ground interface: (2) the geometry factor describing a detector response to scattered gamma rays at the air-ground interface from a point isotropic cobalt-60 source on the ground 100 ft away; and (3) lip scatter and wall backscatter corrections for a detector in an open hole exposed to skyshine radiation from cobalt-60.

The results apply to a variety of shielding problems. One practical application is the shielding provided by basement roofs and exposed basement walls from skyshine radiation originating from fallout.

ACKNOWLEDGMENTS

The authors gratefully acknowledge the many valuable contributions made by L. J. Deal and members of the Civil Effects Branch; Dr. C. M. Huddleston of the Naval Civil Engineering Laboratory (NCEL) and Q. G. Klingler of EG&G for their technical criticisms and suggestions during the project and for their thorough technical review of the manuscript.

CONTENTS

ILLUSTRATIONS

ILLUSTRATIONS (Continued)

ILLUSTRATIONS (Continued)

TABLES

TABLES (Continued)

Chapter 1

INTRODUCTION

1.1 BACKGROUND

About 10% of the gamma-ray exposure rate 3 ft above a contaminated, smooth, infinite plane of fallout consists of air-scattered photons[1], usually referred to as "skyshine radiation." Its energy and angular distribution must be known for hazard assessments of contaminated fields and in many types of shelters. This skyshine contribution takes on special importance in foxholes and building basements where the direct line-of-sight radiation is significantly attenuated. Shielding calculations require a knowledge of the dose-angular distribution of the skyshine component and its attenuation through shields in various configurations.

Theoretical calculations and analytical solutions are available[1, 2] for ideal source-detector geometries. They do not permit exact solutions to particular non-ideal shielding and scattering configurations. The purpose of these experiments was to compare experimental data with calculations of ideal configurations and to obtain empirical solutions for particular problems. The experiments reported here were concerned with measuring the contribution of skyshine radiation and its attenuation through vertical and horizontal barriers. Radioactive sources of cobalt-60 and cesium-137 were used because results can be readily compared to theoretical calculations and are readily adaptable to a fallout energy spectrum, as will be discussed later in this report. Within operational limits, an attempt was made to assure that the relative dose-angular distribution at either the shields or the open hole was a good approximation of the dose-angular distribution that would have resulted from an infinite-plane source.

Some experiments concerned with scattered gamma rays at the air-ground interface from simulated plane sources have been performed.[3, 4] Experiments using a hole in the ground as a collimator for measurements from simulated plane sources have also been reported.[5, 6, 7] Clifford[8] reports some experimental results of

attenuation by horizontal concrete slabs of skyshine radiation originating from a simulated plane source of cesium-137.

Where appropriate, data from this report are compared with other experimental data and with theoretical calculations. Application to a fallout energy spectrum is noted. Results are applicable to a variety of basic shielding problems. Specifically, results provide shielding information for basement roofs and exposed basement walls from skyshine radiation originating from fallout.

1.2 OBJECTIVES

The over-all objective was to measure the attenuation provided by vertical and horizontal barriers of various materials subjected to skyshine radiation originating from simulated plane sources of cobalt-60 and cesium-137. Specific objectives and measurements were:

1. To determine quantitatively the skyshine dose rate* in an open hole as a function of distance from a cobalt-60 source on the ground.
2. To determine lip scatter and wall backscatter corrections for a detector in an open hole exposed to skyshine radiation from a simulated plane source of cobalt-60.
3. To determine qualitatively the geometry factor describing a detector response to scattered gamma rays at the air-ground interface from a point isotropic cobalt-60 source on the ground 100 ft away.
4. To determine the attenuation of skyshine radiation from simulated plane sources of cobalt-60 and cesium-137 by vertical barriers of concrete, steel, aluminum, and wood.
5. To determine the attenuation of skyshine radiation from cobalt-60 sources by horizontal barriers of concrete, steel, aluminum, and wood.

REFERENCES

1. L. V. Spencer, Structure Shielding Against Fallout Radiation from Nuclear Weapons; NBS Monograph 42 (National Bureau of Standards, Washington 25, D. C.) June 1, 1962.

2. M. J. Berger and J. C. Lamkin, Sample Calculations of Gamma-Ray Penetration into Shelters: Contributions of Skyshine and Roof Contamination, Journal of Research NBS, Vol. 60, No. 2, Feb. 1958.

*The terms "dose" and "dose rate" as used throughout this report mean "exposure" and "exposure rate," respectively, as defined in ICRU Report 10a, NBS Handbook 84, page 6 (1962).

3. Ralph E. Rexroad and Murray A. Schmoke, Scattered Radiation and Free-Field Dose Rates from Distributed Cobalt-60 and Cesium-137 Sources, NDL-TR-2 (Chemical Corps Nuclear Defense Laboratory, Army Chemical Center, Maryland) September 1960.

4. Keran O'Brien and James E. McLaughlin, Jr., Gamma Radiation At the Air-Ground Interface, CEX-61.1 (Prelim.) Civil Effects Test Operations, U. S. Atomic Energy Commission, May 1963.

5. C. E. Clifford, et al, Scattered Radiation from a Simulated Fallout Field Using Cesium-137, DRCL-296 (Defence Research Chemical Laboratories, Ottawa, Canada) January, 1959.

6. Albert W. Starbird and John F. Batter, Angular Distribution of Skyshine Radiation at the Surface of a Plane of Fallout Contamination. TO-B 63-40 (Technical Operations Research, Burlington, Mass.), March 1964.

7. C. E. Clifford, Dependence of Total Dose Rate and Skyshine Dose Rate on the Area of Contamination (Cesium-137): DRCL-TM-104 (Defence Research Chemical Laboratories, Ottawa, Canada) March 1960.

8. C. E. Clifford, Absorption of Cesium-137 Skyshine Radiation by Concrete Slabs: DRCL - Technical Note No. 62-7 (Defence Research Chemical Laboratories, Ottawa, Canada), May 1962.

Chapter 2

EXPERIMENTAL METHOD

2.1 GENERAL DESCRIPTION

In shielding calculations of protection provided by below-ground structures against fallout radiation, the contribution of skyshine radiation is an important factor. Attenuation of skyshine radiation through a horizontal barrier is important in the case of a covered foxhole or a basement below a light superstructure.

For basements with walls partially exposed above ground, attenuation of skyshine radiation through a vertical barrier is important. The exposed basement wall acts as a vertical barrier and the radiation emerging from this wall is dependent upon the energy and dose-angular distribution of the radiation striking the outside of the wall. If the ground level sloped downward from the building or if the ground was rough, the dose-angular distribution would be exceedingly different than from a level, smooth plane. In these cases, the skyshine contribution passing through the vertical barrier would be of greater relative importance.

In shielding calculations of fallout-protection factors, the attenuation is expressed as a product of two general factors. One factor gives the attenuation in the barrier material, assuming a particularly simple type of source and medium that is completely uniform in density. This factor is termed "barrier factor." The other factor is called "geometry factor" and accounts for the finiteness of the barrier and for the detector locations.

An example of barrier reduction is shown in Fig. 2.1, taken directly from Ref. 1. In all three cases the detector is assumed to be immediately under (or beside) the shielding material and this in turn is assumed to be infinite in extent. These reduction curves were derived from data in Spencer's report.[2] The simple detector-source-medium arrangements for these theoretical calculations are shown in Cases 1, 2 and 3 of Fig. 2.2. (Case 4 depicts a possible

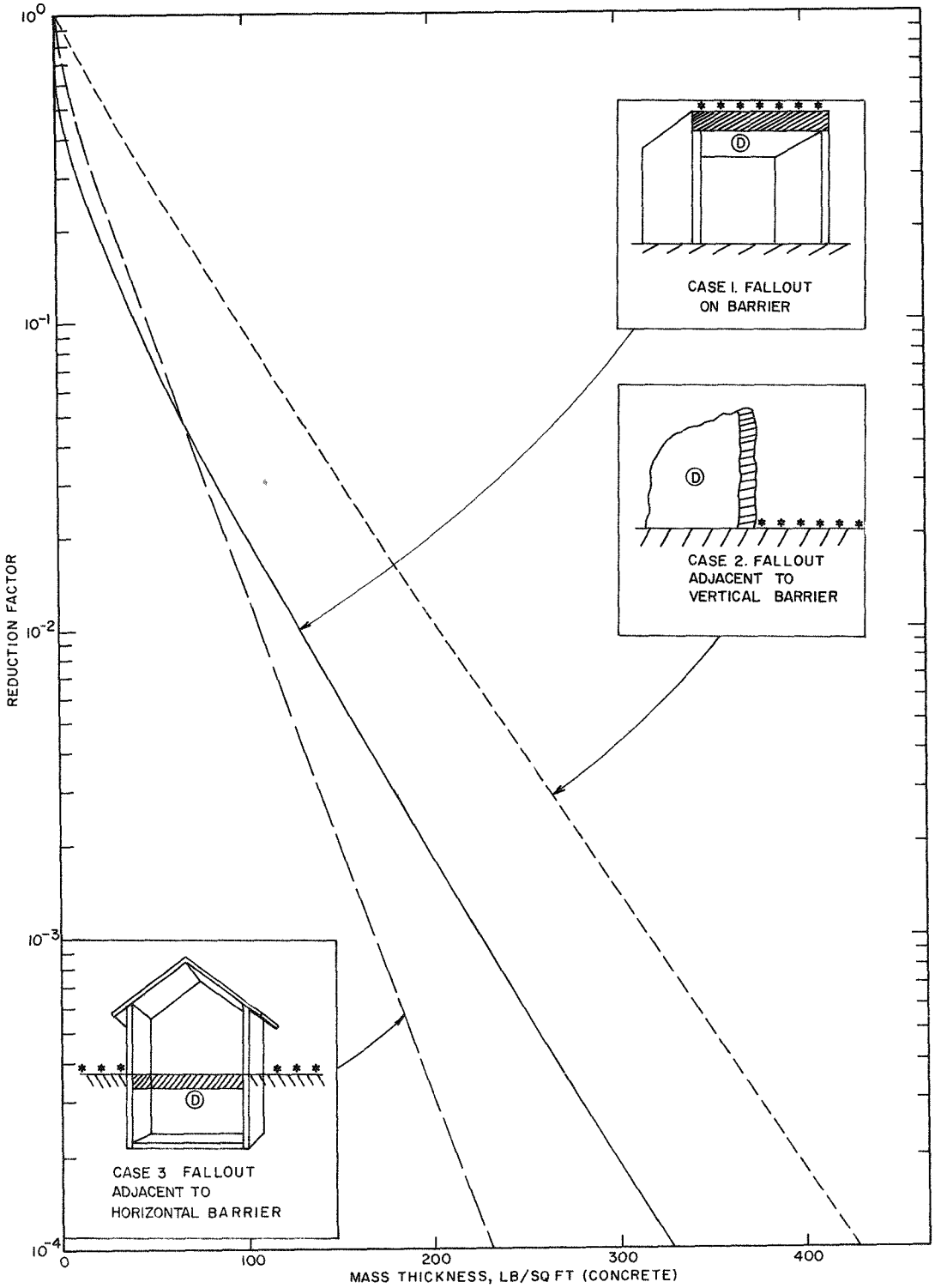

Fig. 2.1 - Barrier shielding effects.

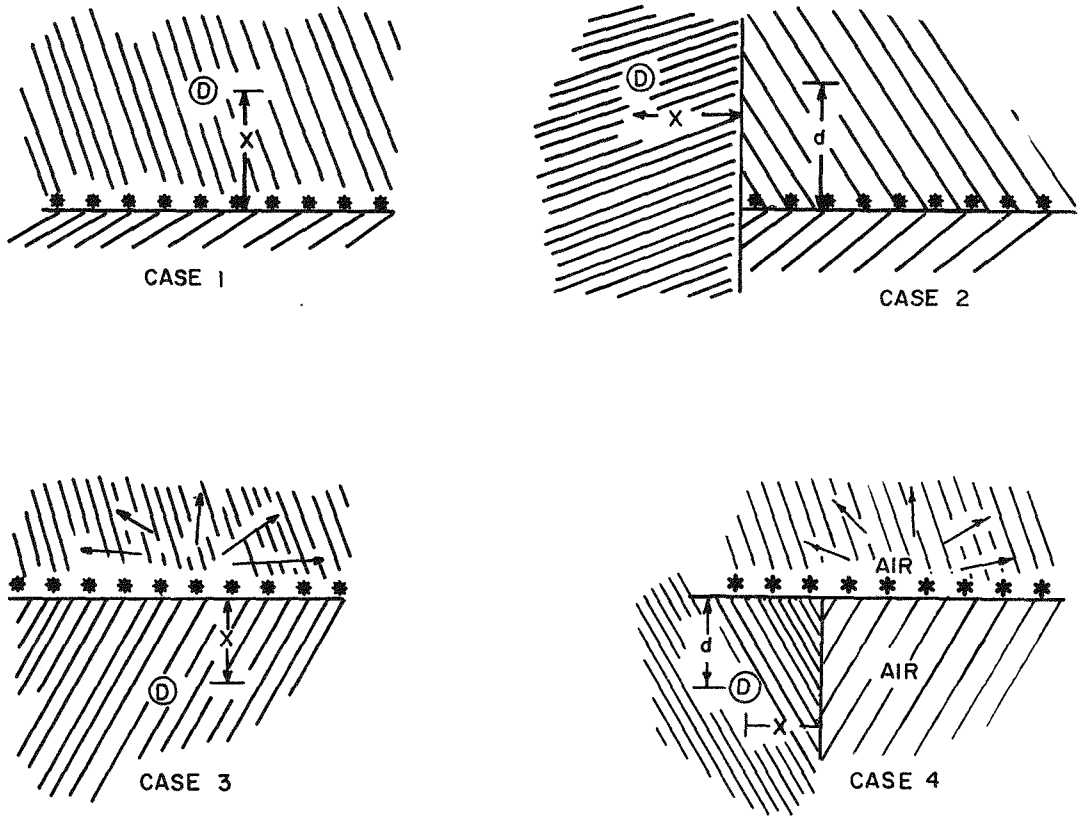

Fig. 2.2 - Simple detector-source-medium arrangements. Case 1 - isotropic detector, plane isotropic source; Case 2 - isotropic detector and plane isotropic source; the radiation field at height d above the primary source is taken as a new source at a penetration distance X to the right of the detector; Case 3 - isotropic detector, source "isotropic" only in directions pointing away from detector; Case 4 - isotropic detector, source "isotropic" only in directions pointing away from detector, $d \gg X$.

arrangement for vertical barrier attenuation of skyshine radiation.) Spencer's calculations assume an infinite-plane source of contamination located in an infinite ocean of air, one side being compressed to the density of earth. Penetration calculations through thickness X of material is for a water medium.

Geometry reduction is illustrated in Fig. 2.3, also taken from Ref. 2. The D = 100-ft curve was obtained by graphical interpolation by using Figs. 28.15, 28.17, B37, B38, B41 and B42 of Ref. 2 as guides.

---

* Cases 1, 2, and 3 were taken from Ref. 2.

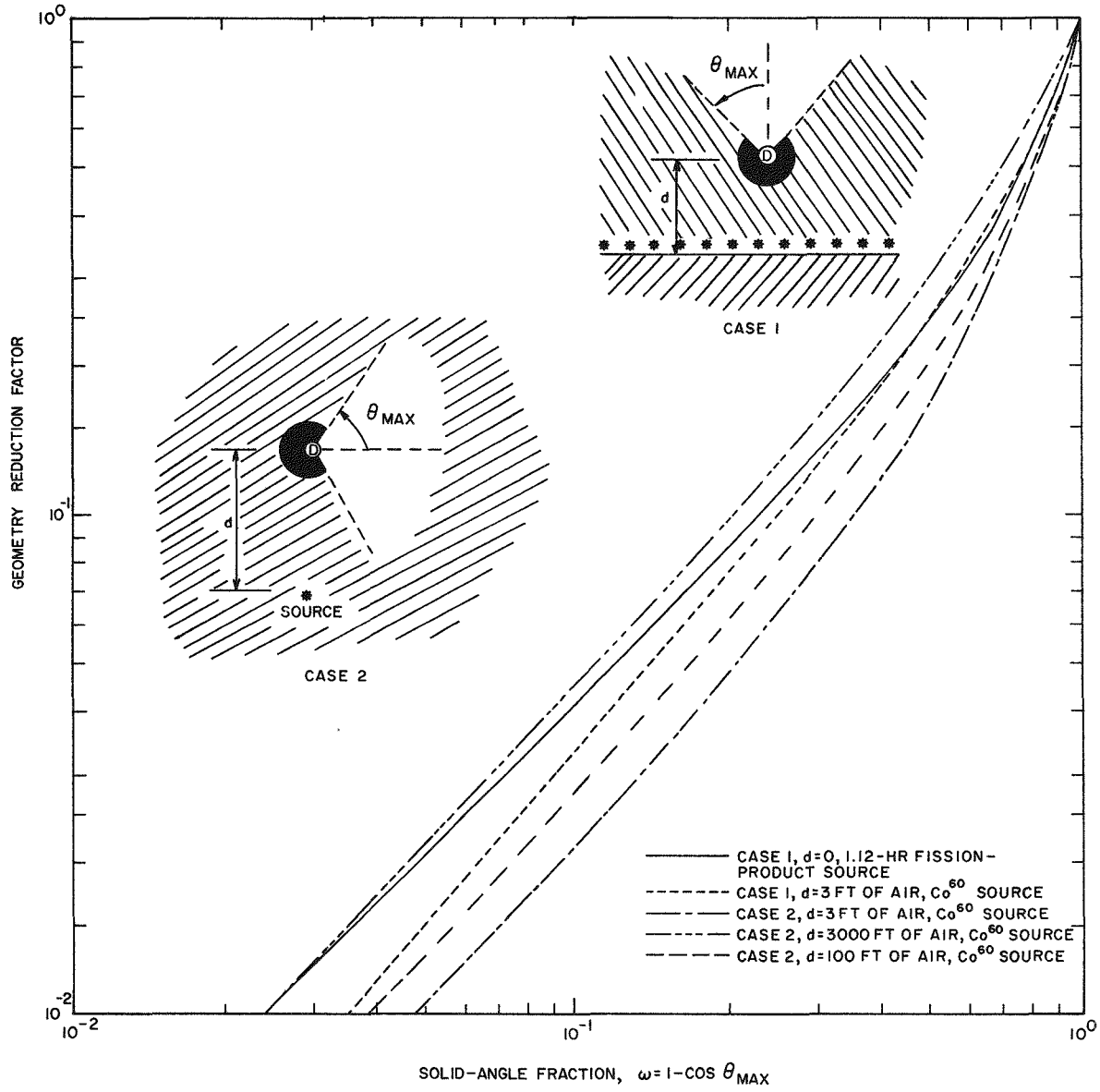

Fig. 2.3 - Geometry factor describing detector response to skyshine radiation.[2] Case 1 - conical detector pointed away from a plane isotropic source; Case 2 - conical detector pointed 90° from the source-detector line, point isotropic source.

2.2 SOURCE-DETECTOR-SHIELD ARRANGEMENTS

Within operational limitations the source-detector-shield arrangements in this experiment were chosen such that the relative dose-angular distribution of radiation at either the shield or open hole was a good approximation of the dose-angular distribution due to an infinite-plane source. Arrangements were chosen to approximate ideal configurations used for calculations and those most readily adaptable to practical applications, such as in a fallout situation.

The shields were 5 ft square. Since we were primarily concerned with barrier-reduction factors, shields were large compared with detector size. Low-Z materials of wood, aluminum, steel, and concrete were used for practical applications.

2.2.1 Open Hole

It was desirable to measure the dose rate of skyshine radiation versus solid angle subtended by a detector as a function of distance from a cobalt-60 source. In Area 1 at NTS an area 35 ft wide and 560 ft long was graded and smoothed. At one end, a hole 4 ft in diameter and 6 ft deep was dug. Steel casing 3/16 in. thick was placed in the hole as an earth retainer. A lead lip 4 in. wide and 4 in. deep was placed around the hole such that the top was flush with the ground surface. To reduce wall backscattering, a 1/8-in. lead liner was placed on the walls and floor of the hole.

A cobalt-60 source was placed on the ground at varying distances ranging from 5 to 440 ft from the center of the hole. Dose rate measurements were made at various depths along the centerline of the hole for each source position. Measurements were repeated many times at the 100-ft distance since this was the position in which all of the shield data were taken. Later, another hole of the same dimensions was dug in Yucca dry-lake bed and measurements were made with source-detector separation distances from 60 to 1500 ft. This dry-lake bed was extremely flat, thus providing very good geometry for simulated smooth-plane sources.

To evaluate the lip scatter and wall backscatter component in the open hole, measurements were made with the hole having the following lip and wall configurations:

1. Lead lip and steel wall liner.
2. Lead lip and lead wall liner.
3. Earth lip and earth wall.

Photographs and drawings showing open-hole configurations appear in Figs. 2.4 thru 2.6. Figures 2.4 and 2.5 show the tubing layout and detector-positioning mechanism for the "Cutie Pie" set of

open-hole measurements. The mechanism for positioning this detector was designed such that there would be no scattering or absorbing material above the detector (see Fig. 2.6). The data by the "Cutie Pie" instrument were taken every 6 in. going down into the hole, starting with the top of the detector 1 in. below ground level.

Most of the open-hole data were taken with 10-mr and 1-mr chambers. To minimize the effect of detector anisotropy the top chamber was oriented such that the stem was pointed perpendicular to the source-detector line. For other positions the stem pointed down. The top position was such that the top of the 10-mr chamber was 5/8 in. below ground level, and the 1-mr chamber, 1/8 in. below ground level. Other positions were located about every 6 in. down into the hole.

For the large-distance measurements in Yucca dry-lake bed a spherical air-equivalent ion chamber 7-1/2 in. in diameter was used. It was located at only one position, the top of the chamber being 1/8 in. below ground level.

2.2.2 Vertical Shield

In Figs. 2.1 and 2.2 simple detector-source-shield arrangements in infinite media are used for theoretical calculations readily adaptable to practical applications. A simple detector-source-medium arrangement that might show the desired geometry for the vertical barrier appears as Case 4 of Fig. 2.2. In this configuration, detector response will depend upon (among other factors) the dose-angular distribution of gamma radiation at the vertical wall. The distribution is expected to be isotropic in a plane parallel to the source plane and to follow the geometry reduction as in Case 1 of Fig. 2.3 in a plane perpendicular to the source plane. In designing the actual experimental arrangement, these expected distributions were kept in mind.

By choosing a ring source the distribution in a plane parallel to the source plane at the detector-shield arrangement (at the center of the ring) was expected to be isotropic. An examination of theoretical curves from Spencer indicates an ideal radius for the ring source in a homogeneous medium of air would be about 300 ft for the correct relative dose distribution for a plane perpendicular to the source plane. However, an examination of the same curves indicates the angular distribution is a slowly varying function of source-detector separation distance. We arbitrarily chose a radius of 100 ft because of the limitation of source strengths and detector sensitivity.

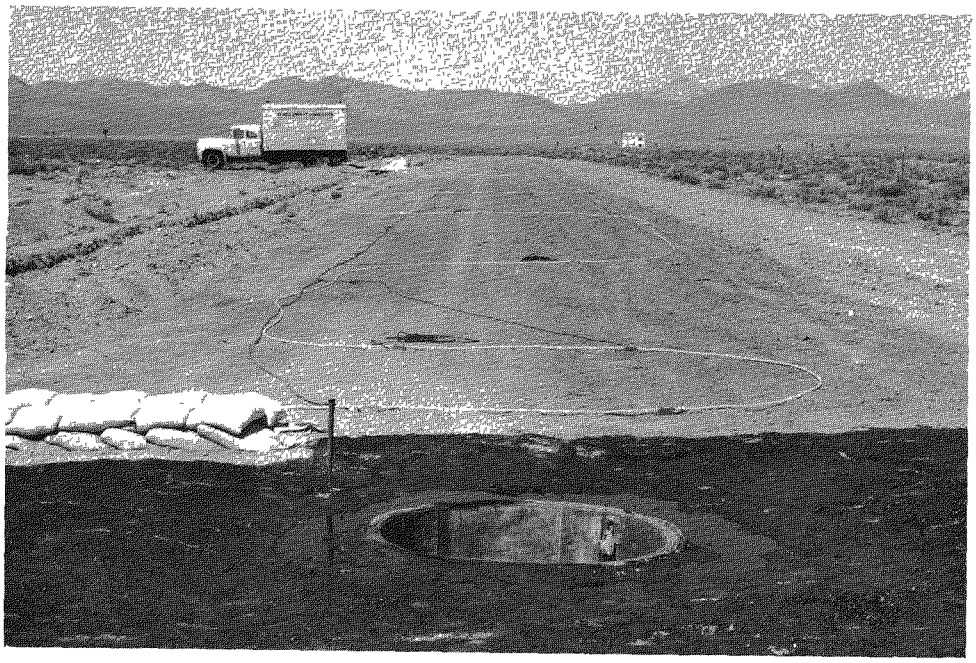

Fig. 2. 4 - Open-hole configuration and tubing distribution for source positioning.

Fig. 2. 5 - Detector positioning in open hole.

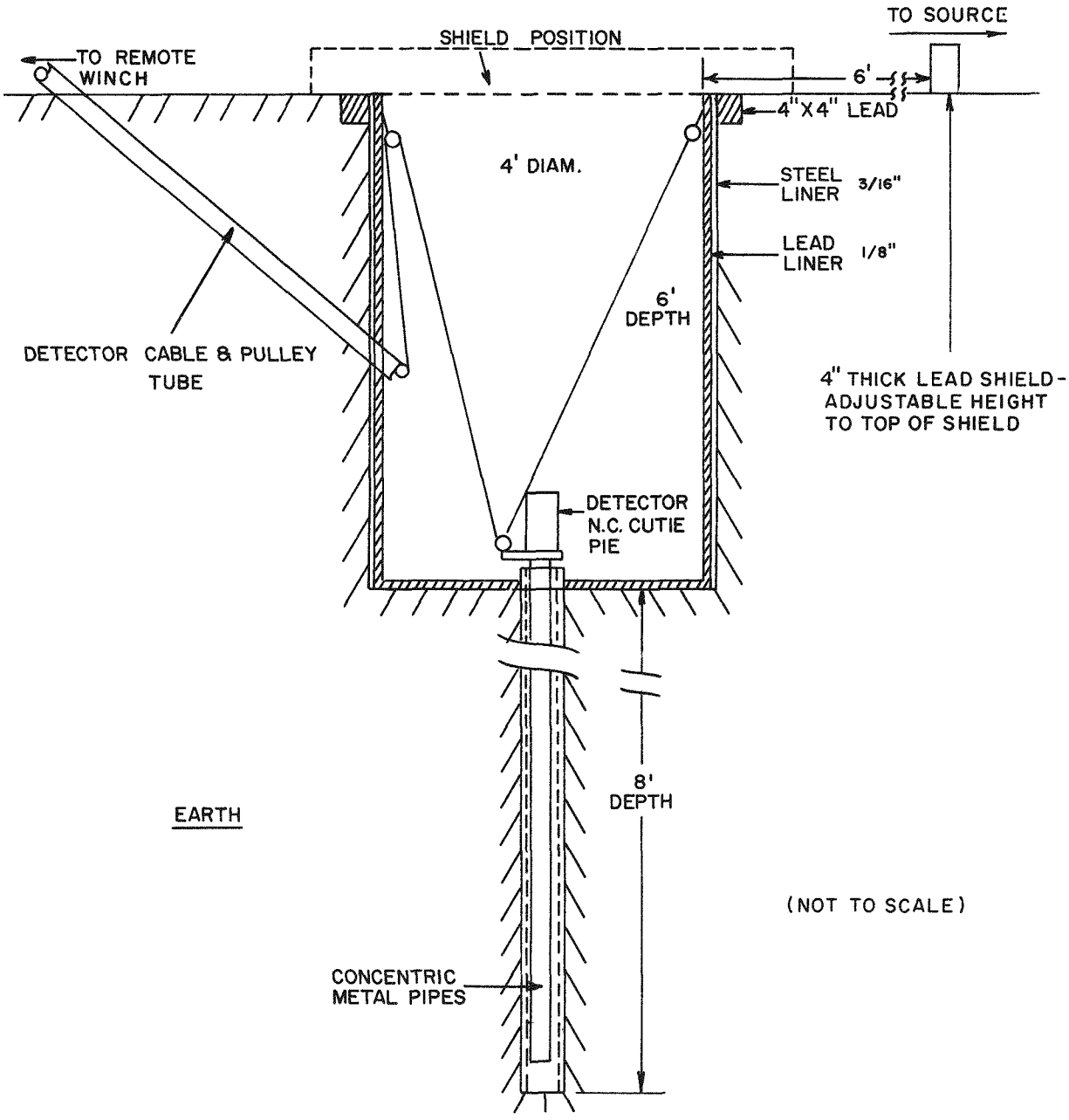

Fig. 2.6 - Detector positioning in open hole.

To lessen the air-ground interface influence, we chose to shield the unscattered component near the source rather than near the detector (Fig. 2.7). This also insured that gamma rays striking the shield had already undergone at least one air scatter.

Photographs and drawings showing locations of detectors, sources, and shields appear in Figs. 2.8 through 2.11.

Note in Fig. 2.7 that the bunker arrangement also included a square bunker open at the top. This was to be used for the horizontal barrier experiments but was abandoned after the first set of measurements because of presumed poor geometry. (Gamma rays that had scattered less than about 4° could not reach the horizontal shield.)

A lead liner was mounted on the inside walls of the vertical bunker to reduce backscatter. Another lead sheet was formed over the sandbags around the edge of the bunker to reduce radiation leakage through the sandbags and wood framing.

Figure 2.8 is an aerial photograph of the vertical bunker site. The test pad and approaches were oiled to reduce the dust problem.

Figures 2.9 through 2.11 show detector positions in relation to bunker dimensions. Detectors were mounted and held in place by 1/8 in. of plexiglass. Temperature effects were minimized by shading the detectors in the unshielded case. Shields were placed at the face of the bunker.

2.2.3 Horizontal Shield

The horizontal shield measurements were made by placing the shields over the hole used for the open-hole experiments (see Fig. 2.6). Data were taken at various depths in the center of the hole from a point source located 100 ft away. Care was taken to obtain as close to an ideal geometry as feasible.

To prevent any direct radiation from reaching the shields, sandbags and/or lead bricks were placed on the ground about 6 ft in front of the hole. The height of this barrier in each instance was the exact height of the top of the shield. This also insured that the top of the shield was exposed to the total skyshine component.

The shields were placed over the hole such that the overlap was greatest in the direction of the source. Figure 2.12 shows this orientation. This insured that the overlap was greater than the shield thickness in this direction. The maximum shield thickness was 4 in. for concrete, 2-1/2 in. for steel, 5 in. for aluminum, and 10 in. for wood. A small error probably occurred in the 10-in. wood measurements because of only an 8-in. overlap. Any error because of the 4-in. overlap in the opposite direction is assumed to be negligible.

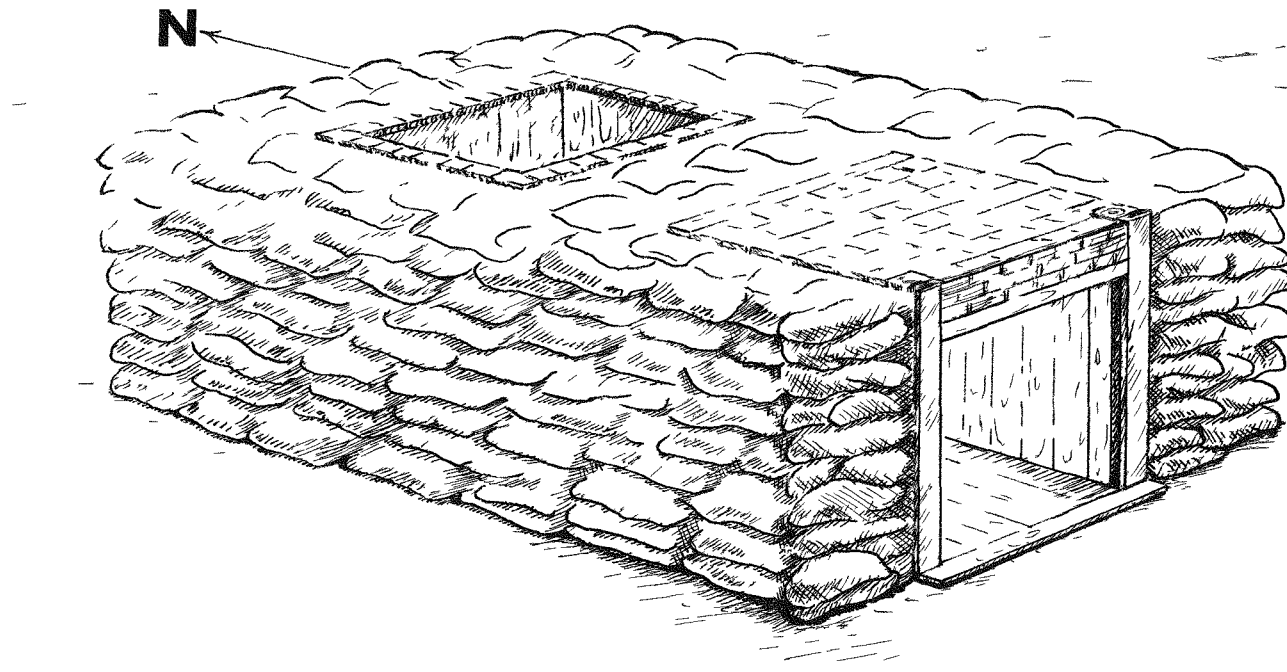

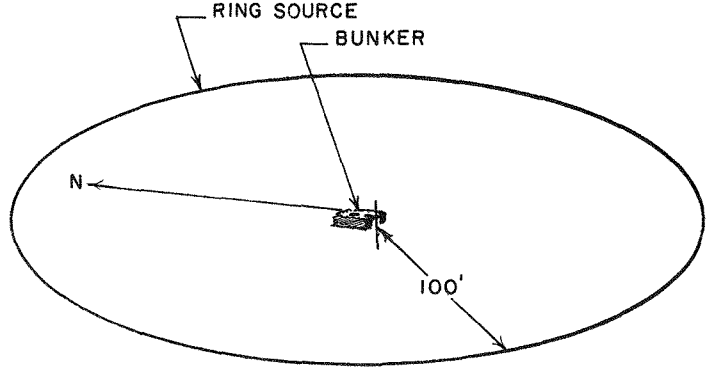

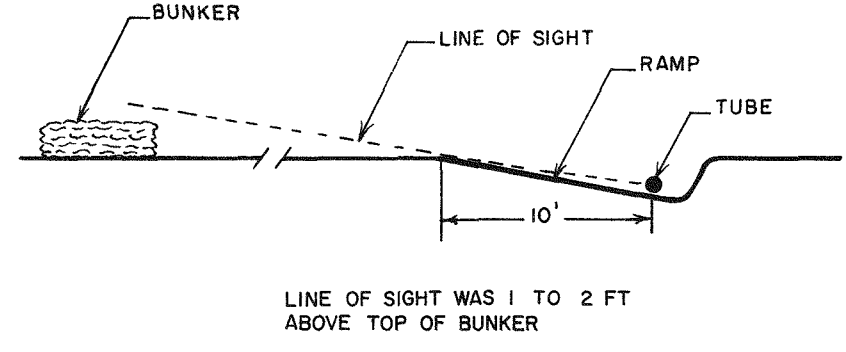

Fig. 2.7 - Vertical shield bunker arrangement.

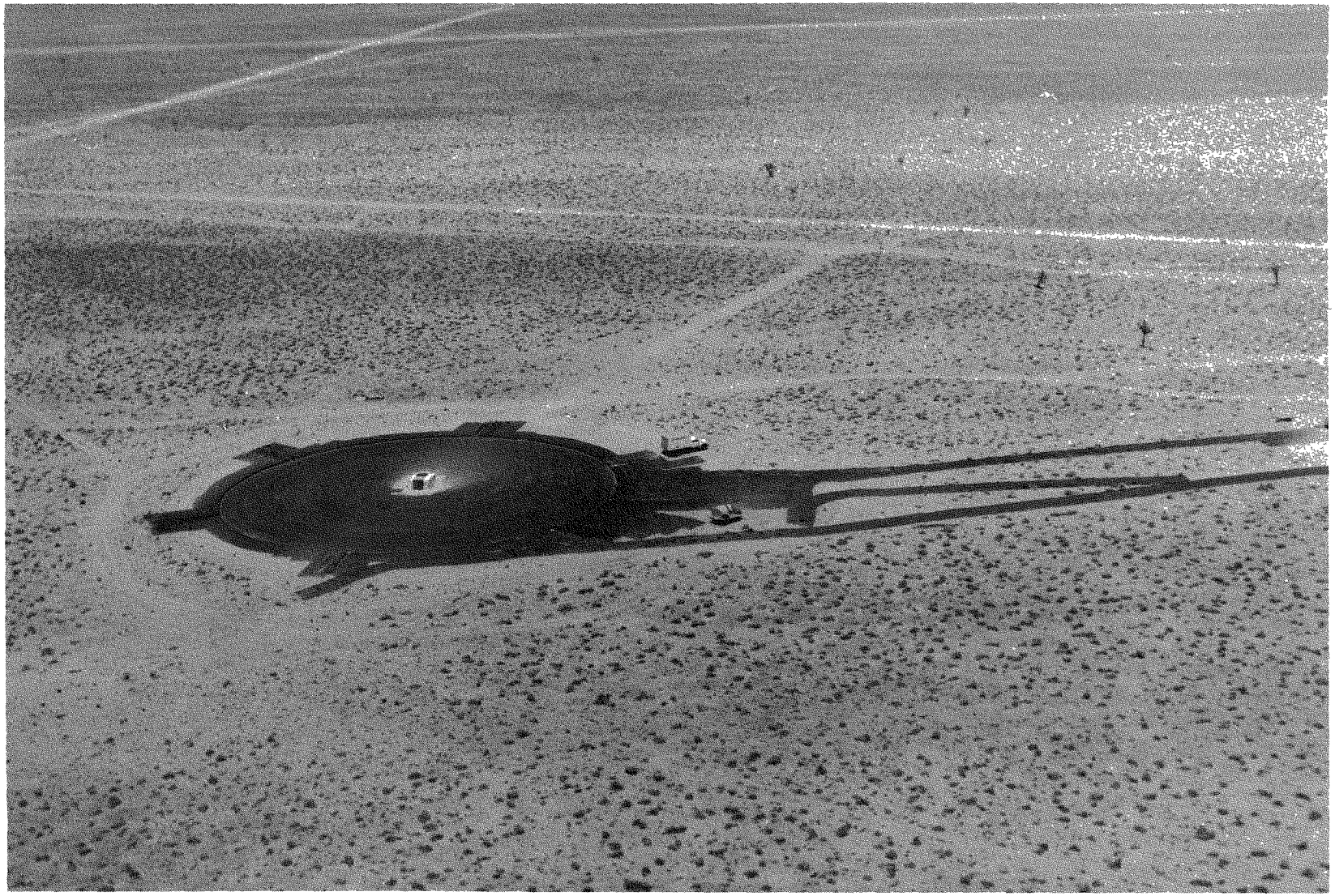

Fig. 2.8 - Aerial view of vertical shield bunker site.

Fig. 2.9 - Vertical shield bunker, showing detector positions.

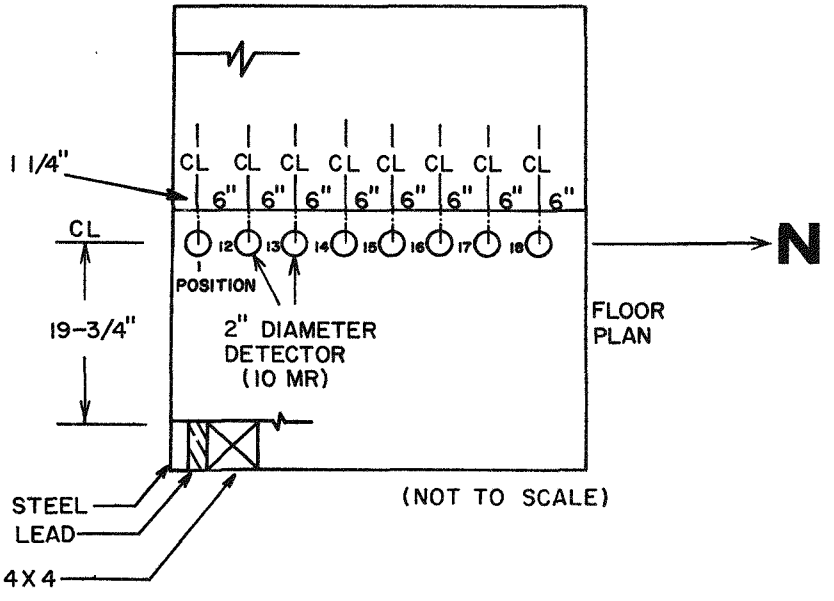

Fig. 2.10 - Detector positions, 10-mr chambers, vertical shield bunker.

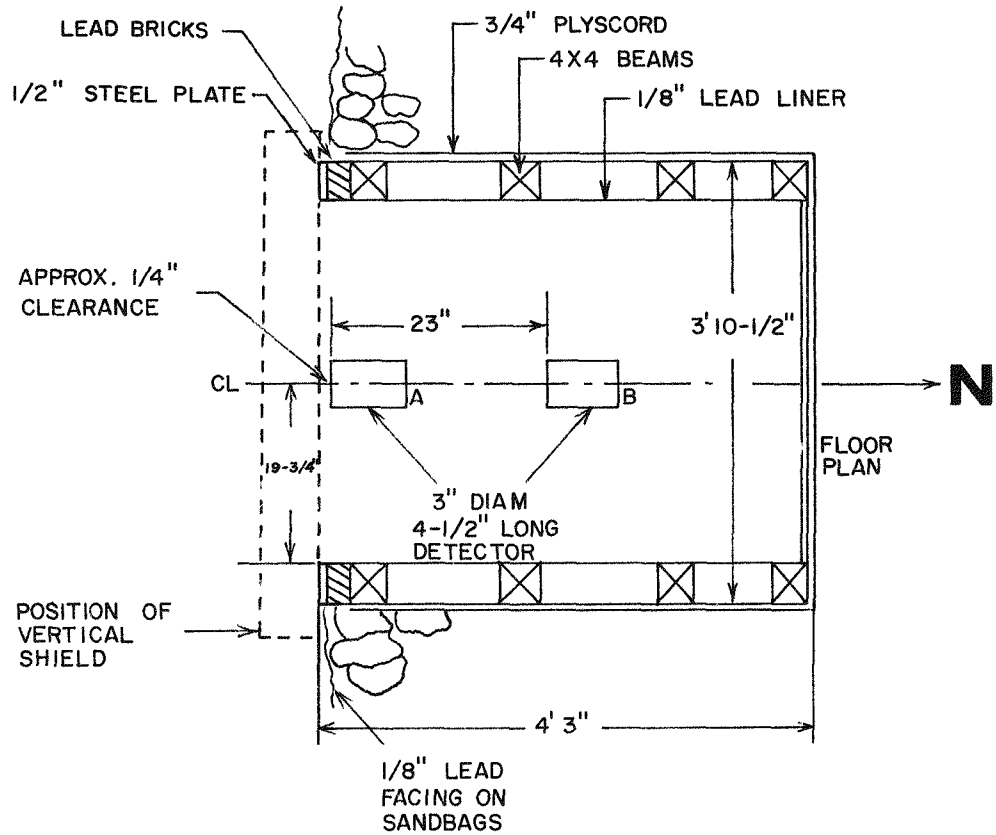

Fig. 2.11 - Detail plan, vertical shield bunker, showing Nuclear Chicago Cutie Pie Detector Positions.

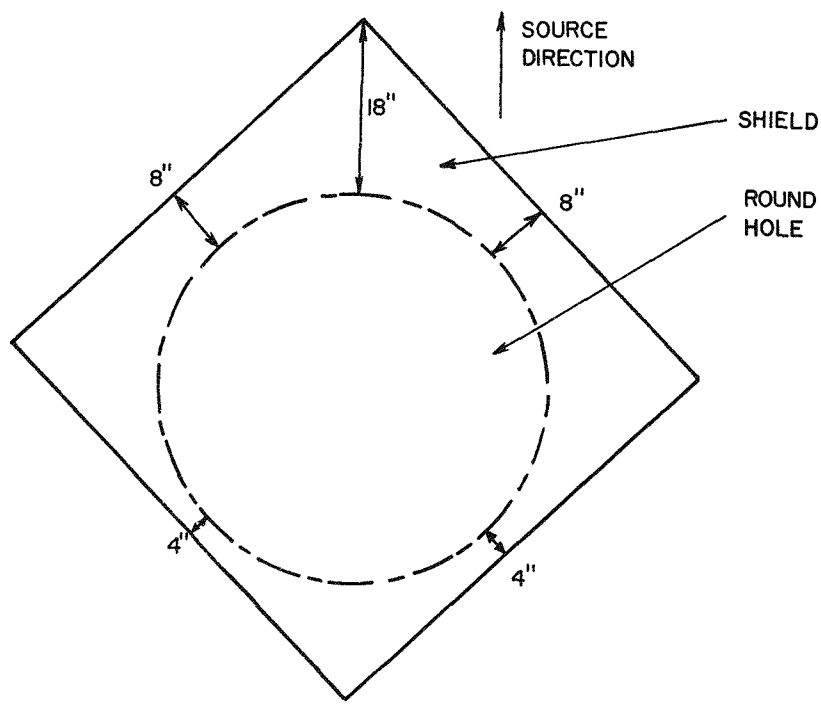

Fig. 2.12 - Horizontal shield-source orientation.

2.3 EXPERIMENTAL TECHNIQUE

2.3.1 Source-Handling System

Handling of the radioactive sources for this experiment was done by the Mobile Radiological Measuring Unit (MRMU). This system used a moving, radioactive source hydraulically pumped through polyethylene tubing. Since the source traveled at a uniform speed, a ring source or area source could be simulated. The source could also be pumped to a location and stopped, enabling point-source experiments to be made. Equipment required for pumping the source through the polyethylene tubing has been described in detail in previous reports[3-6] and is therefore only mentioned briefly here.

A schematic diagram of the hydraulic system for source circulation is shown in Fig. 2.13. The polyethylene tubing was attached to a cobalt-60 multi-source shield (S-1). Within this shield were seven S-shaped stainless-steel tubes in which a total of six radioactive sources could be stored. One tube was reserved for the water-return line but could also provide emergency storage of a radioactive source, if needed. A means had been provided to completely secure and lock sources not in use.

The source could be started, stopped, reversed, and completely controlled remotely by a control console in a laboratory trailer located up to 1000 ft away. The small metal boxes attached to the tubing in Fig. 2.4 were source-position indicators, allowing the console operator to know the location of the source at all times.

2.3.2 Sources

The sources used in this experiment were cobalt-60 and cesium-137. The cobalt-60 source strengths were approximately 12.5, 200, and 1100 curies. The cesium-137 source strength was approximately 300 curies.

All the sources were encapsulated in magnetic stainless-steel containers accurately machined to pass through the polyethylene tubing. The capsules were Heliarc-welded and passed all AEC leak tests. (See Figs. 2.14 and 2.15.)

All sources were calibrated at the CETO-EG&G Nevada Test Site calibration facility. A photograph and drawing of this facility appear in Figs. 2.16 and 2.17. Two sets of NBS-calibrated Victoreen condenser-R-chambers were used. A source was pumped by the MRMU system into calibration position directly between two posts (A and B) at a height of 10 ft. Dose-calibration measurements were made perpendicular to the long axis of the source at a distance of

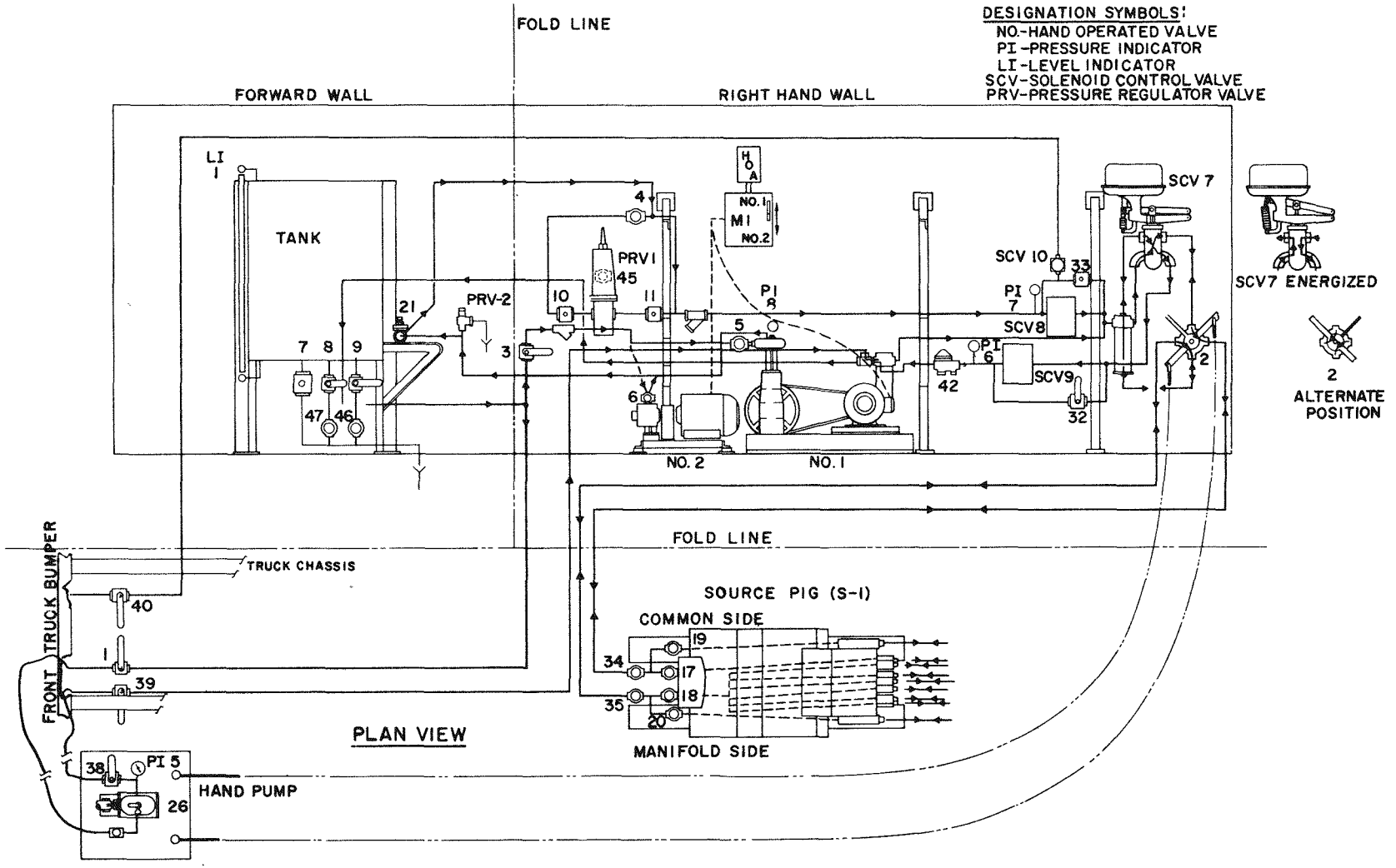

Fig. 2.13 - Hydraulic piping flow diagram.

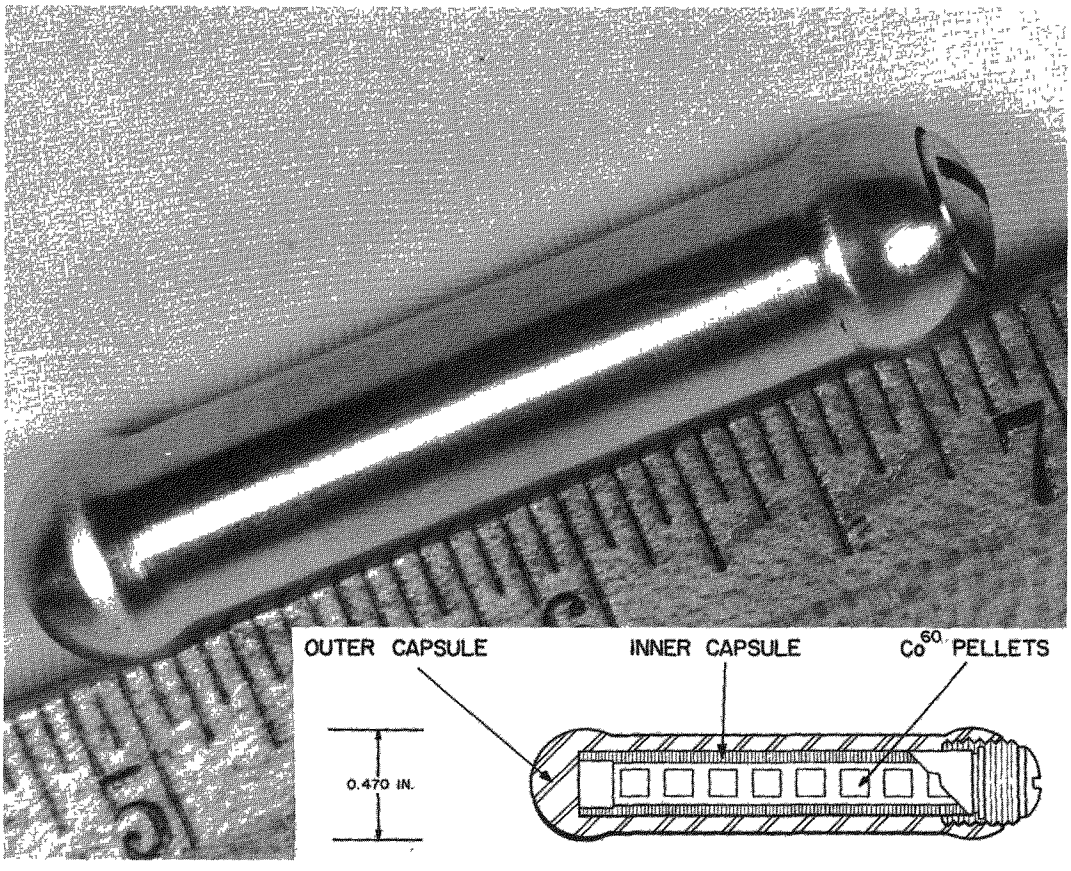

Fig. 2.14 - Photo and detail drawing of 200-curie cobalt-60 source.

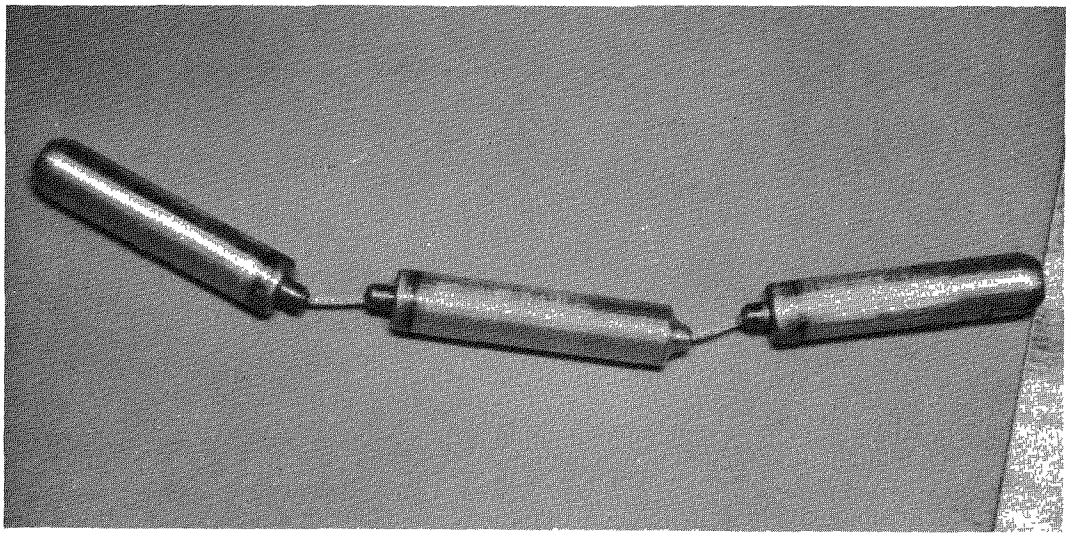

Fig. 2.15 - 300-curie cesium-137 source.

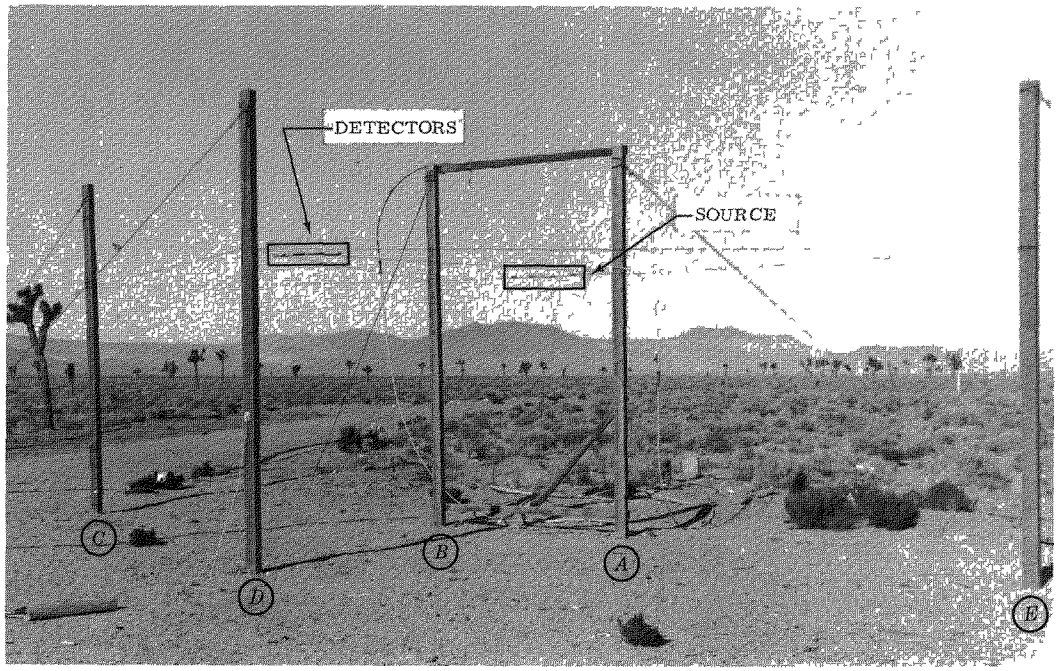

Fig. 2.16 - Calibration facility, CETO-EG&G, Nevada Test Site.

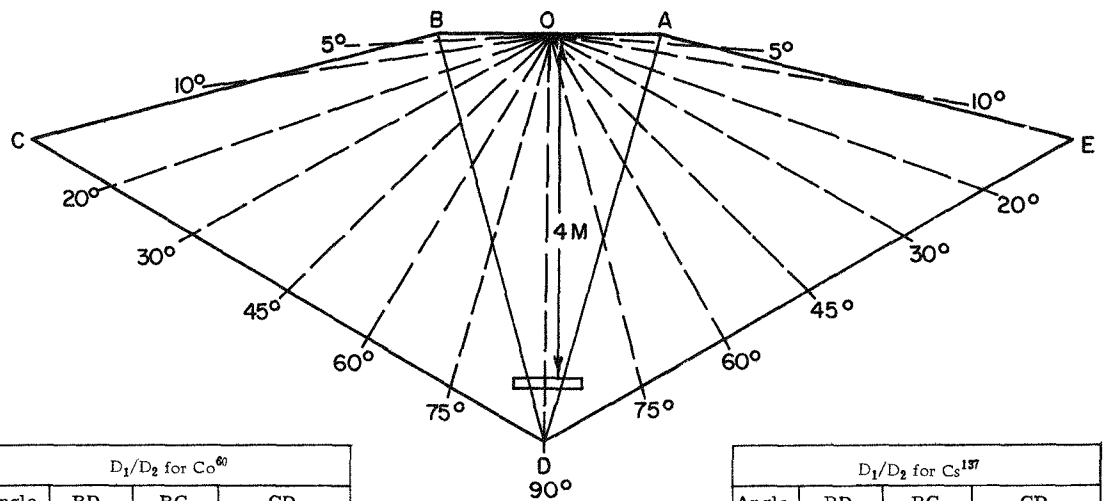

D_1/D_2 for Co^{60}			
Angle	BD	BC	CD
5°	16.95	31.45	
10°	16.95	141.64	
20°	16.95		268.27
30°	17.98		237.35
45°	22.44		194.09
60°	32.79		180.90
75°	65.18		194.09
90°	240.93		
4m	167.79		

$$\frac{D_1}{D_2} = \frac{X^2}{Be^{-\mu x}K}$$

where D_1 = dose rate at 1 ft
D_2 = measured dose rate corrected to S.T.P.
X = distance from source to detector
B = air-buildup factor
μ = linear absorption coefficient
K = ground backscatter correction factor
Co^{60} = 14.53 r/hr/curie at 1 ft
Cs^{137} = 4.19 r/hr/curie at 1 ft

D_1/D_2 for Cs^{137}			
Angle	BD	BC	CD
5°	17.00	31.44	
10°	17.00	141.55	
20°	17.00		268.07
30°	18.03		237.04
45°	22.47		194.33
60°	32.78		180.79
75°	65.16		194.33
90°	241.56		
4m	167.74		

Fig. 2.17 - Plan view, CETO-EG&G calibration facility.

4 meters and at the same height above ground as the source. Relative directional calibrations were also done on all the sources and are illustrated in Figs. 2.18 and 2.19 for two of the sources. Exposure times were approximately 1 hour. The choice of dosimeters was such that the dose received was about mid-scale on the recording instrument. Several exposures were made for each source. All readings were within 5% of the average for a particular source. Effective source strengths were determined by correcting for distance, air attenuation, air buildup, and ground backscattering.

2.3.3 Instrumentation

Instruments used for radiation measurements included stray-radiation chambers, Victoreen model 239 (0 to 10 mr) and Victoreen model 208 (0 to 1 mr). These instruments were charged and read on a Victoreen model 687c minometer. Spherical air-equivalent ionization chambers with an electrometer system, designed and built by EG&G Santa Barbara were also used and, in addition, a Nuclear Chicago model 2586 Cutie Pie and two low-range (0-1 mr) Landsverk model 120 chambers.

The energy and angular response of the Victoreen model 239 and Nuclear Chicago Cutie Pie were measured at EG&G Santa Barbara. The energy response curves are presented in Fig. 2.20. Angular response measurements of the 10-mr Victoreen chambers show a 7% decrease in sensitivity in the direction of the stem.

The integrating ion chambers were calibrated with an NBS-calibrated cobalt-60 source. Actual doses given to these detectors were calculated by considering distance, air attenuation, air buildup, and ground backscatter. Several chambers were selected at random and exposed several times to obtain an average dose and standard deviation at several points over the entire range of the instruments. Both source and detectors were placed about 6 ft above the ground on thin aluminum stands. Other detectors were calibrated in like manner.

2.3.4 Shields

Shielding materials tested were wood, aluminum, steel, and concrete and were all 5 by 5 ft and varied in thickness. The plywood slabs were from 1/4 to 1 in. thick. The aluminum was type 61S and 1/2 in. thick. The steel was 400 series mild steel 1/4 in. thick. The concrete was pea gravel (less than 3/8 in. aggregate) and cement poured in a steel peripheral framework with reinforcement rods extending from the periphery 6 in. into the concrete. The thickness of

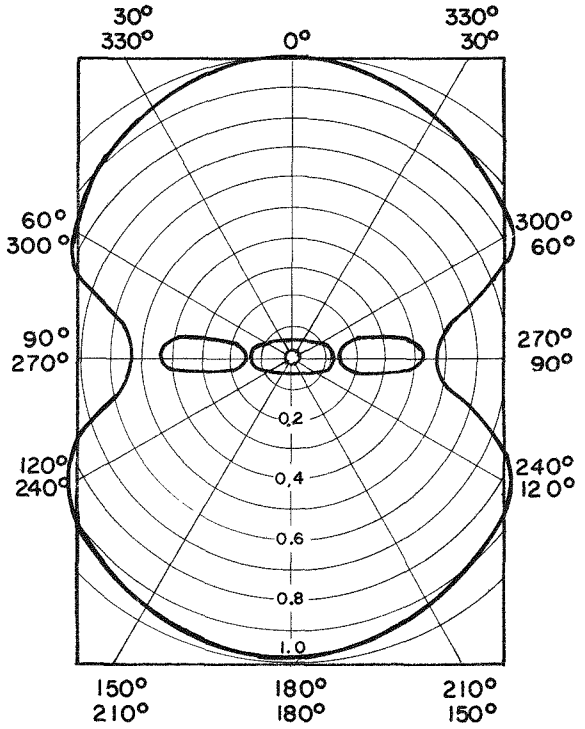

Fig. 2.18 - Relative directional calibration, cesium-137 source.

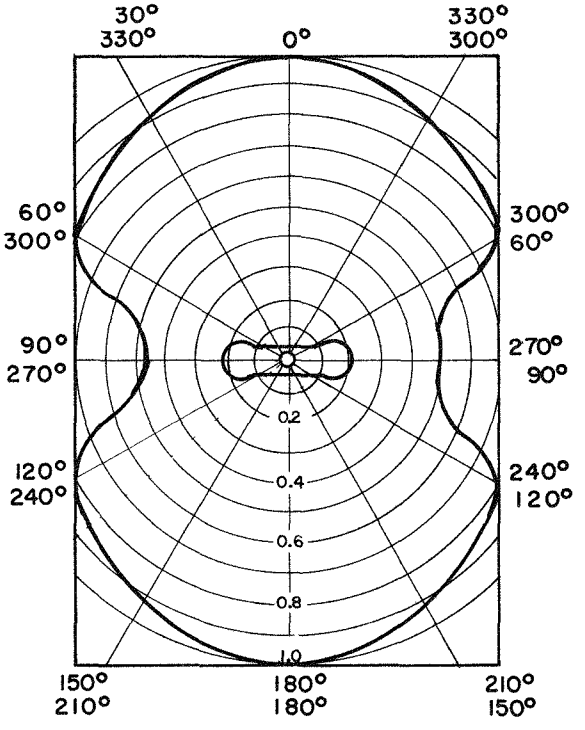

Fig. 2.19 - Relative directional calibration, cobalt-60 source.

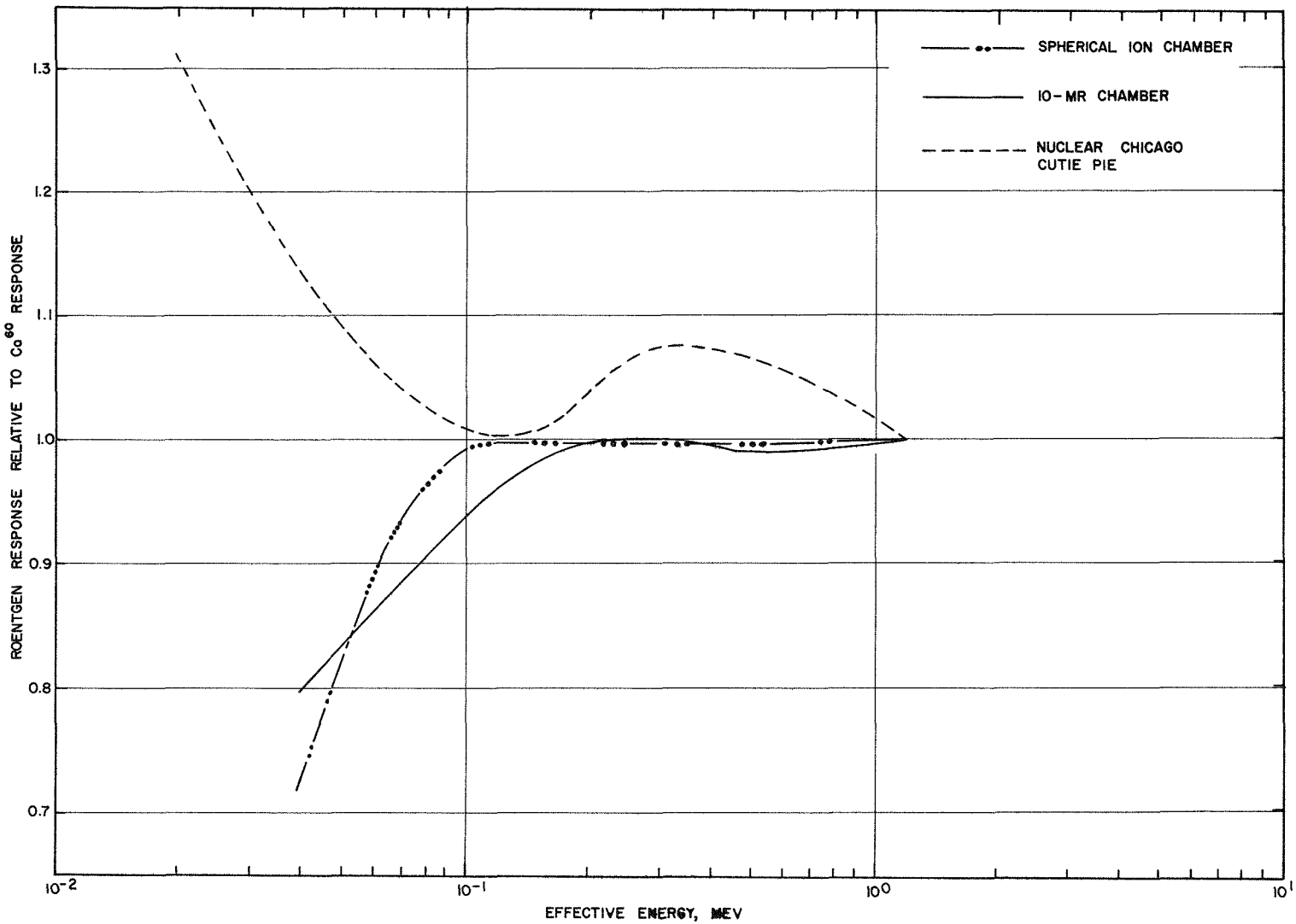

Fig. 2.20 - Energy response of detectors used in experiment.

this shield was 2 in. Each shield was weighed individually to obtain the mass per unit area.

REFERENCES

1. Engineering Manual: Design and Review of Structures for protection from Fallout Gamma Radiation, Office of Civil Defense, revised 1 October 1961.

2. L. V. Spencer, Structure Shielding Against Fallout Radiation from Nuclear Weapons, NBS Monograph 42 (National Bureau of Standards, Washington 25, D. C.), June 1, 1962.

3. H. Borella, Z. Burson and J. Jacovitch, Evaluation of the Fallout Protection Afforded by Brookhaven National Laboratory Medical Research Center, Report CEX-60. 1, February 1961.

4. Z. G. Burson, Experimental Evaluation of the Fallout-radiation Protection Provided by Selected Structures in the Los Angeles Area, Report CEX-61.4, February 26, 1963.

5. Z. G. Burson, Experimental Radiation Measurements in Conventional Structures, Report CEX-59. 7B, Part II, February, 1963.

6. Z. G. Burson et al., Description and Operating Procedures for the Mobile Radiological Measuring Unit, Report CEX-63. 11, to be published.

Chapter 3

PRESENTATION OF DATA

Experimental data are presented in tabular form separately for the three major sets of measurements. Point-source data were normalized to milliroentgens per hour per curie (mr/hr/c) and ring-source data to milliroentgens per hour per curie per foot of circumference (mr/hr/c/ft). Thicknesses of shields are given in mass thickness (lb/sq ft) instead of linear thickness. For open-hole and horizontal-shield data, solid-angle fractions (ω) are also given at each detector position. These were calculated by assuming the center of the detector as the detector location. The value of ω was set equal to 1.0 at a solid angle of 2π steradians. Nearly all data presented in the tables are averaged from at least two exposures.

All data have been corrected for chamber temperature and pressure, calibration, and for background. For information and comparison, some of the data are also presented in graphical form.

3.1 OPEN HOLE

The first set of measurements in an open hole were made by the Cutie Pie instrument with the cobalt-60 source at 100 ft. Measurements were made before and after the lead liner was added to the already in-place steel liner. No significant changes in dose rates or angular distribution could be detected within the limits of experimental error. It is concluded that the dose contribution due to wall backscatter was negligible for this configuration.

About nine sets of measurements were made with the 10-mr chambers with the cobalt-60 source placed at 100 ft. These data were taken with the lead liner (and lead lip) in place. Measurements were also made at 60 ft. The data are plotted in Fig. 3.1

A smooth curve was drawn through the data points for d = 60 ft. For d = 100 ft and small values of ω data points were scattered. A straight line was assumed for data points at small values of ω and a least squares fit was calculated. A smooth curve was then drawn

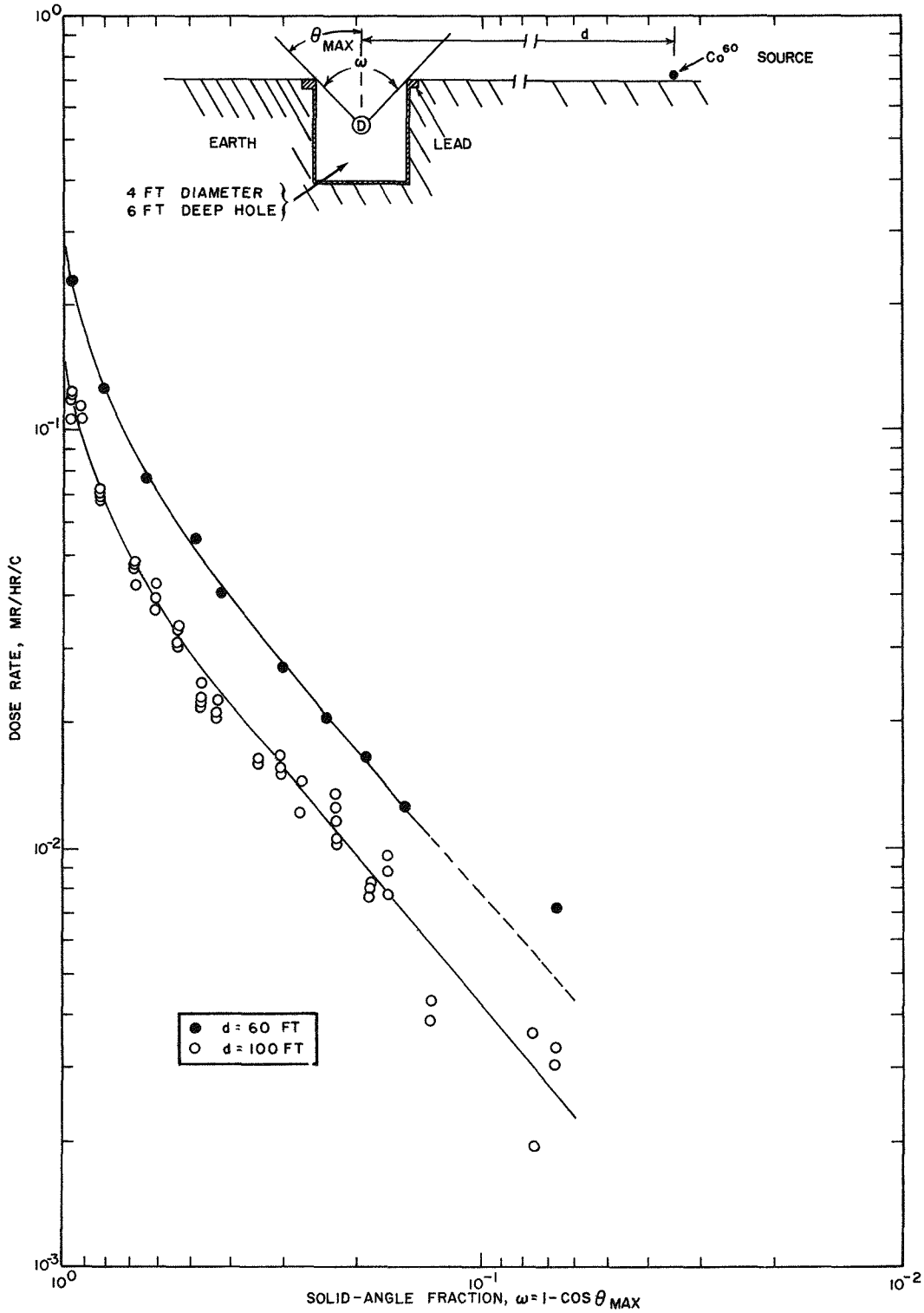

Fig. 3.1 - Experimental data at various depths in the center of the open hole, using 10-mr chambers and cobalt-60.

through the data points, using as guidelines the least squares fit for small solid angles and the average of the data points for large solid angles.

It is interesting to note that the two curves are parallel and the ratio between the curves is about 1.8. Thus, for these two distances, the quantity of skyshine radiation from a point source falls off inversely with the distance (rather than distance squared). The relative dose rate versus solid-angle fractions (geometry factors) are about the same. For the same solid-angle fractions, values were read from the two smooth curves in Fig. 3.1 and are tabulated in Table 3.1.

TABLE 3.1. SMOOTHED DATA AT VARIOUS DEPTHS IN THE CENTER OF THE OPEN HOLE*

	Dose rate, mr/hr/c	
Solid angle fraction, ω	d = 100 ft	d = 60 ft
1.0	0.15	0.28
0.9	0.10	0.19
0.8	0.070	0.13
0.7	0.052	0.096
0.5	0.030	0.056
0.25	0.013	0.023
0.15	0.0070	0.013
0.10	0.0044	
0.06	0.0024	

*Interpolated from Fig. 3.1.

Several measurements were made with the Cutie Pie instrument with the cobalt-60 source placed from 5 to 440 ft from the center of the hole. The data points were consistent within themselves but did not compare well with data from the 10-mr chambers. These data are therefore not listed. They were examined, however, and no changes in geometry factors with distance from the source were noted. If small changes occurred, they were overshadowed by the experimental error.

Further measurements were made in an open hole in Yucca dry lake. Two sets of measurements with the 10-mr chambers were made with the cobalt-60 source placed at 100 ft. In this case, the walls and lip of the open hole were of earth, not lead. The readings were averaged; these are listed in Table 3.2 and plotted in Fig. 3.2. After measurements were taken, it was discovered the earth

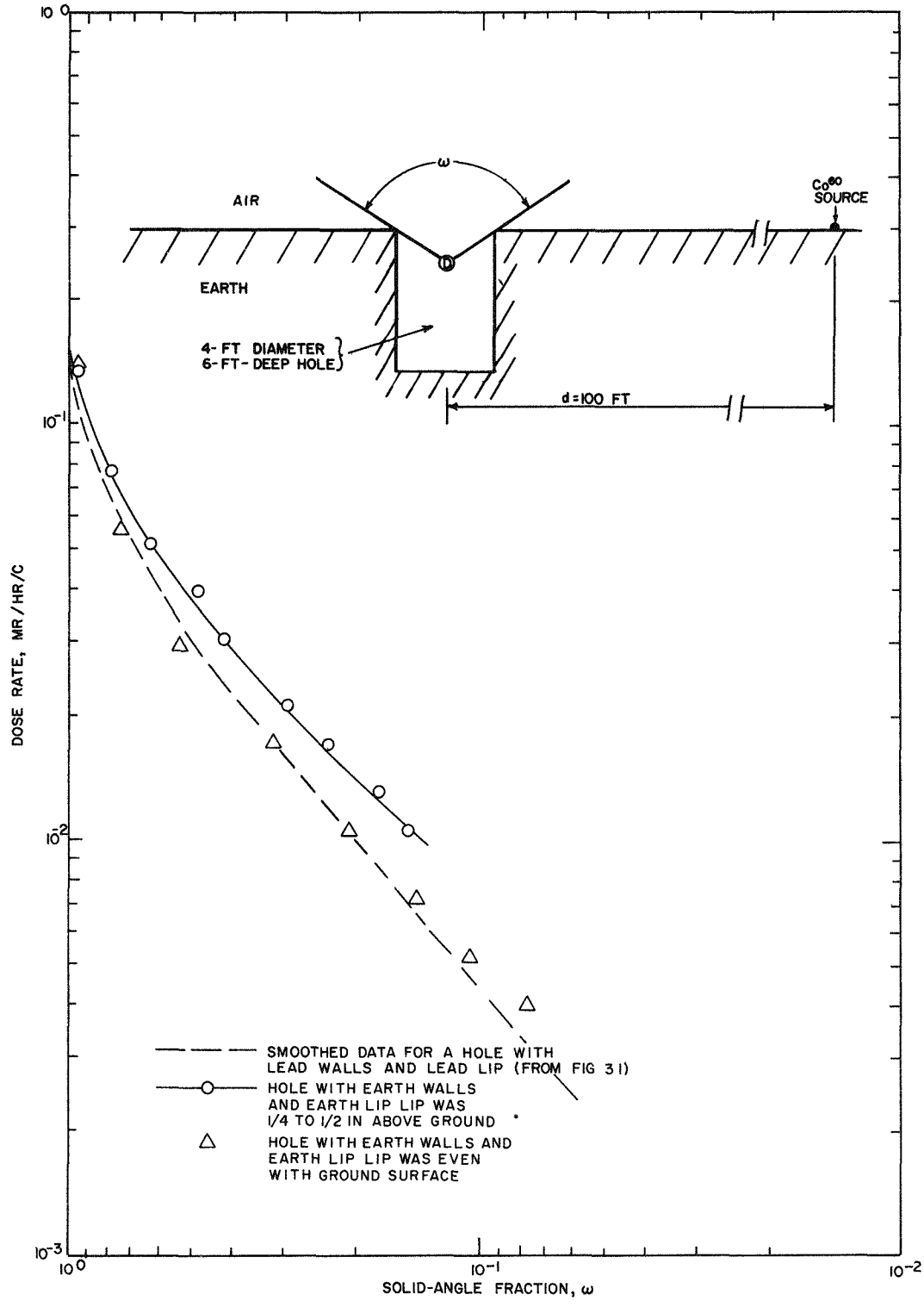

Fig. 3.2 - Dose rate on centerline of open hole 4 ft in diameter and 6 ft deep, cobalt-60 source at 100 ft.

lip actually protruded above ground surface about 1/4 in. in the direction of the source and about 1/2 in. at the back of the hole. Evidently during the drilling process, pressure had forced the earth lip slightly upward.

TABLE 3.2. EXPERIMENTAL DATA IN OPEN HOLE IN YUCCA DRY LAKE. 10-mr CHAMBERS, COBALT-60 AT 100 ft, WITH EARTH WALLS AND EARTH LIP

Lip ¼ to ½ in. above ground surface		Lip even with ground surface	
Solid-angle fraction, ω	Dose rate, mr/hr/c	Solid-angle fraction, ω	Dose rate, mr/hr/c
0.942	0.13	0.958	0.137
0.785	0.077	0.739	0.055
0.630	0.051	0.535	0.029
0.485	0.039	0.319	0.017
0.415	0.030	0.208	0.0104
0.295	0.021	0.143	0.0072
0.232	0.017	0.103	0.0052
0.184	0.013	0.077	0.0040
0.150	0.010		

The lip was smoothed until it was even with the ground surface and then measurements were repeated. The repeated measurements showed a marked difference, shown in Table 3.2 and Fig. 3.2. As is shown in Fig. 3.2 it makes very little difference if the lip and walls are of lead or of earth, except for small solid angles.

In addition to the 100-ft measurements, data were taken with the 10-mr chambers and the spherical ion chamber and electrometer system with the cobalt-60 source placed at distances up to 1500 ft. Data are presented at a solid-angle fraction value of 0.86 in Table 3.3, as this corresponded to the position of the spherical ion chamber. The data have been corrected for background.

TABLE 3.3. EXPERIMENTAL DATA IN YUCCA DRY LAKE FOR ω = 0.86, Cobalt-60

Distance from source, ft	Dose rate, mr/hr/c	
	10-mr chamber	Spherical ion chamber
100	0.086	0.078
175	0.033	
250	0.020	
440	0.0079	0.0078
700	0.0031	0.0025
1000		0.00122
1500		0.00030

3.2 VERTICAL BARRIERS

Before the experiment was begun, measurements were made in the vertical bunker (see Fig. 2.7) before and after the lead liner was installed. Very little difference was observed. Another set of measurements was made at locations around the periphery and on top of the bunker to assure the experimenters that the bunker was not exposed to any direct radiation and that the direct beam was intersected at about 1 ft above the bunker.

The 10-mr chambers (Victoreen model 268) were initially used for measuring the dose rate attenuated by the steel and aluminum shields from cobalt-60. These data along with barrier reduction factors are listed in Tables 3.4, and 3.5. Detector locations are shown in Figs. 2.9 and 2.10. Some of the steel data are shown in graphical form in Fig. 3.3.

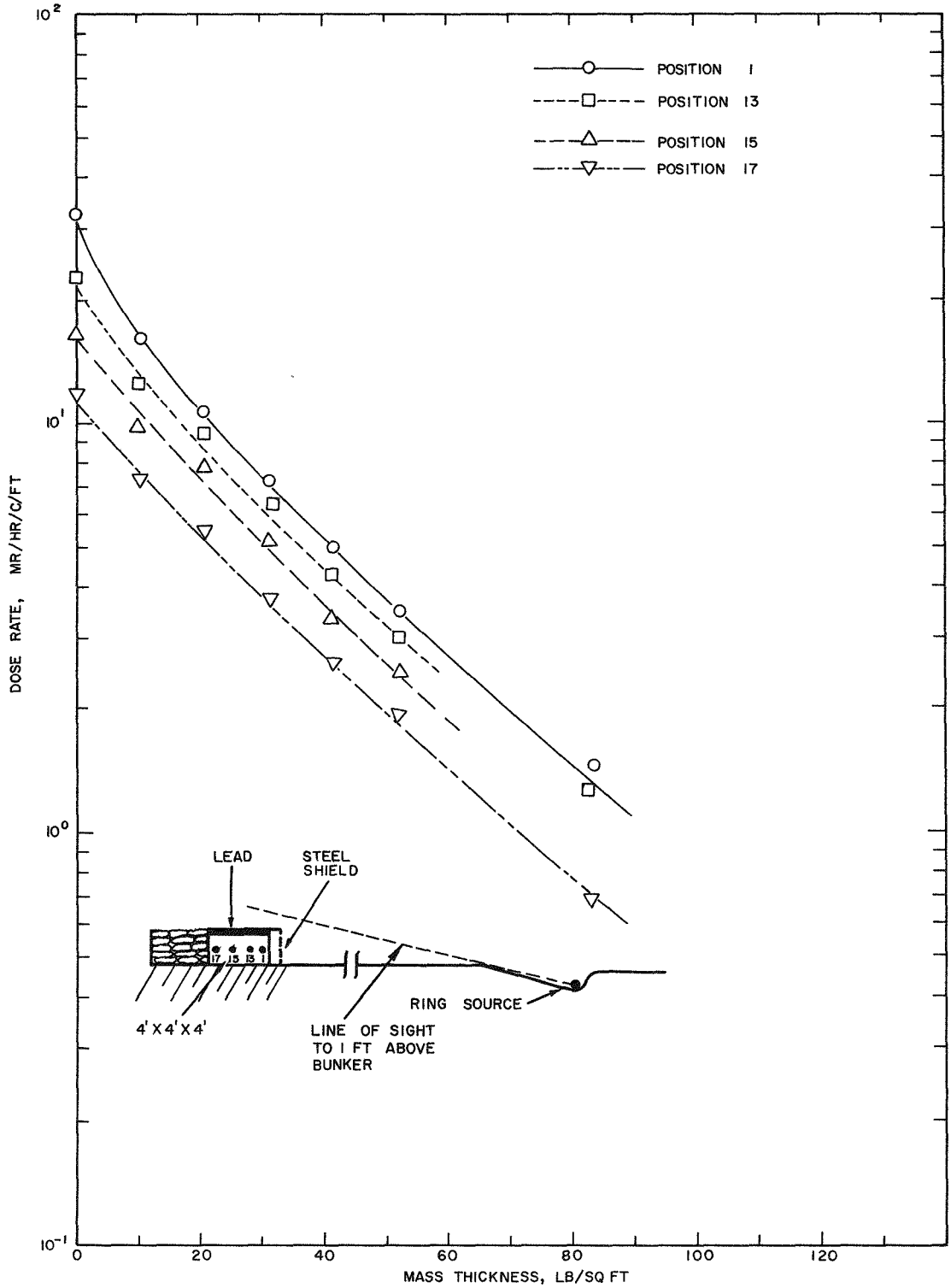

Fig. 3.3 - Vertical barrier data for steel, cobalt-60 ring source at a 100-ft radius, 10-mr chambers.

TABLE 3.4. VERTICAL BARRIER STEEL SHIELDING DATA, 100-FOOT-RADIUS RING COBALT-60 SOURCE, 10-mr CHAMBERS

Detector Position*	Mass Thickness, lb/sq ft						
	0	10.48	20.96	31.44	41.92	52.40	83.84
	Dose Rate, mr/hr/c/ft						
1	32.4	16.9	10.6	7.23	4.93	3.53	1.43
2, 3, 4, &5 averaged	32.0	16.6	10.8	7.20	4.76	3.27	1.28
6	34.7	18.3	11.8	7.83	5.13	3.66	1.51
7	33.9	17.7	11.4	7.59	5.05	3.33	1.50
8	33.7	17.2	11.1	7.31	4.97	3.53	1.55
9	31.1	16.1	10.5	7.00	4.55	3.11	1.28
10	30.1	15.5	10.1	6.64	4.40	3.04	1.20
11	28.3	14.6	9.49	6.30	4.09	2.91	1.05
12	27.7	15.2	10.1	6.84	4.62	3.12	1.32
13	22.5	13.2	9.31	6.35	4.28	3.00	1.29
14	19.8	11.5	8.32	5.69	3.85	2.74	1.22
15	16.5	9.83	7.70	5.13	3.36	2.47	
16	13.6	8.04	6.06	4.28	2.95	2.06	
17	11.6	7.17	5.33	3.68	2.60	1.94	0.68
18	10.2	6.31	4.80	3.39	2.34	1.52	
	Barrier Reduction Factor						
1	1.0	0.522	0.327	0.223	0.152	0.109	0.0441
2, 3, 4, &5 averaged	1.0	0.519	0.338	0.225	0.149	0.102	0.0400
6	1.0	0.527	0.340	0.226	0.148	0.105	0.0435
7	1.0	0.522	0.336	0.224	0.149	0.0982	0.0442
8	1.0	0.510	0.329	0.217	0.147	0.105	0.0460
9	1.0	0.518	0.338	0.225	0.146	0.100	0.0412
10	1.0	0.515	0.336	0.221	0.146	0.101	0.0399
11	1.0	0.516	0.335	0.223	0.145	0.103	0.0371
12	1.0	0.549	0.365	0.247	0.168	0.113	0.0477
13	1.0	0.587	0.414	0.282	0.190	0.133	0.0573
14	1.0	0.581	0.422	0.287	0.194	0.138	0.0616
15	1.0	0.596	0.467	0.311	0.204	0.150	
16	1.0	0.591	0.446	0.315	0.217	0.151	
17	1.0	0.618	0.459	0.317	0.224	0.167	0.0586
18	1.0	0.619	0.471	0.332	0.229	0.149	

*See Figs. 2.9 and 2.10

TABLE 3.5. VERTICAL BARRIER ALUMINUM SHIELDING DATA, 100-FT-RADIUS RING COBALT-60 SOURCE, 10-mr CHAMBERS

Detector position*	Mass thickness, lb/sq ft			Mass thickness, lb/sq ft		
	0	7.5	36.67	0	7.5	36.67
	Dose rate, mr/hr/c/ft			Barrier reduction factor		
1	32.4	18.7	6.08	1.0	0.577	0.188
2, 3, 4, &5 averaged	32.0	18.9	6.13	1.0	0.591	0.192
12	27.7	16.0	5.90	1.0	0.578	0.213
13	22.5	14.8	5.39	1.0	0.658	0.240
14	19.8	11.8	4.67	1.0	0.600	0.236
15	16.5	8.95	3.80	1.0	0.542	0.230

*See Figs. 2.9 and 2.10

For more expediency and little loss of accuracy, the Nuclear Chicago Cutie Pie was used for the rest of the vertical barrier experiment. All the aluminum and part of the steel attenuation measurements were repeated. The cesium-137 measurements were made at only three or four thicknesses of shield material and at only Position A. (See Fig. 2.11). Data were taken at Position B from the cobalt-60 source for wood and aluminum. The Cutie Pie data along with barrier reduction factors are tabulated in Tables 3.6, 3.7 and 3.8.

TABLE 3.6. VERTICAL BARRIER SHIELDING DATA, 100-FT-RADIUS RING COBALT-60 SOURCE, NUCLEAR CHICAGO CUTIE PIE, POSITION A*

Mass thickness, lb/sq ft	Dose rate, mr/hr/c/ft	Barrier reduction factor
Wood shield		
0	31.9	1.00
3.02	25.9	0.813
5.98	22.6	0.709
8.89	20.7	0.649
11.86	18.6	0.583
14.80	16.5	0.518
20.78	13.4	0.420
29.84	9.32	0.292
35.64	8.45	0.262
Concrete shield		
0	31.9	1.00
21.52	12.3	0.386
43.26	5.75	0.180
64.70	2.94	0.0923
85.98	1.65	0.0518
129.34	0.69	0.0216
Aluminum shield		
0	31.9	1.00
7.16	20.9	0.655
14.52	15.3	0.480
21.66	11.7	0.367
36.64	7.00	0.219
59.12	3.44	0.108
88.29	1.34	0.0420
Steel shield		
0	31.9	1.00
10.48	15.9	0.498
20.96	9.83	0.308
52.40	3.22	0.101
83.84	1.35	0.0424

*See Fig. 2.11

TABLE 3.7. VERTICAL BARRIER SHIELDING DATA, 100-FT-RADIUS RING CESIUM-137 SOURCE, NUCLEAR CHICAGO CUTIE PIE, POSITION A*

Mass thickness, lb/sq ft	Dose rate, mr/hr/c/ft	Barrier reduction factor
	Wood shield	
0	13.8	1.00
3.02	11.4	0.828
5.98	9.93	0.720
14.80	6.76	0.490
	Concrete shield	
0	13.8	1.00
21.52	4.7	0.346
43.26	2.07	0.150
	Aluminum shield	
0	13.8	1.00
7.16	8.74	0.634
14.52	5.99	0.434
36.64	2.34	0.170
	Steel shield	
0	13.8	1.00
10.48	6.41	0.464
20.96	3.65	0.264
52.40	0.93	0.0674

*See Fig. 2.11.

TABLE 3.8. VERTICAL BARRIER SHIELDING DATA, 100 FT-RADIUS RING COBALT-60 SOURCE, NUCLEAR CHICAGO CUTIE PIE, POSITION B*

Mass Thickness, lb/sq ft	Dose rate, mr/hr/c/ft	Barrier reduction factor
	Wood shield	
0	13.2	1.00
3.02	11.8	0.895
5.98	11.0	0.834
8.89	10.0	0.758
11.86	9.15	0.693
14.80	8.50	0.644
20.78	7.20	0.546
29.84	5.62	0.425
35.64	4.95	0.375
	Aluminum shield	
0	13.2	1.00
7.16	10.1	0.770
14.52	7.81	0.592
21.66	6.44	0.487
36.64	4.39	0.333
59.12	2.45	0.186
88.29	1.30	0.0985

*See Fig. 2.11

There was some radiation leakage through the sides of the bunker. To estimate this dose rate, measurements were made by placing all the steel and concrete sheets at the bunker face. Data were plotted and extrapolated to a mass thickness of 1000 lb/sq ft. The value at this thickness was 0.3 mr/hr/c/ft for cobalt-60 data. It is noted in Table 3.6 that the dose rate through the largest shield (129 lb/sq ft of concrete) is more than twice this leakage dose rate.

An estimate of this radiation leakage for cesium-137 was made from the cobalt-60 data.

3.3 HORIZONTAL BARRIERS

The first set of horizontal barrier measurements was made for steel slabs at the vertical bunker arrangement (see Fig. 2.7) from a ring source of cobalt-60. These data are shown in graphical form in Fig. 3.4. The geometry was such that the top of the shield was not exposed to scattering angles of less than about 4^{o}. This bunker did not have a lead liner. The solid-angle fraction values (ω) given in the graph refer to the detector-shield geometry.

The remainder of the horizontal shield data were taken in the round hole, the top of which was flush with the ground. The walls and lip were of lead. All data have been corrected for background.

The primary detector for the wood and aluminum sheets was the 10-mr ion chamber. Its small physical size provided good geometry for the experiment. A few other measurements were made with the 1-mr chambers and the Cutie Pie instrument for large thicknesses to support those from the 10-mr chambers. Data for the wood shielding material are tabulated in Table 3.9, and shown in Fig. 3.5. Data for the aluminum shielding material are tabulated in Table 3.10 and shown in Fig. 3.6.

TABLE 3.9. HORIZONTAL BARRIER DATA FOR WOOD, 100 FT DISTANCE, COBALT-60 SOURCE, 10-mr CHAMBERS

Det. depth, in.	ω	Mass thickness, lb/sq ft						
		0	0.75	1.50	3.0	6.0	15.0	30.0
		Dose rate, mr/hr/c						
1.37	0.949	0.121	0.084	0.065	0.057	0.045	0.034	0.021
5.12	0.813	0.0705	0.054	0.047	0.043	0.037	0.028	0.017
9.62	0.664	0.0465	0.037	0.034	0.031	0.028	0.022	0.013
14.37	0.530	0.0325	0.027	0.024	0.023	0.021	0.017	0.010
17.12	0.464	0.0275	0.022	0.020	0.019	0.018	0.014	0.0086
23.87	0.339	0.0184	0.016	0.013	0.013	0.012	0.0098	0.0061
28.87	0.269	0.0140	0.012	0.010	0.0098	0.0092	0.0075	0.0048
33.62	0.220	0.0110	0.0098	0.0079	0.0078	0.0073	0.0061	0.0039
38.50	0.181	0.00880	0.0080	0.0063	0.0062	0.0058	0.0049	0.0032
63.00	0.0655	0.00270	0.0032	0.0020	0.0020	0.0019	0.0016	0.0012

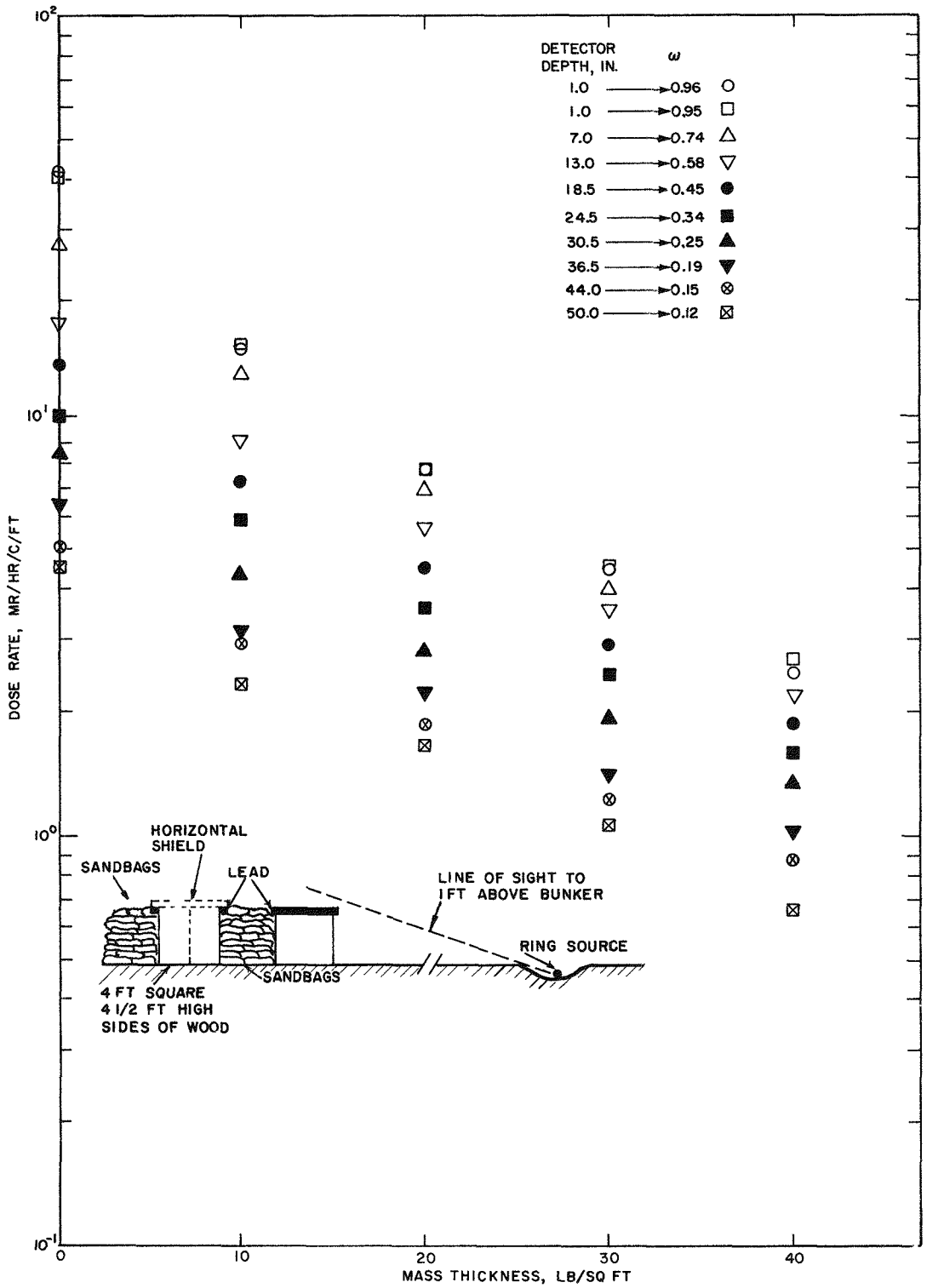

Fig. 3.4 - Horizontal barrier data for steel, cobalt-60 ring source at a 100-ft radius, 10-mr chambers.

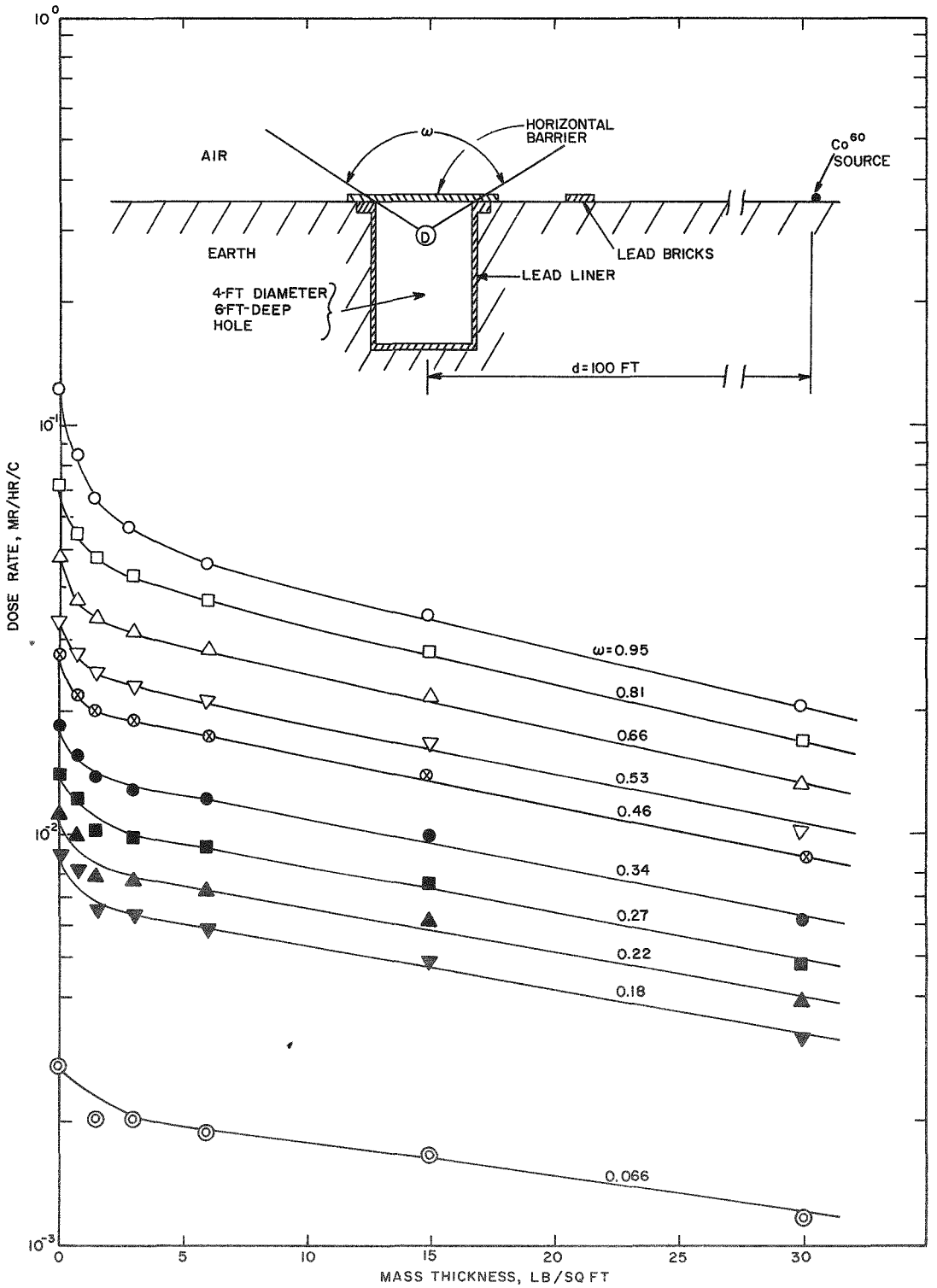

Fig. 3.5 - Horizontal barrier data for wood, cobalt-60 source at 100 ft, 10-mr chambers.

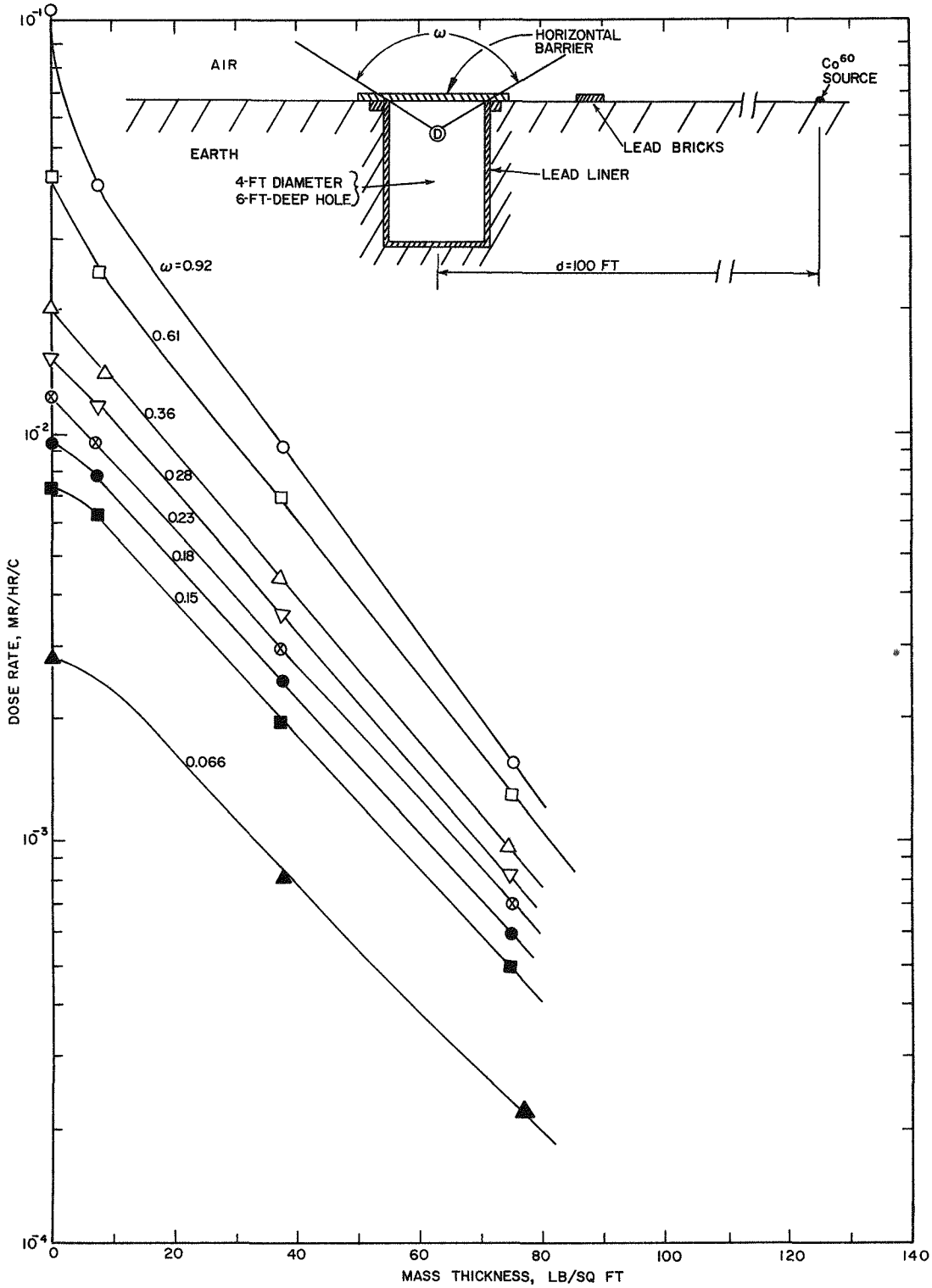

Fig. 3.6 - Horizontal barrier data for aluminum, cobalt-60 source at 100 ft, 10-mr chambers.

TABLE 3.10. HORIZONTAL BARRIER DATA FOR ALUMINUM, 100 FT DISTANCE, COBALT-60 SOURCE, 1 mr AND 10 mr CHAMBERS

Det. depth, in.	ω	Mass thickness, lb/sq ft			
		0	7.5	37.5	75
		Dose rate, mr/hr/c			
2.00	0.917	0.107	0.039	0.0088	0.0015
10.25	0.607	0.0402	0.024	0.0066	0.0013
20.00	0.360	0.0198	0.014	0.0043	0.00093
24.75	0.282	0.0148	0.011	0.0035	0.00080
29.25	0.227	0.0113	0.0090	0.0029	0.00068
34.00	0.183	0.00900	0.0075	0.0023	0.00057
38.75	0.150	0.00700	0.0061	0.0019	0.00048
63.00	0.0655	0.00270	0.0029	0.00079	0.00021

The main detector for the steel shields was the 1-mr chambers. A few measurements with the 10-mr chambers and the Cutie Pie instrument confirmed the 1-mr chamber findings. Data for the steel sheets are tabulated in Table 3.11 and shown in Fig. 3.7.

TABLE 3.11. HORIZONTAL BARRIER DATA FOR STEEL, 100 FT DISTANCE, COBALT-60 SOURCE, 1-mr CHAMBERS

Det. depth, in.	ω	Mass thickness, lb/sq ft				
		0	10.5	20.0	52.0	105
		Dose rate, mr/hr/c				
1.58	0.945	0.120	0.027	0.016	0.0041	0.00048
14.25	0.490	0.0295	0.015	0.010	0.0030	0.00034
27.25	0.250	0.0128	0.0077	0.0055	0.0018	0.00020
49.54	0.100	0.00440	0.0029	0.0019	0.00070	0.000078
63.00	0.0655	0.00270	0.0018	0.0012	0.00042	0.000049

All concrete data were taken with 1-mr chambers. These data are tabulated in Table 3.12. Data were also taken for 132 lb/sq ft mass thickness of concrete but are not included because of poor geometry. It turned out that the overlap of the shield over the edge of the hole was not as much as the thickness; therefore the data were considered invalid. Time did not permit larger shields to be constructed.

The "no shield" data in Tables 3.9 through 3.12 were taken from the smoothed curve in Fig. 3.1.

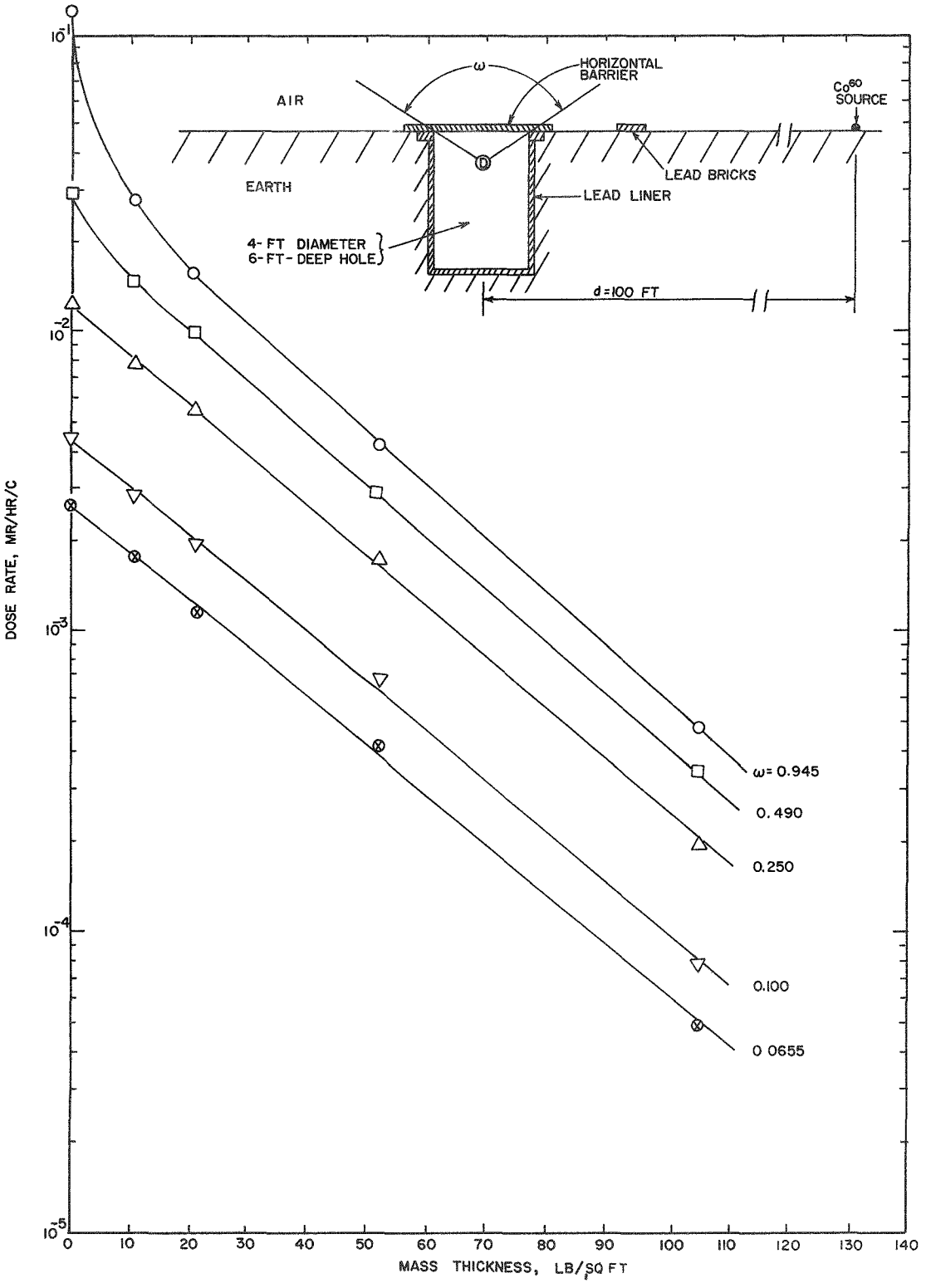

Fig. 3.7 - Horizontal barrier data for steel, cobalt-60 source at 100 ft, 1-mr chambers.

TABLE 3.12. HORIZONTAL BARRIER DATA FOR CONCRETE, 100 FT DISTANCE, COBALT-60 SOURCE, 1-mr CHAMBERS

Det. depth, in.	ω	Mass thickness, lb/sq ft		
		0	22	44
		Dose rate, mr/hr/c		
2.25	0.907	0.103	0.015	0.0053
36.00	0.168	0.00800	0.0043	0.0016
62.00	0.067	0.00278	0.0021	0.00075

Chapter 4

ANALYSIS AND CONCLUSIONS

4.1 OPEN HOLE

4.1.1 Dose Versus Distance

The total scattered gamma radiation, D^s, at a detector in an infinite medium of air a distance, d, from an isotropic point source of radiation can be represented as:

$$D^s = \frac{Qe^{-\mu d}}{d^2} \left[B(\mu d) - 1 \right] \qquad (4.1)$$

where D^s = total scattered gamma radiation
Q = A source strength normalization factor, 14.53×10^3 mr/hr 1 ft from a 1-curie cobalt-60 source
d = source-to-detector distance in feet
μ = the total linear absorption coefficient for air
$B(\mu d)$ = the dose buildup factor

Berger[1] has expressed the buildup factor, $B(\mu d)$, for a 1.25-Mev isotopic point source in an infinite water medium as:

$$B(\mu d) = 1 + \mu d \left[1.325 \; e^{0.0314 \mu d} - 0.461 \; e^{-0.244 \mu d} \right] \qquad (4.2)$$

To compare with experimental data, the collimation of the detector and the presence of the ground must be considered (see Fig. 4.1).

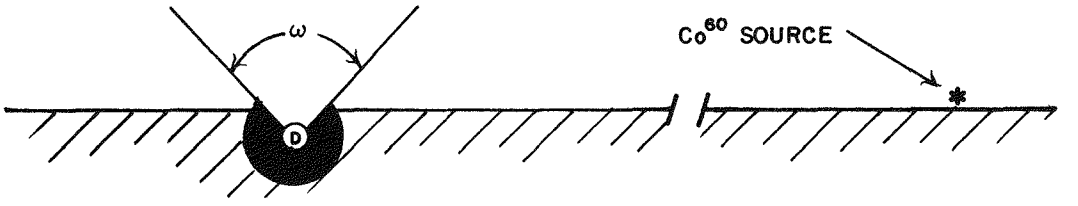

Fig. 4.1 - Conical detector pointing 90° away from the source-detector line, isotropic point cobalt-60 source, source and detector at the air-ground interface.

The detector response, S, of a conical detector pointing 90^{o} away from the source detector line as in Fig. 4.1 can be expressed as:

$$S = G K_a D^s \qquad (4.3)$$

where G is a directional response correction factor to correct for the collimation of the detector and K_a is an interface correction factor to correct for the presence of the ground. The value of G is taken as half the geometry reduction factor of Case 2 in Fig. 2.3. These reduction factors were taken from Spencer[2], who assumes an ideal collimated detector in an infinite medium of air. Because of the strong forward component of the air-scattered radiation, one would expect the single scattered photons to dictate the angular distribution and, therefore, the presence of the ground is not expected to greatly influence their angular distribution. One further assumes the buildup factor expression for water (Equation 4.2) is applicable for air with suitable density scaling.

It is of interest to calculate values of S for the homogeneous medium case (K_a=1). These calculations will later be compared to experimental data to derive values of K_a. The value of G was taken as 0.30 for a solid-angle fraction of 0.86 (Fig. 2.3) corresponding to the detector position of the spherical ion chamber. This value of G was assumed to be constant for all values of d. The air density for the conditions of this experiment was used for the calculations.

The results of the calculations are given in Table 4.1 for point sources and for ring sources.

TABLE 4.1. CALCULATED SKYSHINE DOSE RATE FOR A COLLIMATED DETECTOR (ω = 0.86) a DISTANCE d FROM A COBALT-60 SOURCE IN AN INFINITE HOMOGENOUS MEDIUM OF AIR

Distance d, ft	Point Source, mr/hr/c	Ring Source, mr/hr/c/ft
10	0.615	38.6
50	0.121	38.0
100	0.0600	37.7
150	0.0382	36.0
250	0.0195	30.6
440	0.00780	21.5
700	0.00329	14.5
1000	0.00144	9.04
1500	0.000479	4.21

For ease of presentation, the data from a point source of cobalt-60 were multiplied by $2\pi d$ to correspond to a ring-source configuration. The resulting values along with the calculations are shown in Fig. 4.2. Some measurements made by other experimenters[3,4] corrected for the appropriate solid-angle fraction, are also presented for comparison. The dashed line was drawn through the experimental points available. The value of K_a for a given distance corresponds to the ratio of the experimental value to the calculated value. These values, taken from the smoothed curves, are listed in Table 4.2 for several distances corresponding to 0.1 to 2.5 mean free paths (mfp). Under the experimental conditions of this project, a mfp in air was about 530 feet.

In evaluating experimental data, Fig. 4.2 shows that results are consistent and compare well with other experimental data. Also listed in Table 4.2 for comparison are values of K, representing correction factors for the total radiation at or slightly above the interface for cobalt-60 sources at the interface (as defined by Berger[1]). For both cases (total and skyshine radiation) and for sources near the detector, the earth acts effectively as a scatterer and hence the values of the correction factors (K and K_a) are greater than one. For large source-to-detector distances, the earth acts effectively as an absorber of air-scattered radiation and thus the values are less than one. For both small and large source-detector distances, values of K_a were found to be greater than

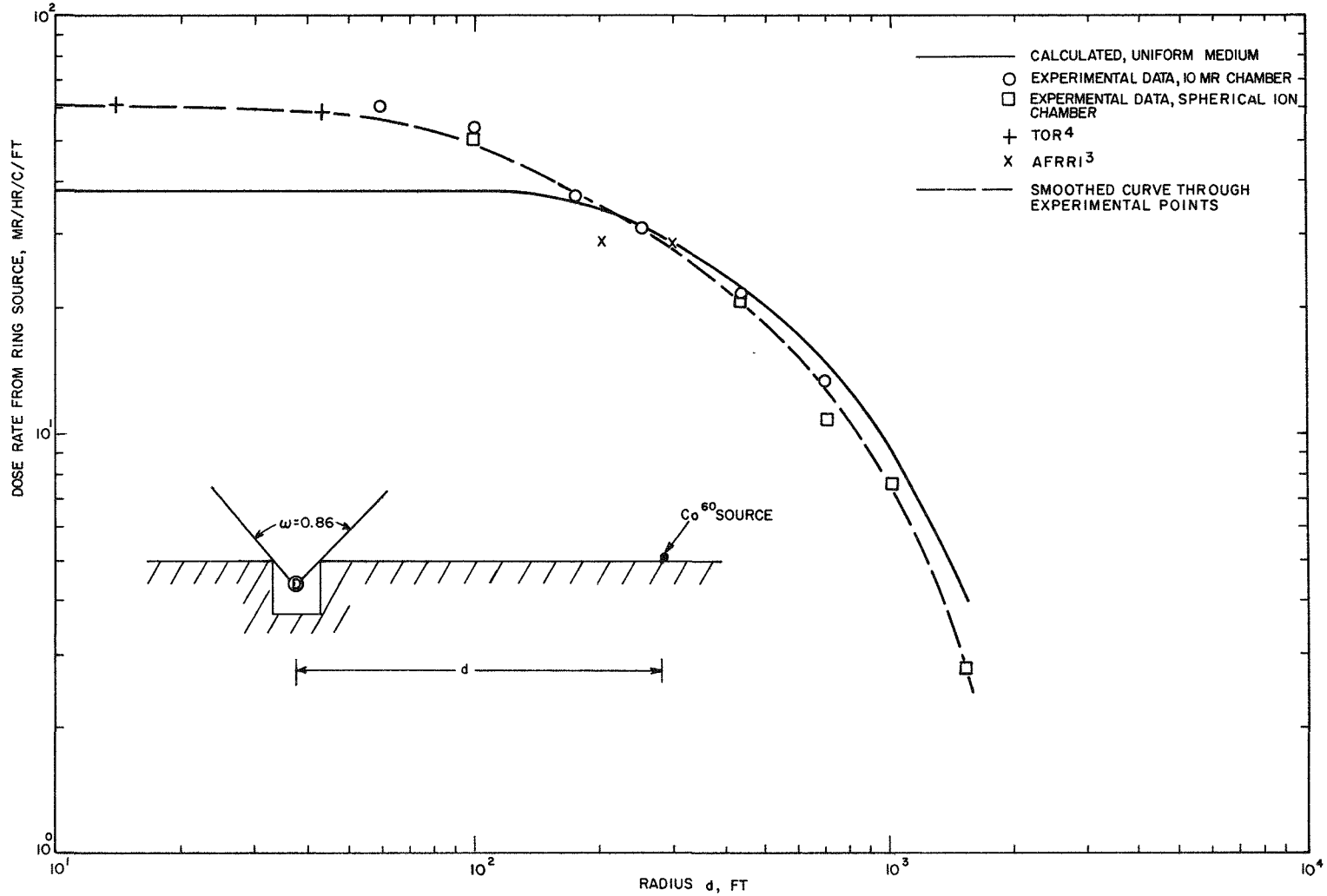

Fig. 4.2 - Skyshine dose rate for a collimated detector ($\omega = 0.86$) a distance d from a cobalt-60 source.

TABLE 4.2. AIR-GROUND INTERFACE CORRECTION FACTORS, FOR RADIATION FROM COBALT-60. (Source and Detector at or near the interface.)

Mean free path in air, mfp	K_a(experimental) for skyshine radiation	K(theoretical)* for total radiation
0.1	1.53	1.18
0.2	1.28	1.17
0.3	1.11	1.14
0.4	1.01	1.07
0.5	0.97	1.01
0.75	0.92	0.91
1.0	0.91	0.83
1.5	0.85	0.72
2.0	0.79	0.64
2.5	0.70	0.58

*Calculated by Berger[1]

the values of K. For intermediate distances (0.5 mfp) both values are about 1.0.

The calculations may slightly overestimate the buildup for large distances because of the assumption that the buildup factor expression for water applies to air.[5] However, a compensating effect may be the slight change of angular distribution with distance.

Factors influencing the accuracy of the experimental data were:

1. Source calibration.
2. Detector accuracy and calibration.
3. Temperature-and-pressure correction for detectors.
4. Nonisotropy of the source.
5. Nonisotropy of the detectors.
6. Detector positioning.
7. Source-detector geometry.
8. Energy response of the detectors.

Source calibration was considered accurate to within 3%. Detectors after calibration correction were assumed to be accurate to ± 10%. However, most of the reported data points are an average of two or more readings and thus should be accurate to within approximately 7%. A maximum of 1% error was possible for the temperature-and-pressure correction. As can be seen in Figs. 2.18 and 2.19, the source was nonisotropic. However, it was always placed such that the long axis was perpendicular to the line

from source to detector. Since radiation tends to be scattered preferentially in the forward direction, and since most of the large-angle scattered radiation reaching the detector had been scattered near the detector rather than near the source, the effect of the anisotropy of the source is considered negligible, especially for large source-detector distances. Detectors were positioned such that the effect of their anisotropy was minimized. Detectors were placed within 1/8 in. of the desired locations. The center of the detector was assumed to be the effective detector location. This assumption may have resulted in small errors for the larger detectors.

The geometry of the hole was as ideal as was consistent with practical field operations. However, there were probably some errors due to source-height effects and scattering off near-by material (sandbags 1-1/2 ft high a few yards away, for example) for small source-detector distances.

As can be seen in Fig. 2.20 the chamber responses were essentially flat for energies from 1.25 Mev down to about 100 kev and dropping to 20 to 25% low at 40 kev. The contribution of low-energy radiation may be large. Clifford[6] reports "that at angles greater than 30° above the horizon the bulk of the scattered radiation and hence the bulk of the dose received is due to energies less than 300 kev." He also reports that at a depth of 1 meter in a 2-meter diameter hole, at least one-third of the dose received is from radiation with energies less than 100 kev. His measurements were from a cesium-137 source. Because no measurements were made of the energy spectrum, no corrections were made for energy response of the chambers.

The detectors may have overresponded at small source-detector distances because of electrons, caused by free-air ionization above the ground (an inch or two above the top detector), penetrating the chamber walls. To evaluate this possible error, 1/16 in. of polyethlene was placed around the 10-mr chambers and the 100-ft measurements repeated. The polyethlene plus the chamber walls provided enough mass to stop 1-Mev electrons. The chambers read about 4% lower with the polyethlene cover than without it. While the polyethlene cover probably absorbed some electrons that would have penetrated the chamber walls, it also absorbed some low-energy photons that also would have been read by the chamber. For this reason no correction was made in the data.

Experimental data from this experiment compare satisfactorily with theoretical calculations and with other experimental measurements by AFRRI[3] and TOR[4].

It is of interest to know the skyshine dose rate in the hole as a function of radius of contamination. An estimate of these values was obtained from the data and plotted in Fig. 4.3 for the top of the hole (solid-angle fraction of 1.0). A value of 51 mr/hr is estimated for an infinite plane of cobalt-60 contaminated to a density of 1 mc/sq ft. This value is about 10% of the estimated total dose rate (500 mr/hr) 3 ft above ground. This compares with 8.8% calculated by Spencer[2] for standard temperature and pressure. It is noted that 50% of the skyshine contribution originates from contamination beyond 350 ft.

4.1.2 Geometry Reduction

Note in Fig. 3.1 that experimental data for d = 100 ft are somewhat spotty, especially for positions near the bottom of the hole. However, because of the volume of data taken, a high degree of confidence is placed on the smoothed curve through the experimental points. This smoothed curve was normalized to a dose rate of 1.0 at $\omega = 1.0$ and is compared to a calculated curve for d = 100 ft in Fig. 4.4. The calculated geometry reduction curve is duplicated from Fig. 2.3. It can be seen that the agreement of the two curves is excellent. It is concluded that the calculated geometry factor describing the response of a conical detector pointed 90° away from the source-to-detector line for a source-detector distance of 100 ft in air is confirmed by experimental data.

4.1.3 Lip Scatter and Wall Backscatter

Measurements in a hole with a steel liner and lead lip showed no noticeable difference from those in a hole with a lead liner and lead lip. While no major difference was noted when the hole contained earth walls and an earth lip, a small increase (10 to 20%) was noted at positions near the bottom of the hole ($\omega < 0.15$).

If the lip of the hole would protrude above ground even a small amount, a major increase in dose rate would be observed in the hole. Measurements showed an increase of about 25% at a solid-angle fraction of 0.5 when the earth lip was from 1/4 to 1/2 in. above ground level and the cobalt-60 source was at 100 ft. The height of the source was also about 1/2 in. above ground.

4.2 VERTICAL BARRIERS

The main purpose of the vertical barrier experiment was to study the barrier attenuation of skyshine radiation. The point of

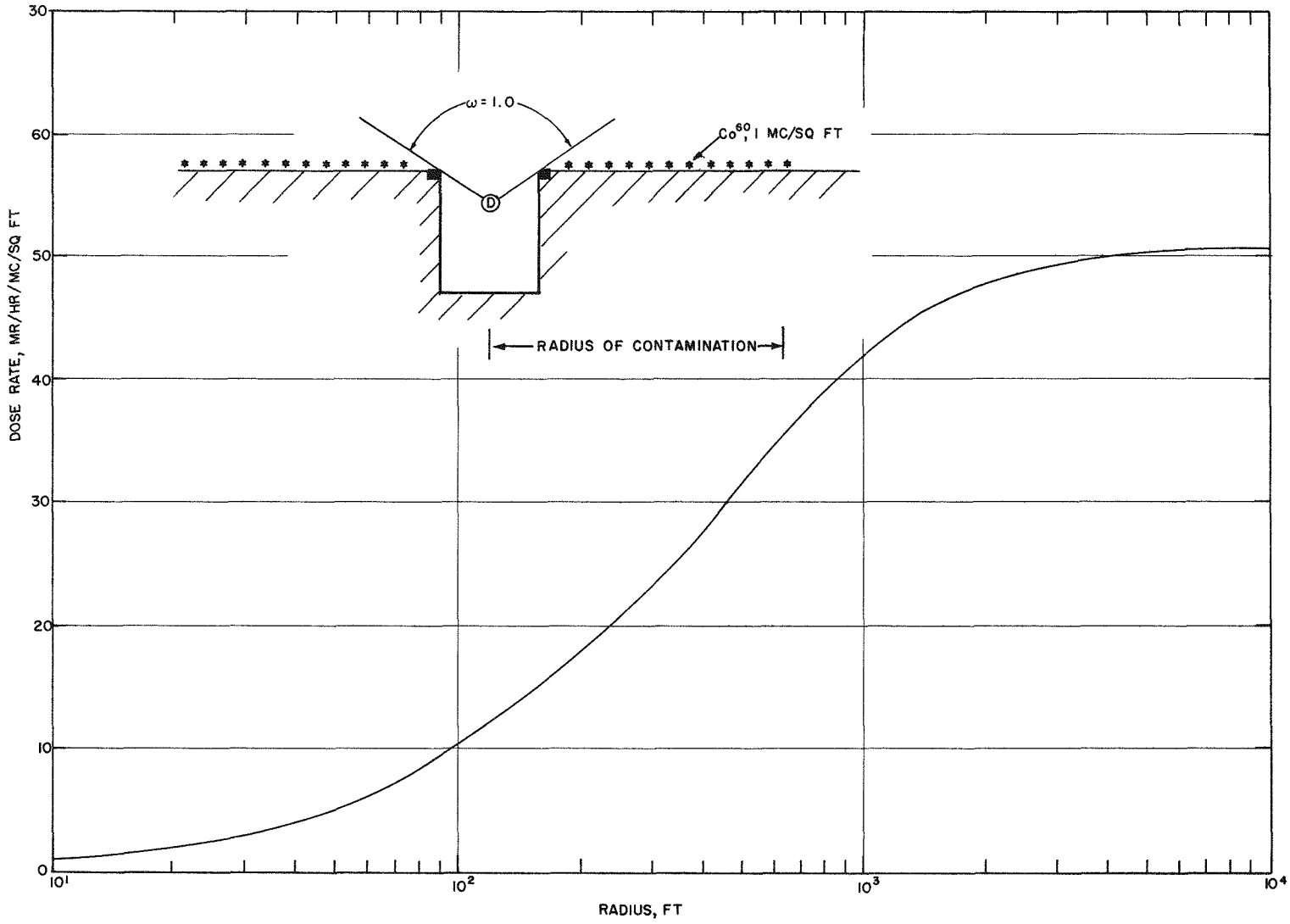

Fig. 4.3 - Dose rate as a function of radius of contamination, cobalt-60, 1 mc/sq ft (integrated from experimental smoothed curve in Fig. 4.2).

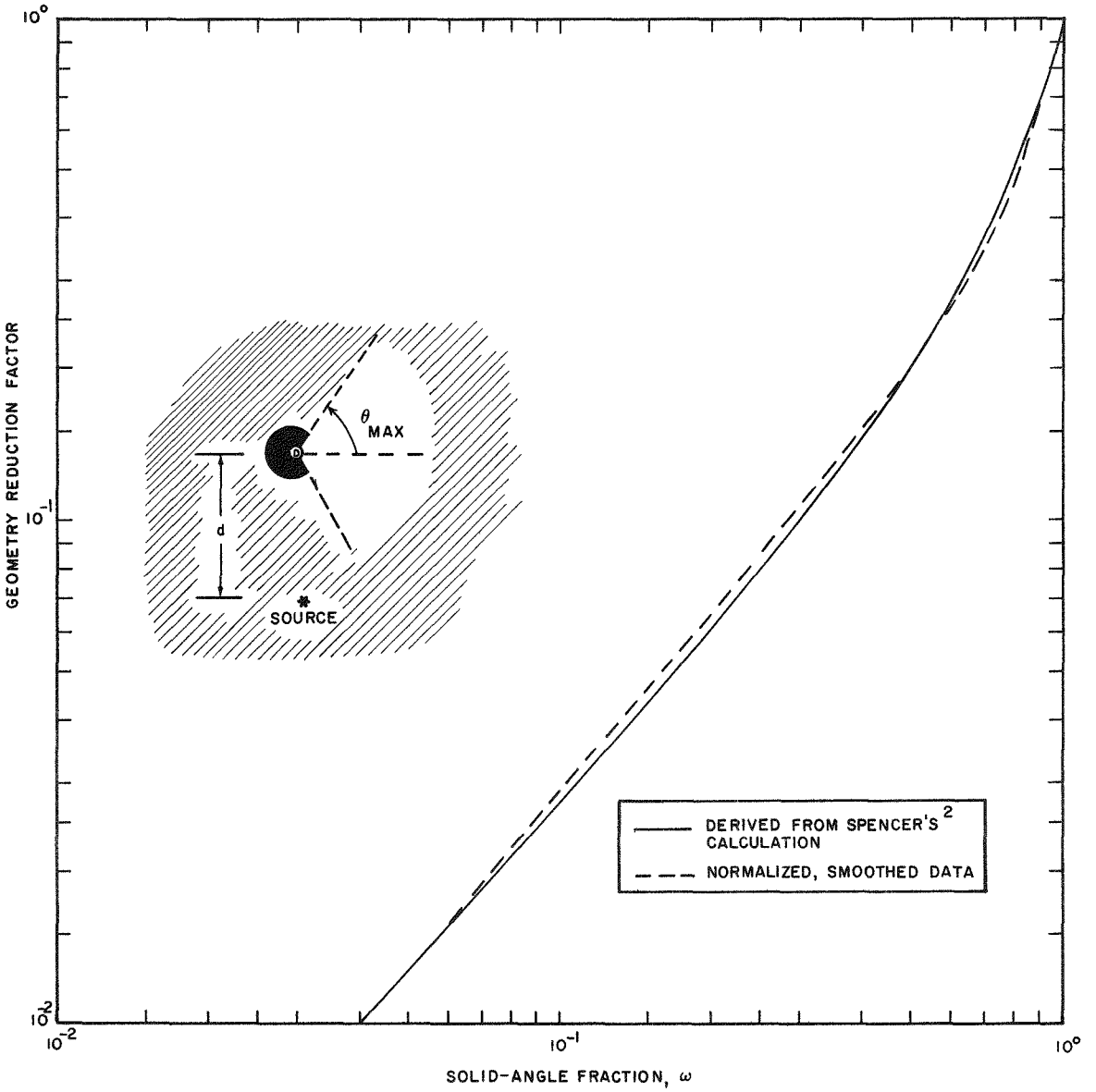

Fig. 4. 4 - Geometry factor describing the detector response to skyshine radiation of a conical detector pointed 90° from the source-to-detector line; source-detector distance in air, 100 ft; cobalt-60 isotropic point source.

interest, therefore, was the detector positions immediately behind the shield. Measurements were also made at other positions for informational purposes.

All data were normalized to the "no shield" dose rate and barrier-reduction factors were determined for each shield material and position. Vertical barrier reduction curves for steel and cobalt-60 are shown in Fig. 4.5. Figures 2.9, 2.10, and 2.11 should be referred to for location of detector positions. The lower curve of Fig. 4.5 is for detectors located immediately behind the shield. Less attenuation is provided at positions further in the bunker. This is understandable since a greater percentage of radiation arriving at these positions has penetrated the shield in a more nearly normal direction.

Figure 4.6 shows the barrier reduction factor curves for aluminum and cobalt-60. For comparison a curve for a vertical barrier exposed to the total radiation (direct plus skyshine) is included. This curve is from Spencer's Monograph[2] for cobalt-60 and is represented schematically in Case 2 in Fig. 2.2.

A comparison of attenuation provided by four different materials for the front position and for cobalt-60 is shown in Fig. 4.7. For this configuration, a steel shield is more efficient than concrete and aluminum, and these in turn are better than wood. This is as one would expect since a large part of the radiation reaching the detector is from low-energy photons. All data points are consistent among themselves, with the exception of the concrete data for 129 lb/sq ft. At this thickness the dose rate is very low and, therefore, errors are large for the instrumentation used.

A comparison of attenuation provided by the four different materials for the front position and for cesium-137 is shown in Fig. 4.8. The same trend is noted for the cesium-137 data as for the cobalt-60 data. Wood and aluminum material attenuation for both cobalt-60 and cesium-137 are presented in Fig. 4.9. The shields provide greater attenuation to skyshine originating from cesium-137 than from cobalt-60 except for very small mass thicknesses.

It must be understood that all vertical shield data have been presented relative to the "no shield" case for each of the two sources separately.

There are no theoretical calculations (known to the authors) directly applicable to the vertical shield configuration. For comparison, results of the concrete data are presented in Fig. 4.10 along with three other source-detector-shield configurations taken from Spencer's Monograph[2] for cobalt-60 contamination. Cases 1 and 2 have been verified by other experimenters.[7-10] Case

(Text continued on page 72)

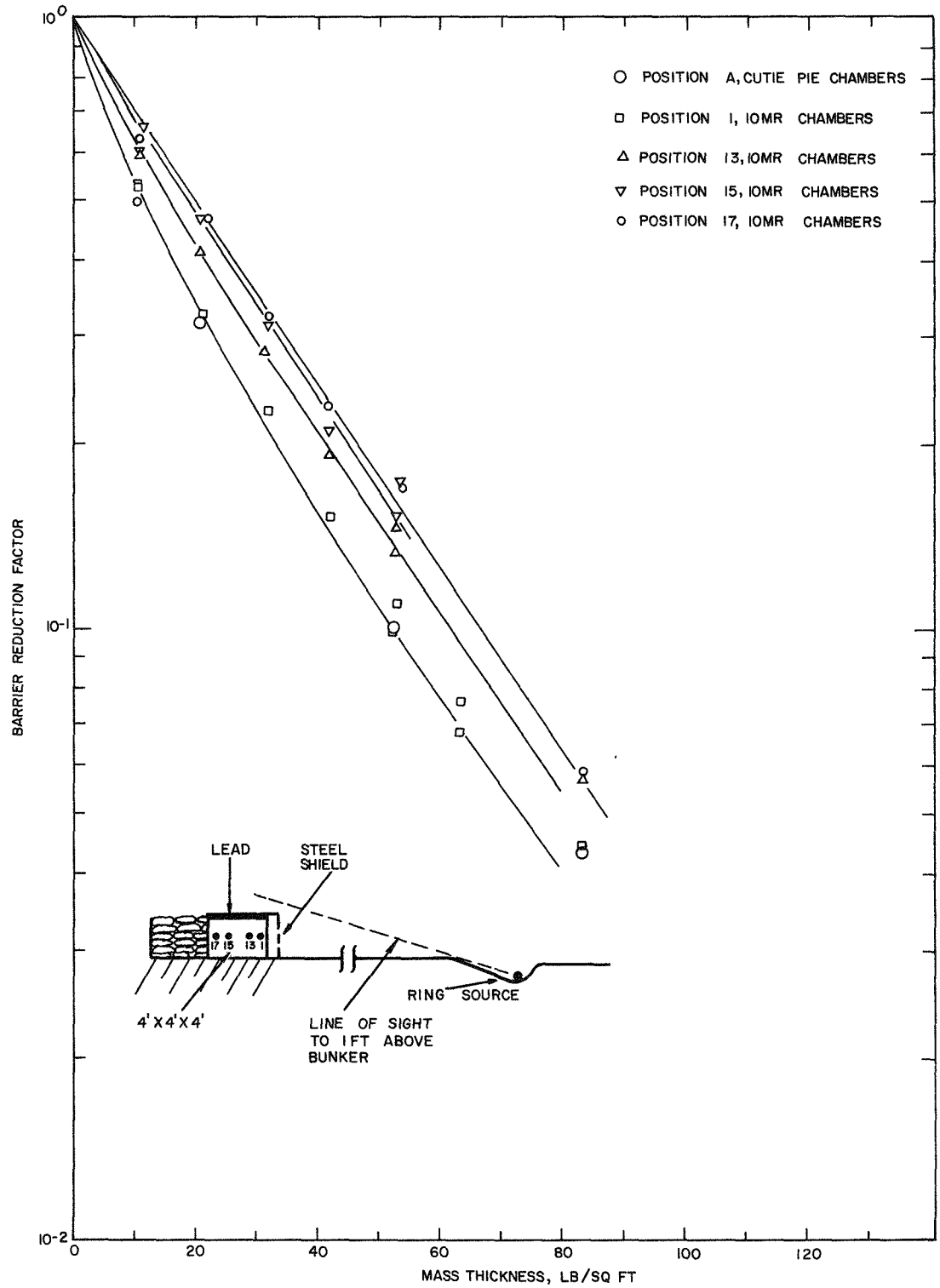

Fig. 4.5 - Vertical barrier reduction for steel from skyshine radiation orginating from a ring source of cobalt-60 at 100 ft.

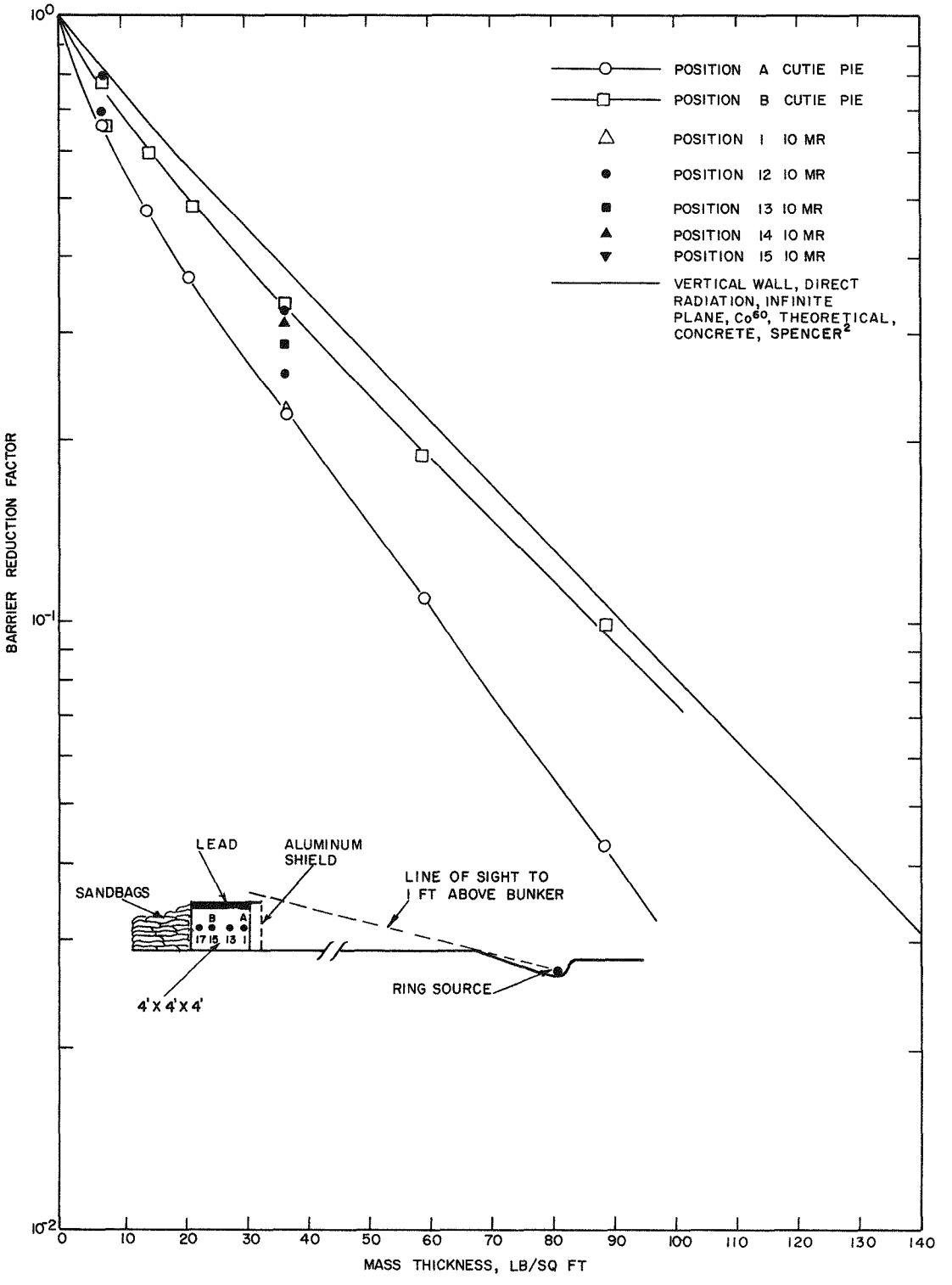

Fig. 4.6 - Vertical barrier reduction for aluminum from skyshine radiation originating from a ring source of cobalt-60 at a 100-ft radius.

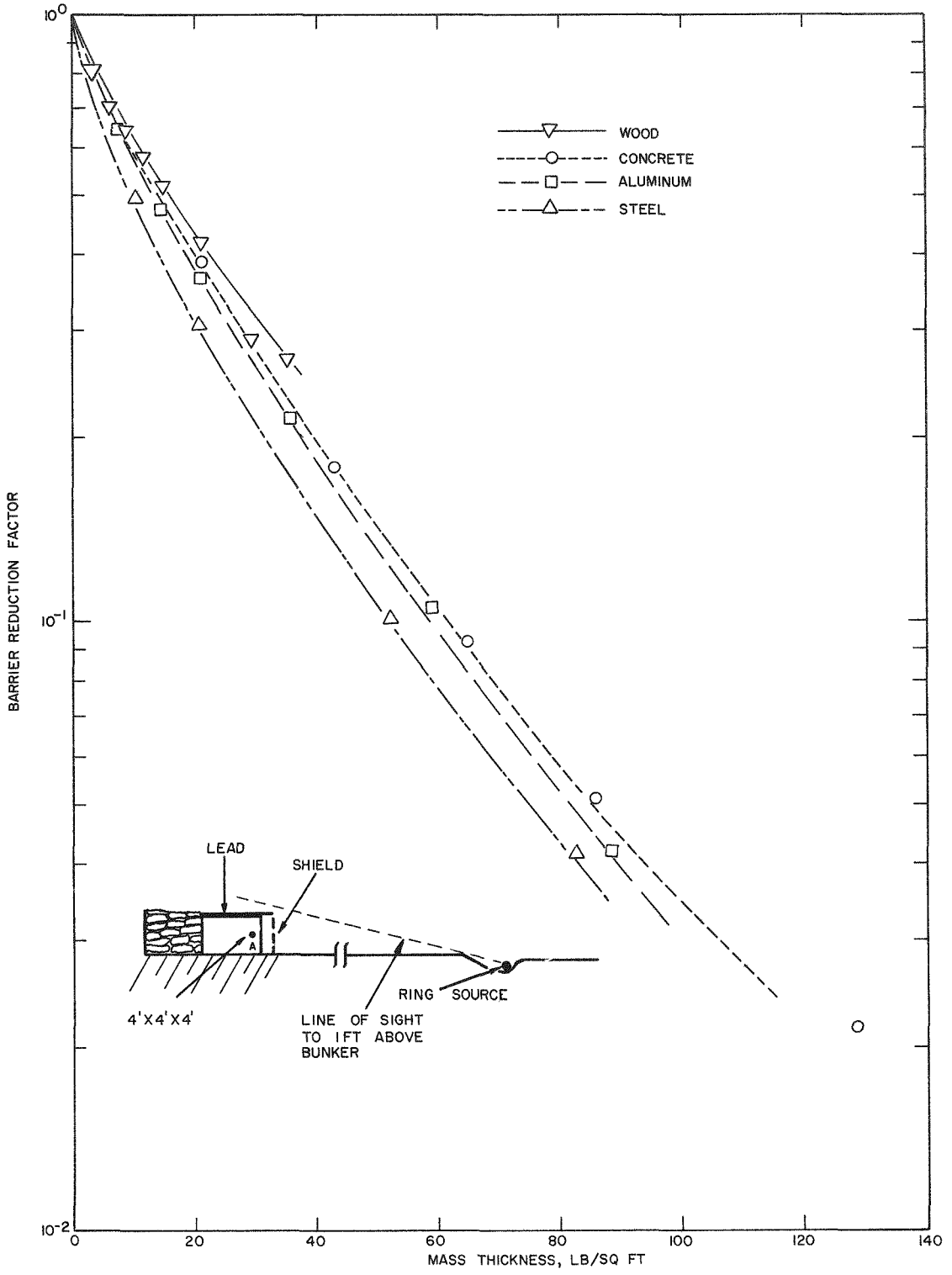

Fig. 4.7 - Vertical barrier reduction from skyshine radiation originating from a ring source of cobalt-60 at a 100-ft radius, Position A.

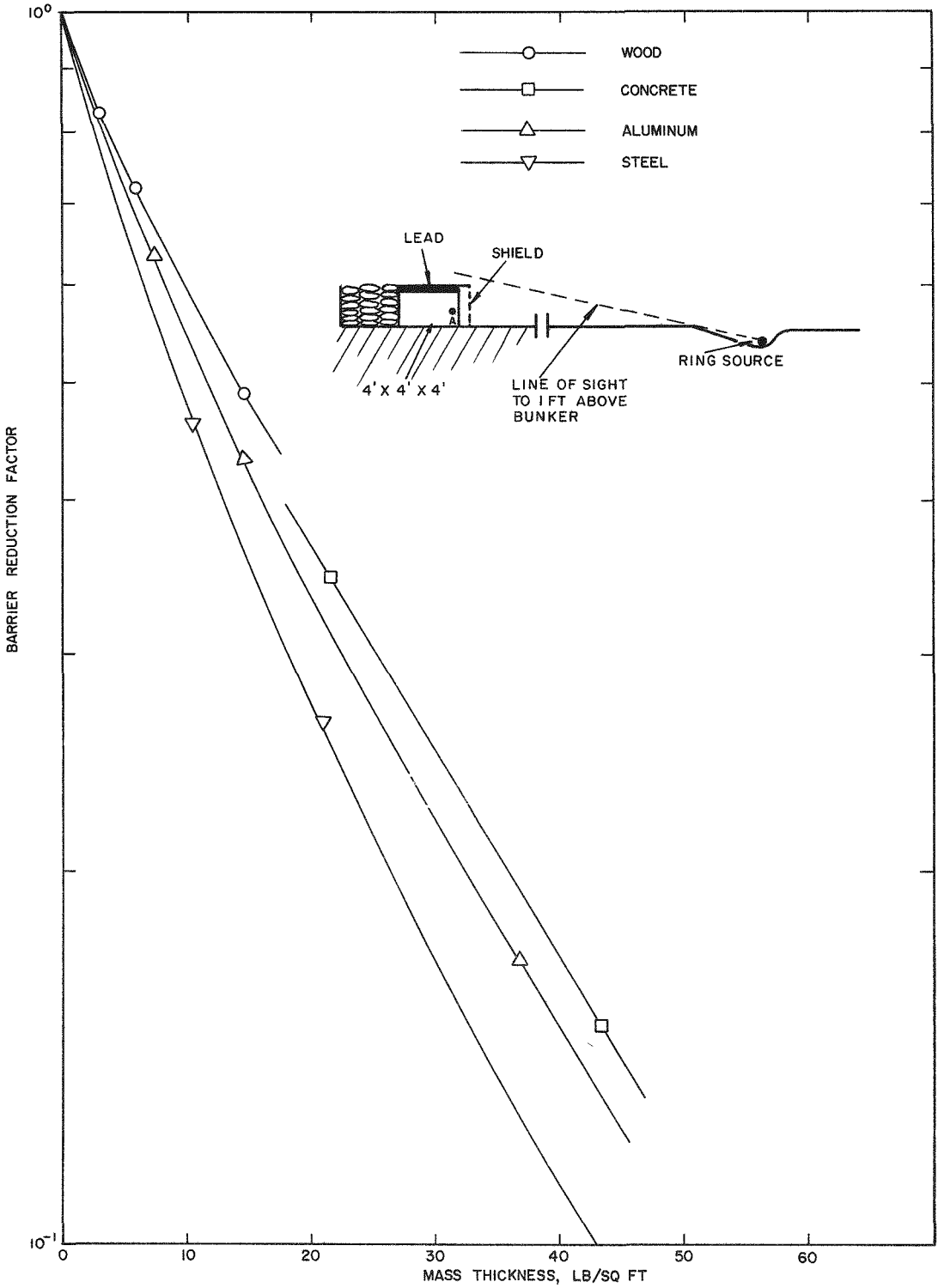

Fig. 4.8 - Vertical barrier reduction from skyshine radiation originating from a ring source of cesium-137 at a 100-ft radius, Position A.

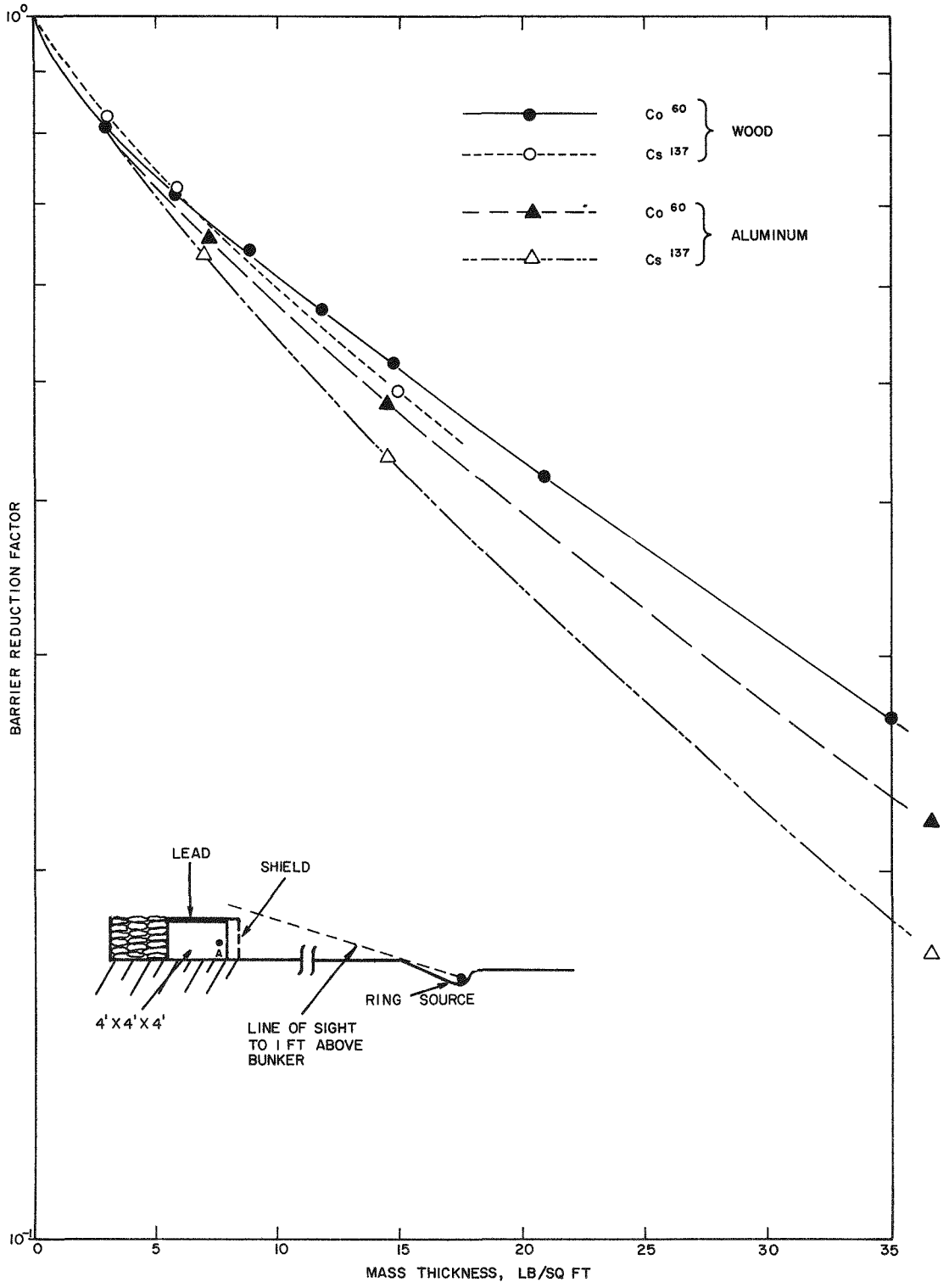

Fig. 4.9 - Vertical barrier reduction from skyshine radiation originating from a ring source of cobalt-60 or cesium-137 at a 100-ft radius, Position A.

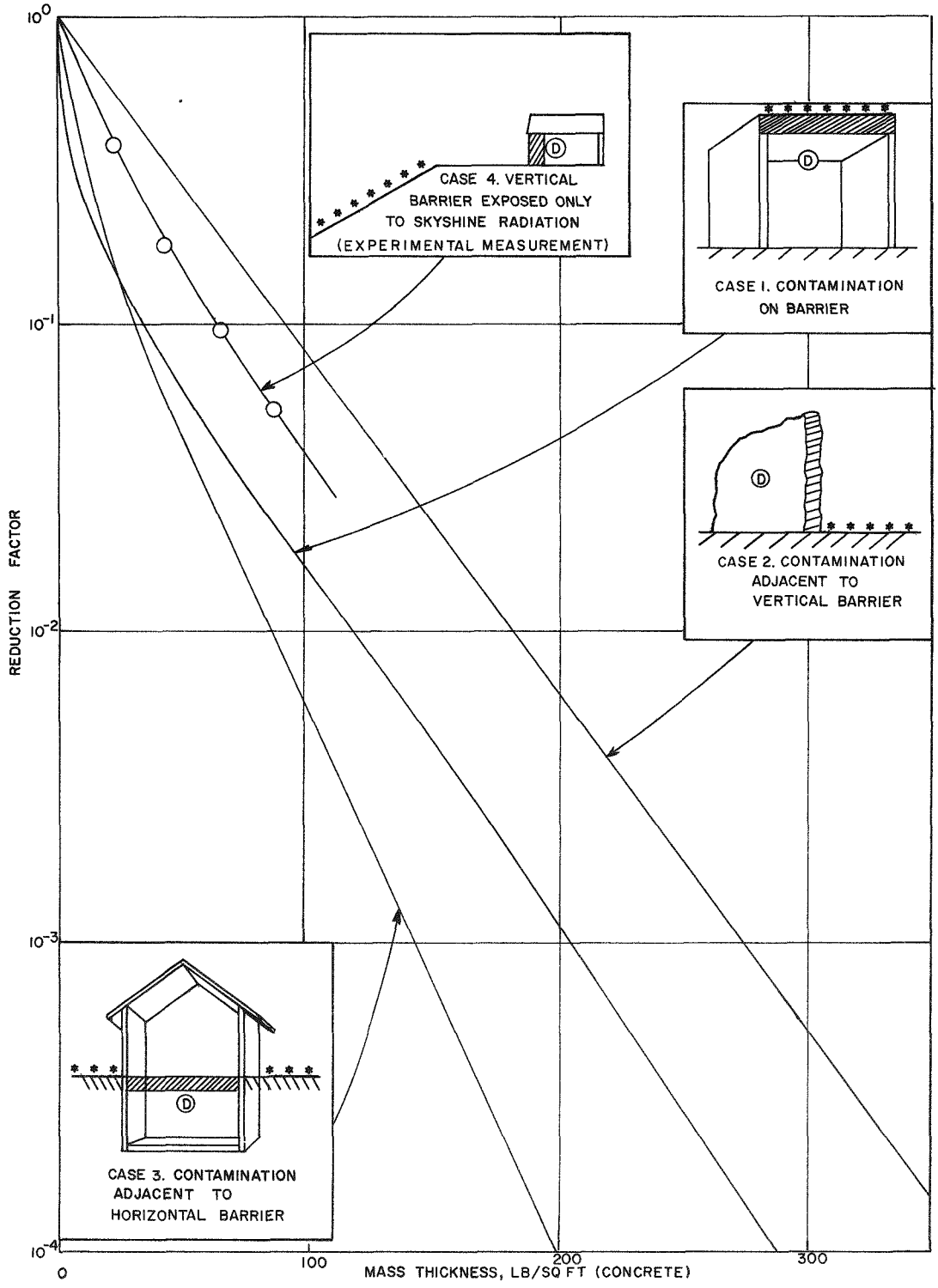

Fig. 4.10 - Barrier shielding effects for cobalt-60 contamination.

3 will be discussed in the next section. Case 4 is the result of the vertical barrier experiment for concrete.

4.3 HORIZONTAL BARRIERS

The point of primary interest in the horizontal barrier experiment was the top detector. Therefore, the time of exposure was such as to obtain maximum accuracy of readings for the top detectors. Since dose rates varied by a factor of 50 from top to bottom of the hole, three separate exposures were needed to get accurate enough readings at all positions. Even then, the lower-position detector readings were low and, therefore, less reliable than readings from the upper detectors. This is noticeable in the spread of data for the thin-shield cases (Figs. 3.5 and 3.6.)

Data in Figs. 3.5, 3.6 and 3.7 were smoothed and plotted as a function of solid-angle fraction (ω) for the various thicknesses. Extrapolations to a solid-angle fraction of one were then obtained for all the materials and thicknesses. Barrier, geometry, and barrier-and-geometry reduction factors were then obtained for various solid-angle fractions. These values are listed in Tables 4.3 through 4.10 and presented in graphical form in Figs. 4.11 through 4.19.

(Text continued on page 75)

TABLE 4.3. SMOOTHED DATA SHOWING BARRIER REDUCTION PROVIDED BY HORIZONTAL WOOD SLABS AGAINST SKYSHINE RADIATION, COBALT-60 SOURCE AT 100 FT

ω	Mass thickness, lb/sq ft						
	0	0.75	1.5	3.0	6.0	15.0	30.0
	Barrier Reduction factor						
1.0	1.0	0.69	0.49	0.43	0.33	0.25	0.15
0.9	1.0	0.71	0.58	0.51	0.42	0.32	0.19
0.8	1.0	0.75	0.66	0.59	0.51	0.39	0.23
0.7	1.0	0.78	0.71	0.64	0.58	0.44	0.27
0.5	1.0	0.81	0.75	0.70	0.64	0.51	0.31
0.25	1.0	0.82	0.74	0.69	0.65	0.54	0.34
0.15	1.0	0.89	0.78	0.73	0.68	0.57	0.38
0.10	1.0	0.91	0.82	0.74	0.68	0.59	0.40
0.060	1.0	0.96	0.87	0.80	0.72	0.63	0.44

TABLE 4.4. SMOOTHED DATA SHOWING BARRIER AND GEOMETRY REDUCTION PROVIDED BY HORIZONTAL WOOD SLABS AGAINST SKYSHINE RADIATION, COBALT-60 SOURCE AT 100 FT

ω	Mass thickness, lb/sq ft						
	0	0.75	0.5	3.0	6.0	15.0	30.0
	Barrier-geometry reduction factor						
1.0	1.0	0.69	0.49	0.43	0.33	0.25	0.15
0.9	0.67	0.47	0.39	0.34	0.28	0.21	0.13
0.8	0.47	0.35	0.31	0.28	0.24	0.18	0.11
0.7	0.35	0.27	0.25	0.22	0.20	0.15	0.093
0.5	0.20	0.16	0.15	0.14	0.13	0.10	0.063
0.25	0.087	0.071	0.064	0.060	0.057	0.047	0.030
0.15	0.047	0.041	0.036	0.034	0.032	0.027	0.018
0.10	0.029	0.027	0.024	0.022	0.020	0.017	0.012
0.060	0.016	0.015	0.014	0.013	0.012	0.010	0.0070

TABLE 4.5. SMOOTHED DATA SHOWING BARRIER REDUCTION PROVIDED BY HORIZONTAL ALUMINUM SLABS AGAINST SKYSHINE RADIATION, COBALT-60 SOURCE AT 100 FT

ω	Mass thickness, lb/sq ft			
	0	7.5	37.5	75
	Barrier reduction factor			
1.0	1.0	0.30	0.061	0.0099
0.9	1.0	0.38	0.086	0.014
0.8	1.0	0.47	0.11	0.020
0.7	1.0	0.54	0.14	0.025
0.50	1.0	0.65	0.19	0.038
0.25	1.0	0.71	0.24	0.056
0.15	1.0	0.79	0.27	0.068
0.10	1.0	0.83	0.28	0.074
0.060	1.0	0.91	0.30	0.081

TABLE 4.6. SMOOTHED DATA SHOWING BARRIER AND GEOMETRY REDUCTION PROVIDED BY HORIZONTAL ALUMINUM SLABS AGAINST SKYSHINE RADIATION, COBALT-60 SOURCE AT 100 FT

ω	Mass thickness, lb. sq ft			
	0	7.5	37.5	75
	Barrier-geometry reduction factor			
1.0	1.0	0.30	0.061	0.0099
0.9	0.67	0.25	0.057	0.0096
0.8	0.47	0.22	0.053	0.0093
0.7	0.35	0.19	0.049	0.0088
0.5	0.20	0.13	0.038	0.0076
0.25	0.087	0.061	0.021	0.0049
0.05	0.047	0.037	0.013	0.0032
0.10	0.029	0.024	0.0083	0.0022
0.060	0.016	0.015	0.0048	0.0013

TABLE 4.7. SMOOTHED DATA SHOWING BARRIER REDUCTION PROVIDED BY HORIZONTAL STEEL SLABS AGAINST SKYSHINE RADIATION, COBALT-60 SOURCE AT 100 FT

ω	Mass thickness, lb/sq ft				
	0	10.5	21.0	52.5	105
	Barrier reduction factor				
1.0	1.0	0.18	0.11	0.027	0.0033
0.9	1.0	0.26	0.15	0.040	0.0046
0.5	1.0	0.51	0.34	0.10	0.012
0.25	1.0	0.59	0.42	0.13	0.016
0.15	1.0	0.63	0.46	0.14	0.018
0.10	1.0	0.65	0.46	0.15	0.019
0.060	1.0	0.68	0.47	0.15	0.020

TABLE 4.8. SMOOTHED DATA SHOWING BARRIER AND GEOMETRY REDUCTION PROVIDED BY HORIZONTAL STEEL SLABS AGAINST SKYSHINE RADIATION, COBALT-60 SOURCE AT 100 FT

ω	Mass thickness, lb/sq ft				
	0	10.5	21.0	52.5	105
	Barrier-geometry reduction factor				
1.0	1.0	0.18	0.11	0.027	0.0033
0.9	0.67	0.17	0.10	0.026	0.0031
0.5	0.20	0.10	0.068	0.020	0.0023
0.25	0.087	0.051	0.036	0.011	0.0014
0.15	0.047	0.029	0.021	0.0067	0.00084
0.10	0.029	0.019	0.013	0.0043	0.00055
0.060	0.016	0.011	0.0075	0.0024	0.00031

TABLE 4.9. SMOOTHED DATA SHOWING BARRIER REDUCTION PROVIDED BY HORIZONTAL CONCRETE SLABS AGAINST SKYSHINE RADIATION, COBALT-60 SOURCE AT 100 FT

ω	Mass thickness, lb/sq ft		
	0	22	44
	Barrier reduction factor		
1.0	1.0	0.11	0.036
0.15	1.0	0.57	0.21
0.060	1.0	0.81	0.28

TABLE 4.10. SMOOTHED DATA SHOWING BARRIER AND GEOMETRY REDUCTION PROVIDED BY HORIZONTAL CONCRETE SLABS AGAINST SKYSHINE RADIATION, COBALT-60 SOURCE AT 100 FT

ω	Mass thickness, lb/sq ft		
	0	22	44
	Barrier-geometry reduction factor		
1.0	1.0	0.11	0.036
0.15	0.047	0.027	0.010
0.060	0.016	0.013	0.0045

In this source-shield-detector configuration, a small amount of shielding material provides a large amount of protection for positions near the shield. This is strongly emphasized in the wood data (Fig. 4.11) where thin sheets of plywood were used. One inch of wood reduced the dose rate a factor of 3. This is not surprising,

(Text continued on page 85)

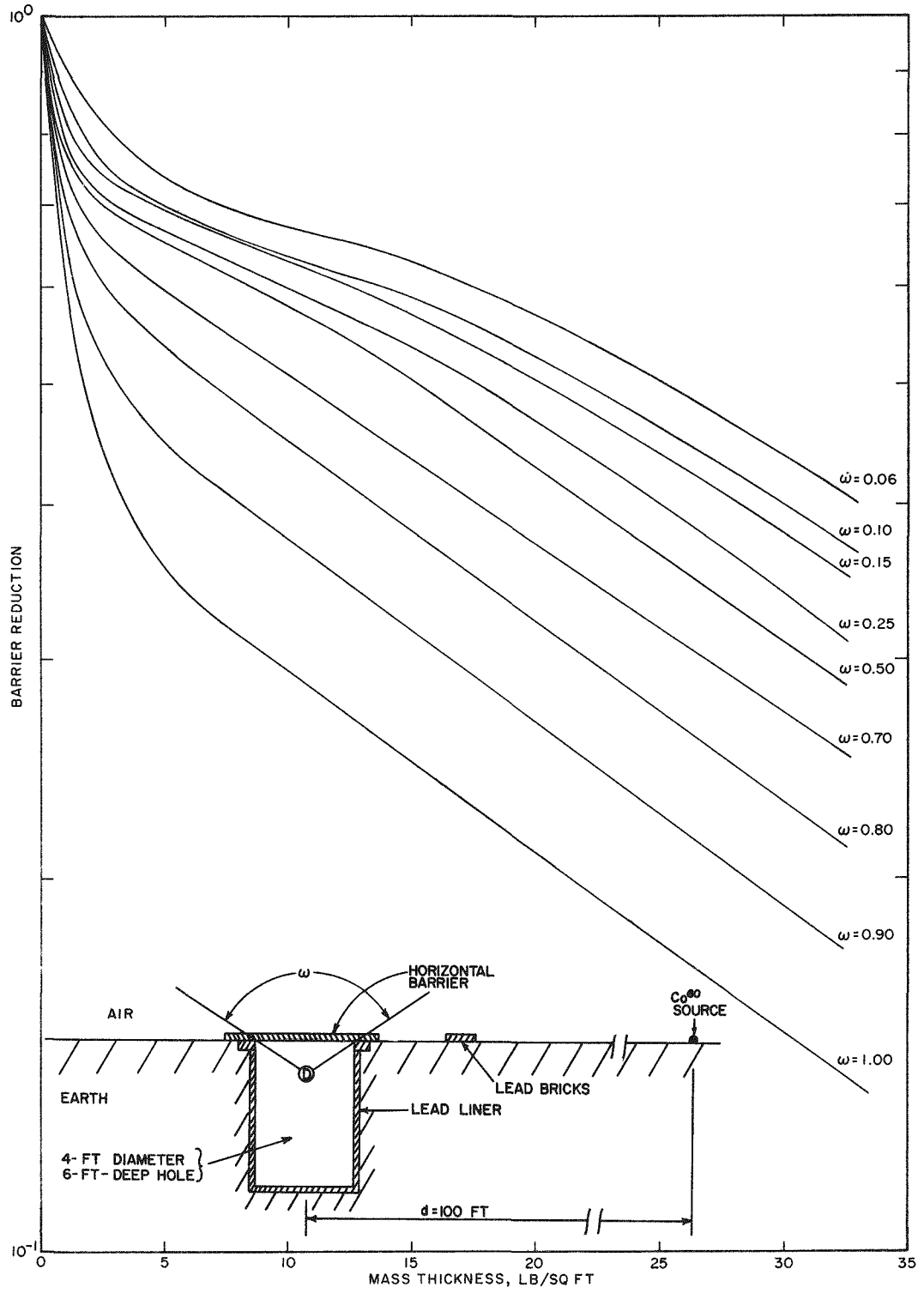

Fig. 4.11 - Smoothed data showing barrier reduction provided by horizontal wood slabs against skyshine radiation from cobalt-60.

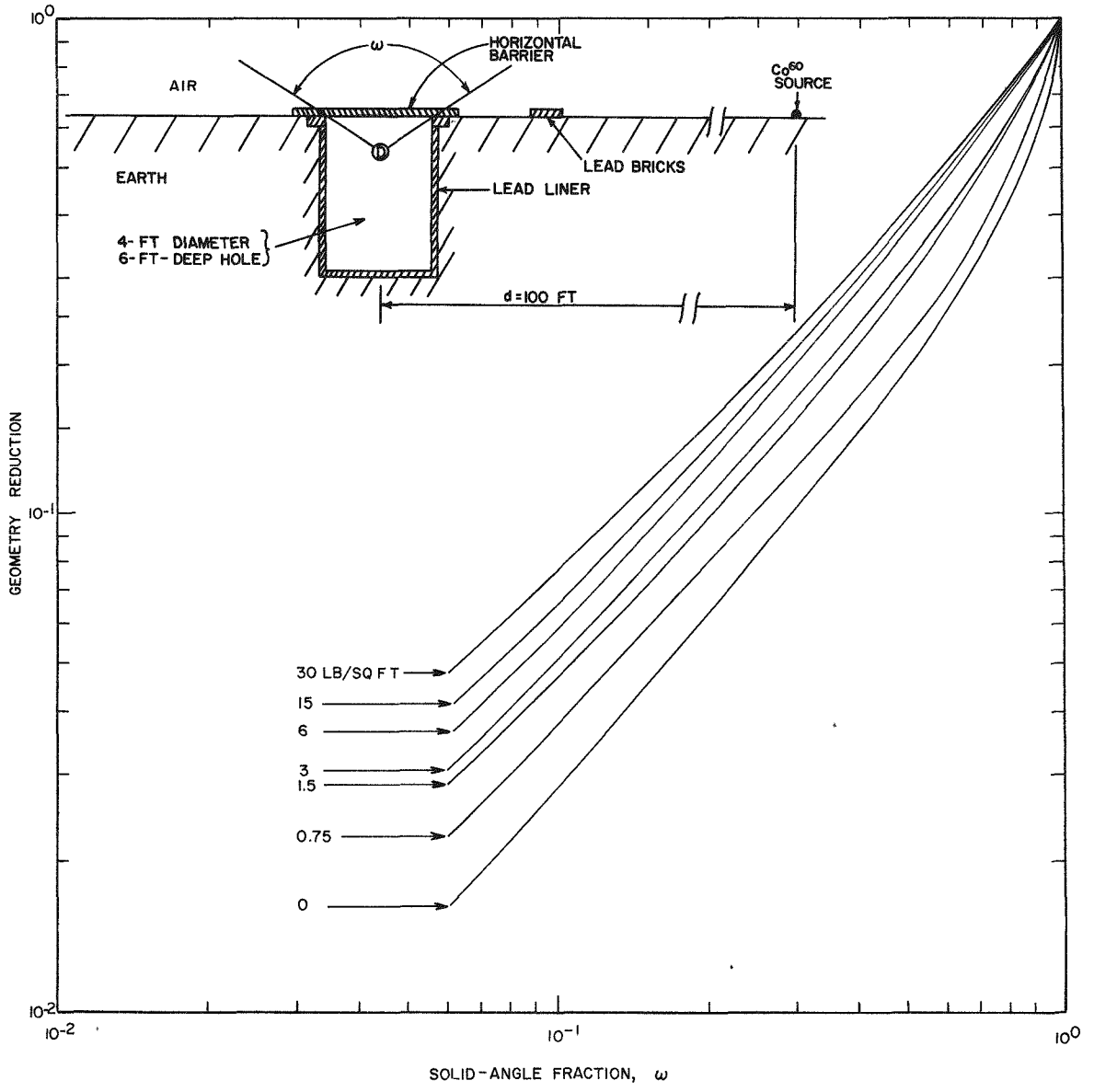

Fig. 4.12 - Smoothed data showing geometry reduction of skyshine radiation from cobalt-60 provided by a round hole covered with horizontal wood slabs.

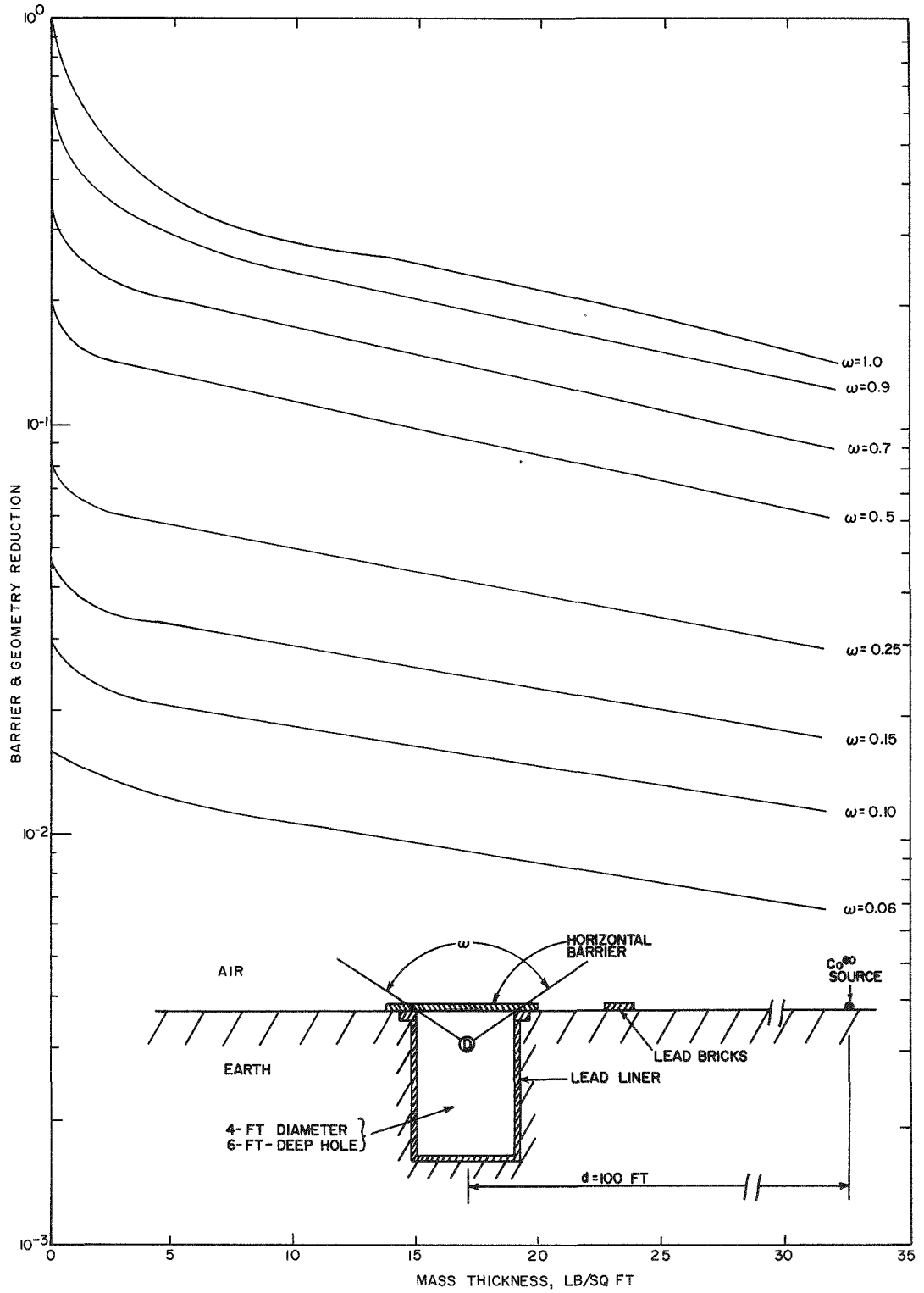

Fig. 4.13 - Smoothed data showing barrier-and-geometry reduction provided by horizontal wood slabs against skyshine radiation from cobalt-60.

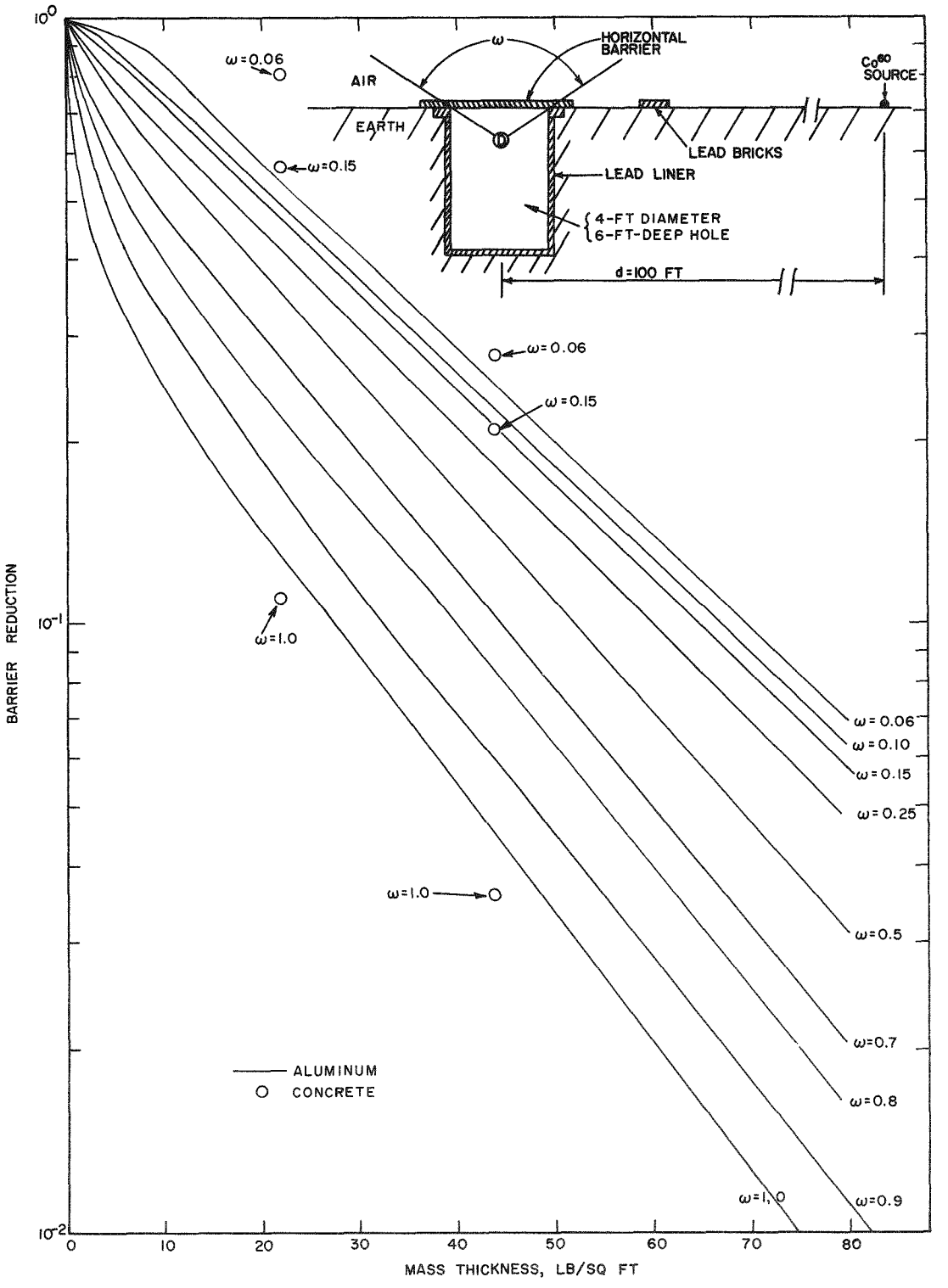

Fig. 4.14 - Smoothed data showing barrier reduction provided by horizontal aluminum and concrete slabs against skyshine radiation from cobalt-60.

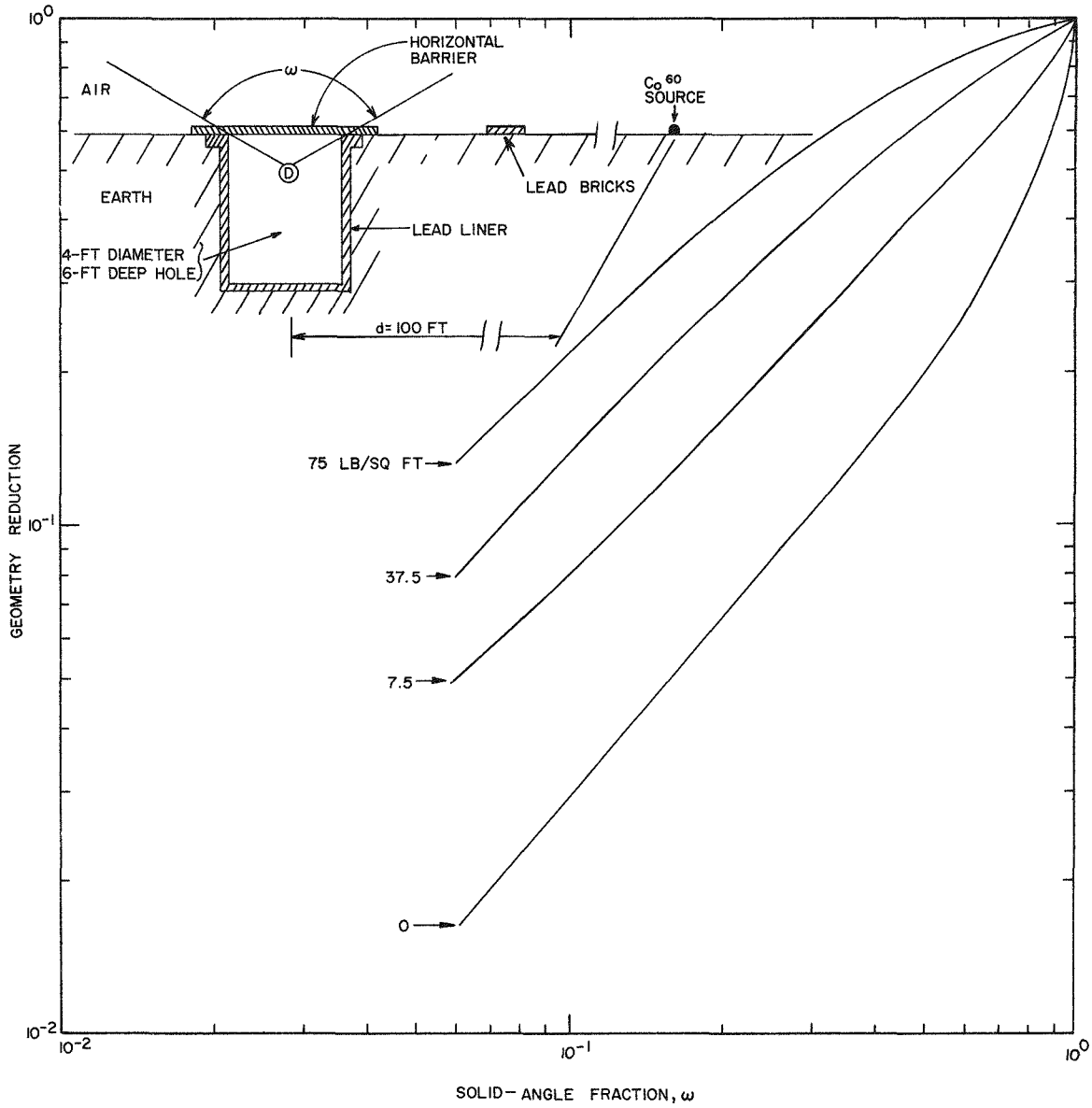

Fig. 4.15 - Smoothed data showing geometry reduction of skyshine radiation from cobalt-60 provided by a round hole covered with horizontal aluminum slabs.

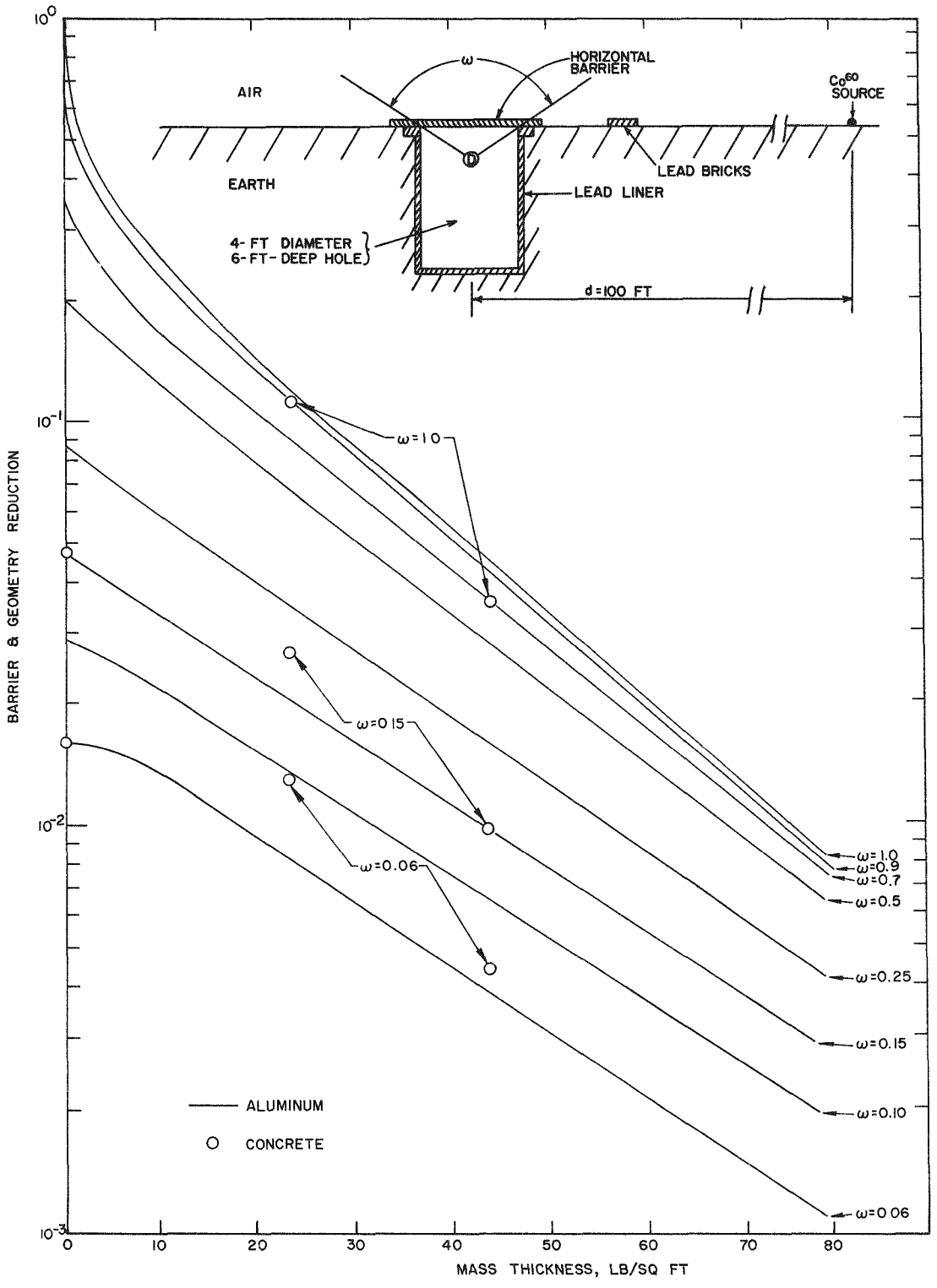

Fig. 4.16 - Smoothed data showing barrier-and-geometry reduction provided by horizontal aluminum and concrete slabs against skyshine radiation from cobalt-60.

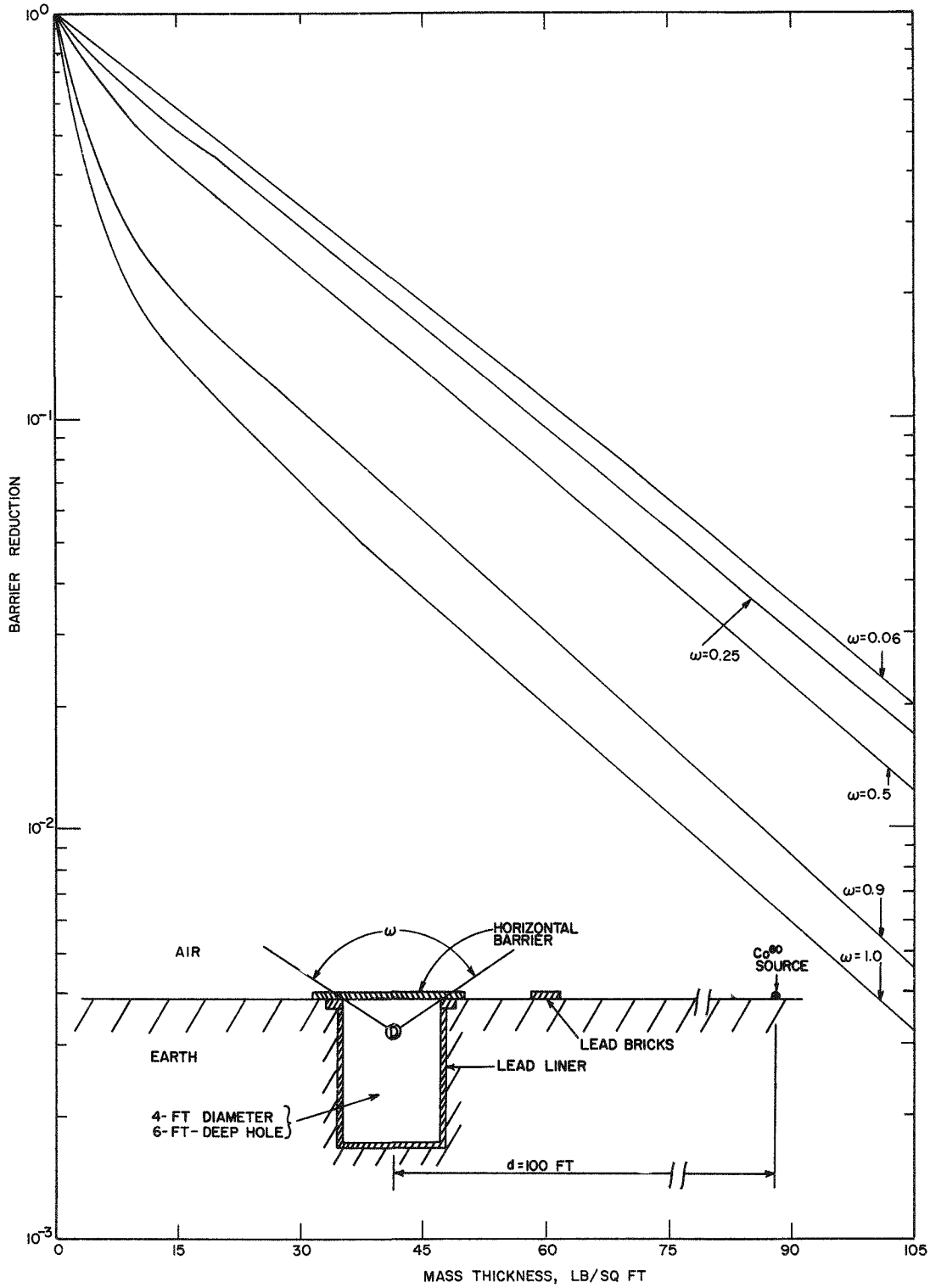

Fig. 4.17 - Smoothed data showing barrier reduction provided by horizontal steel slabs against skyshine radiation from cobalt-60.

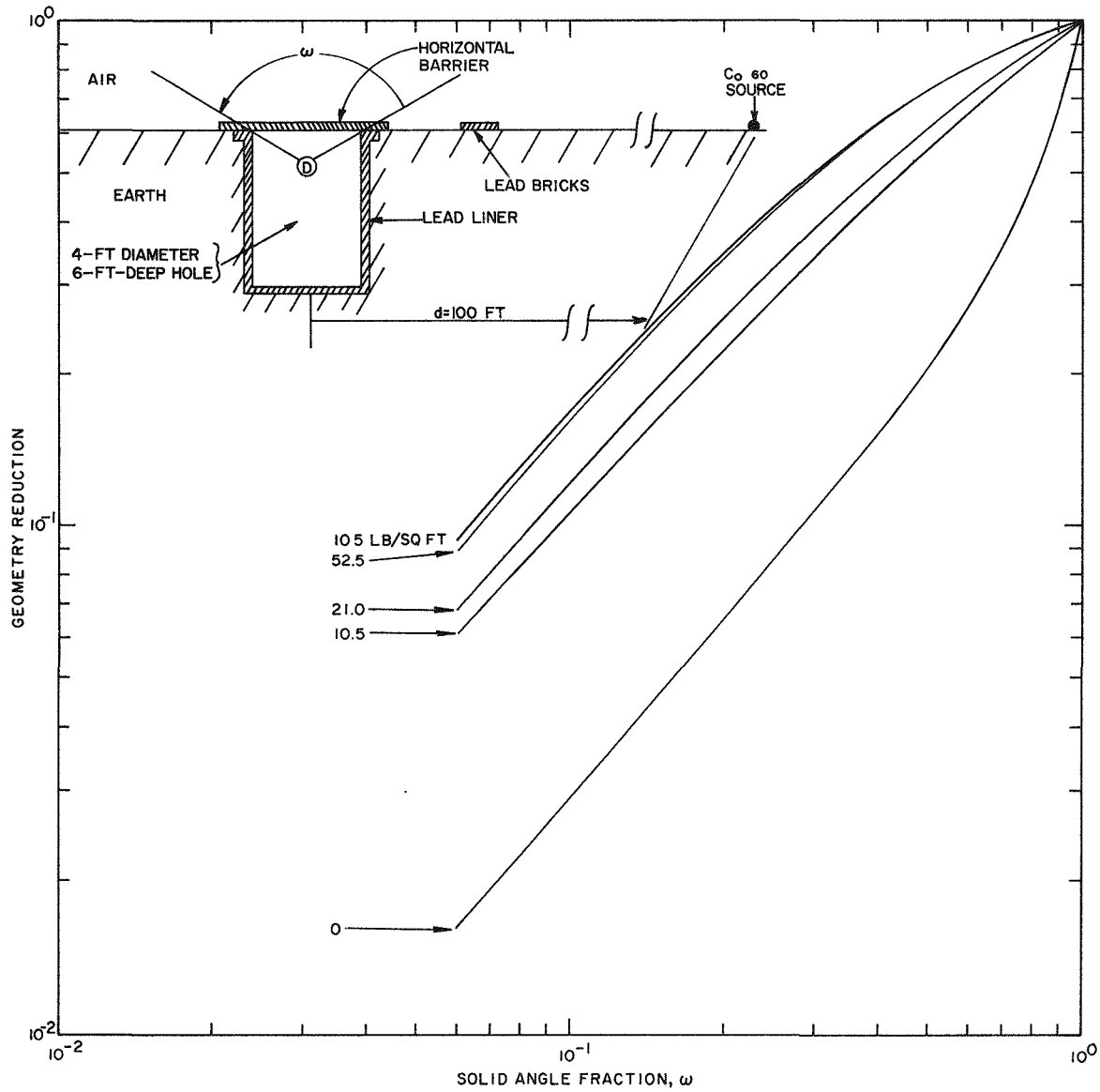

Fig. 4.18 - Smoothed data showing geometry reduction of skyshine radiation from cobalt-60 provided by a round hole covered with horizontal steel slabs.

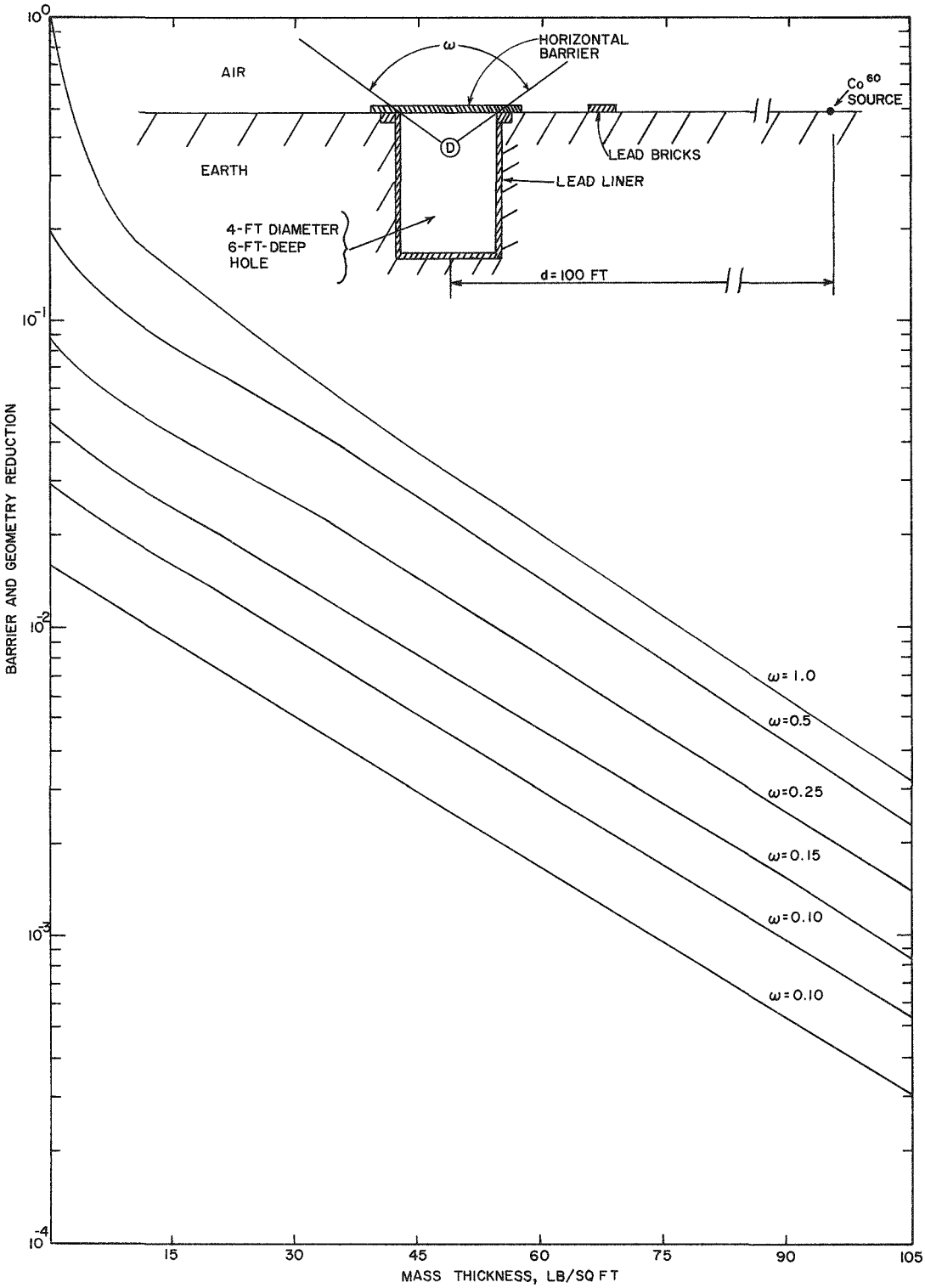

Fig. 4.19 - Smoothed data showing barrier-and-geometry reduction provided by horizontal steel slabs against skyshine radiation from cobalt-60.

however, because of the strong low-angle scatter component. This component must penetrate a large slant thickness to reach the detector.

Much less attenuation (barrier reduction only) is provided for the detector near the bottom of the hole. Presumably a portion of the strong low-angle skyshine component incident on top of the slab is scattered by the slab. This extra secondary, scattered radiation is more isotropic, thereby providing more radiation to the detectors. This was also noted by Clifford[11] in using cesium-137. This extra component is more noticeable for small thicknesses. Material attenuation appears to be logarithmic beyond about 30 lb/sq ft for all positions and materials.

It is interesting to note in the geometry reduction curves that for thin materials the dose rate decreases very rapidly with decrease in solid angle of view. At about 10 to 30 lb/sq ft the dose rate is proportional to the solid angle and at large thicknesses it decreases slowly with decrease in solid angle.

The geometry reduction factor curves in Figs. 4.12, 4.15, and 4.18 are quite similar in shape to those of a more common shield geometry. Figure 4.20 shows this case taken directly from Spencer's Monograph 42.

Even the values are quite similar. This is not surprising when one examines the similarity of the angular distribution of the radiations incident on the shield material in the two cases. The geometry factors are shown in Fig. 4.21 for comparison. The fourth case is for the "poor" geometry case at the ring source bunker arrangement (Fig. 2.7).

For horizontal shields in these instances, the angular distribution appears to have a stronger influence on the barrier or geometry reduction than does either the energy spectrum or the shield material.

Barrier reduction for all shield materials are compared for a solid-angle fraction value of 1.0 in Fig. 4.22. Very little difference is noted between shield materials. The wood data at 30 lb/sq ft is probably too high for all positions because of the small overlap of the slabs at the edge of the hole (see Fig. 2.12). Most data points are below the theoretical curve for an infinite plane. As noted in Figs. 2.3 and 4.21, the geometry reduction for a point source at 100 ft is sharper than that for an infinite plane. One would then expect greater attenuation for this shield geometry. It is also noted that the geometry reduction for the ring-source bunker arrangement more nearly approximates that from an infinite plane for large solid angles. Data points for this case are in excellent agreement with calculations.

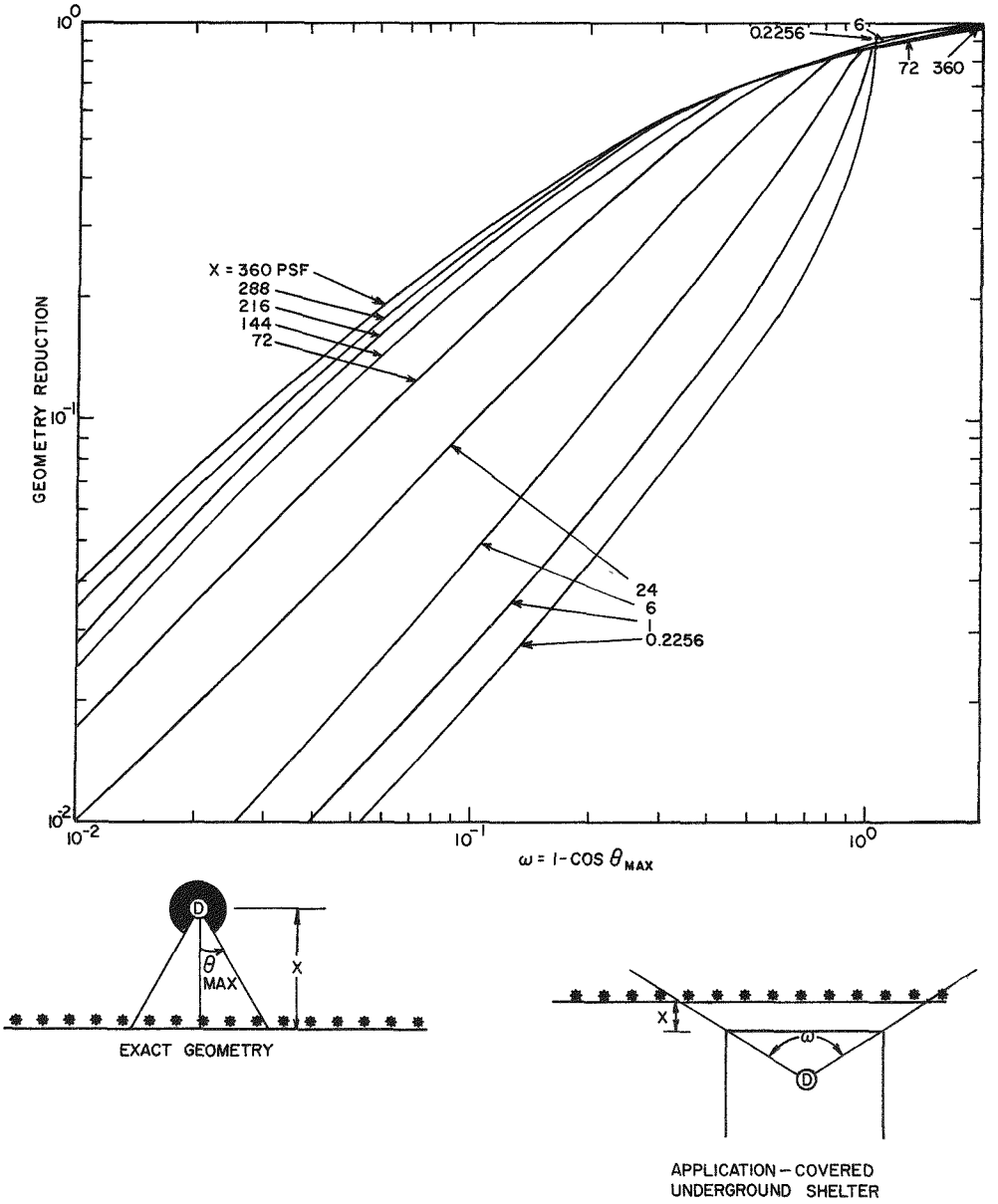

Fig. 4.20 - Geometry factor for detector response to radiation striking the detector from a limited cone of directions, cobalt-60, concrete.

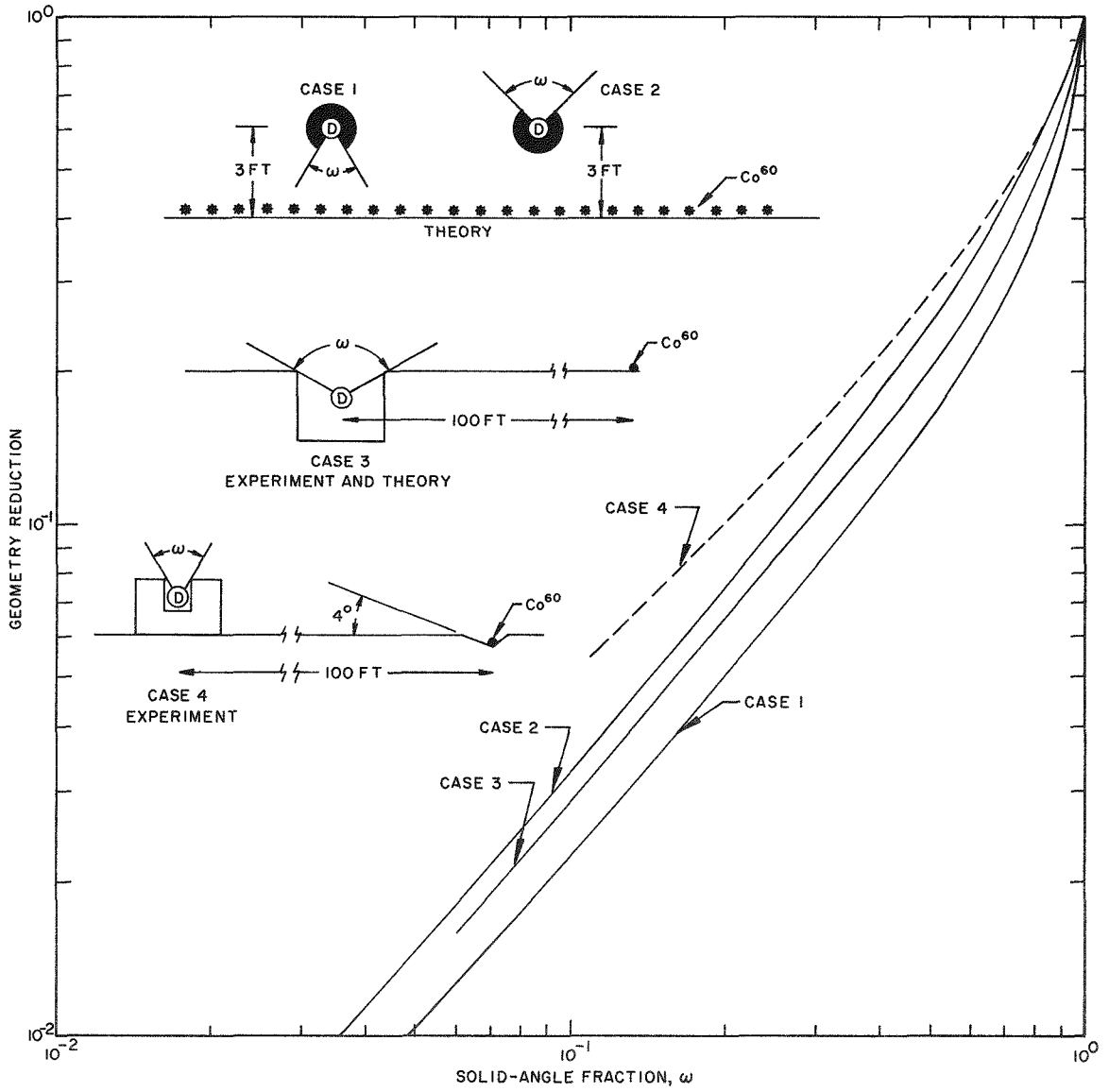

Fig. 4.21 - Geometry reduction for various source-detector configurations.

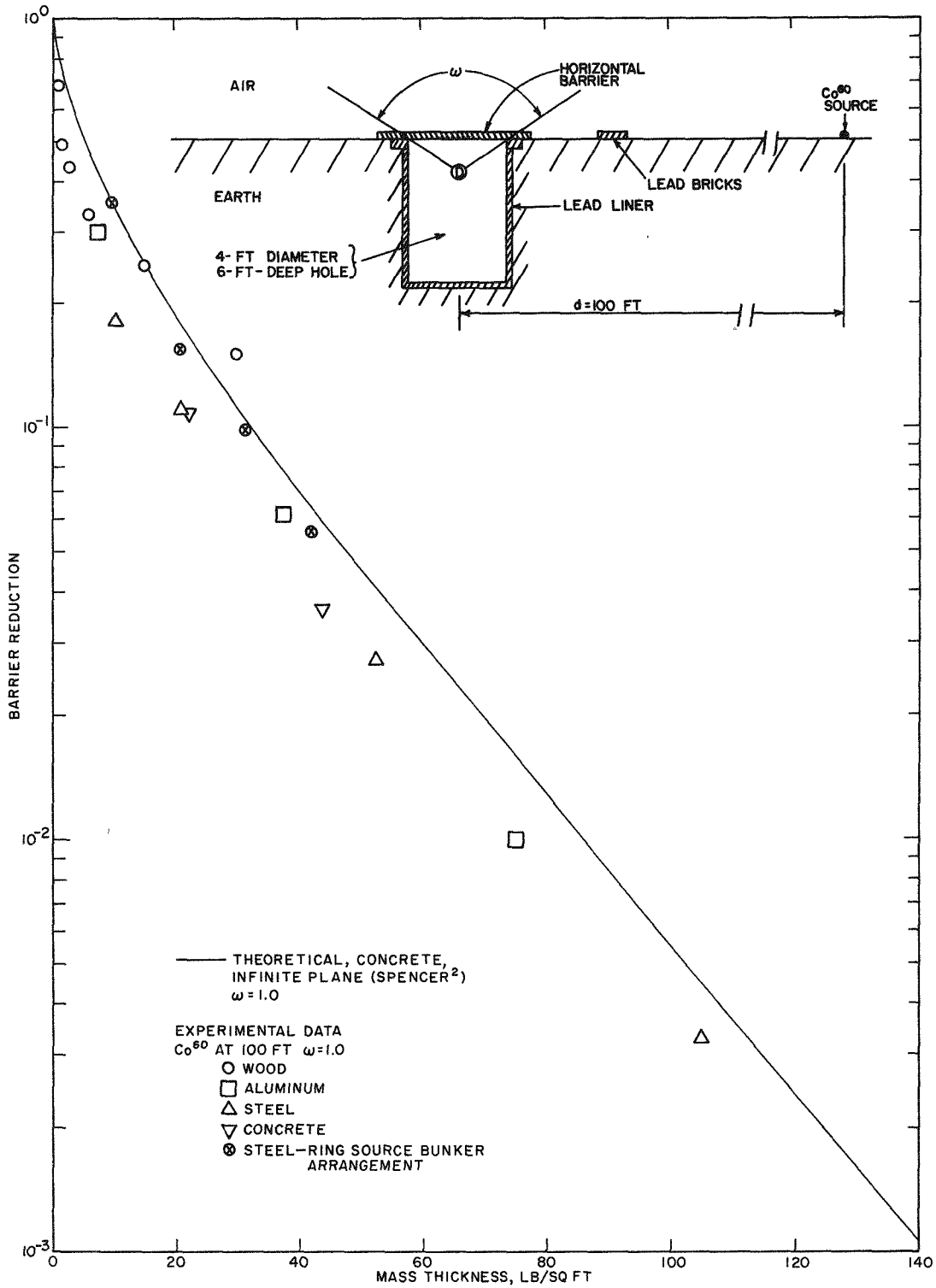

Fig. 4.22 - Barrier reduction provided by a horizontal shield against skyshine radiation originating from cobalt-60.

Data points for solid-angle fraction values of 0.5, 0.15, and 0.06 are shown in Fig. 4.23 for all shield materials. Some difference in materials is noted for small thicknesses and for small solid angles.

REFERENCES

1. M. J. Berger, Calculation of Energy Dissipation by Gamma Radiation near the Interface between Two Media, Journal of Applied Physics, Vol. 28. No. 12, 1502-1508, December, 1957.
2. L. V. Spencer, Structure Shielding Against Fallout Radiation from Nuclear Weapons; NBS Monograph 42 (National Bureau of Standards, Washington 25, D. C.) June 1, 1962.
3. Measurements by the Armed Forces Radiobiology Research Institute (AFRRI) to be reported in Report CEX 63.8, Mr. C. Garrett.
4. A. W. Starbird and J. F. Batter, Angular Distribution of Skyshine Radiation at the Surface of a Plane of Fallout Contamination; Report No. TO-B 63-40 (Technical Operations Research, Burlington, Mass.) March, 1964.
5. R. L. French (RRA) and C. W. Garrett (AFRRI); Gamma-Ray Energy and Angular Distributions near the Air/Ground Interface from Plane Fallout and Point Cobalt-60 Sources, Report RRA-M42 (Radiation Research Associates, Inc., Fort Worth, Texas) June, 1964.
6. C. E. Clifford, et al, Scattered Radiation from a Simulated Fallout Field Using Cesium-137, DRCL-296 (Defence Research Chemical Laboratories, Ottawa, Canada) January, 1959.
7. Frank Titus, Penetration in Concrete of Gamma Radiation from Fallout; NBS-6143, September, 1958.
8. M. A. Schmoke and R. E. Rexroad, Attenuation of Simulated Fallout Radiation by the Roof of a Concrete Blockhouse; NDL-TR-6, August, 1961.
9. G. E. Plummer, A Study of Geometry and Barrier Attenuation Generated by a Vertical Slab Exposed to a Plane Cobalt-60 Source; Trans. Am. Nucl. Soc. 5, 222.
10. J. Jones and J. Batter, Experimental Determination of the Wall-Scattered Radiation Function $G_s(\omega)$. TO-B 63-88.
11. C. E. Clifford, Absorption of Cesium-137 Skyshine Radiation by Concrete Slabs, TN No. 62-7 (Defence Research Chemical Laboratories, Ottawa, Canada) May 1962.

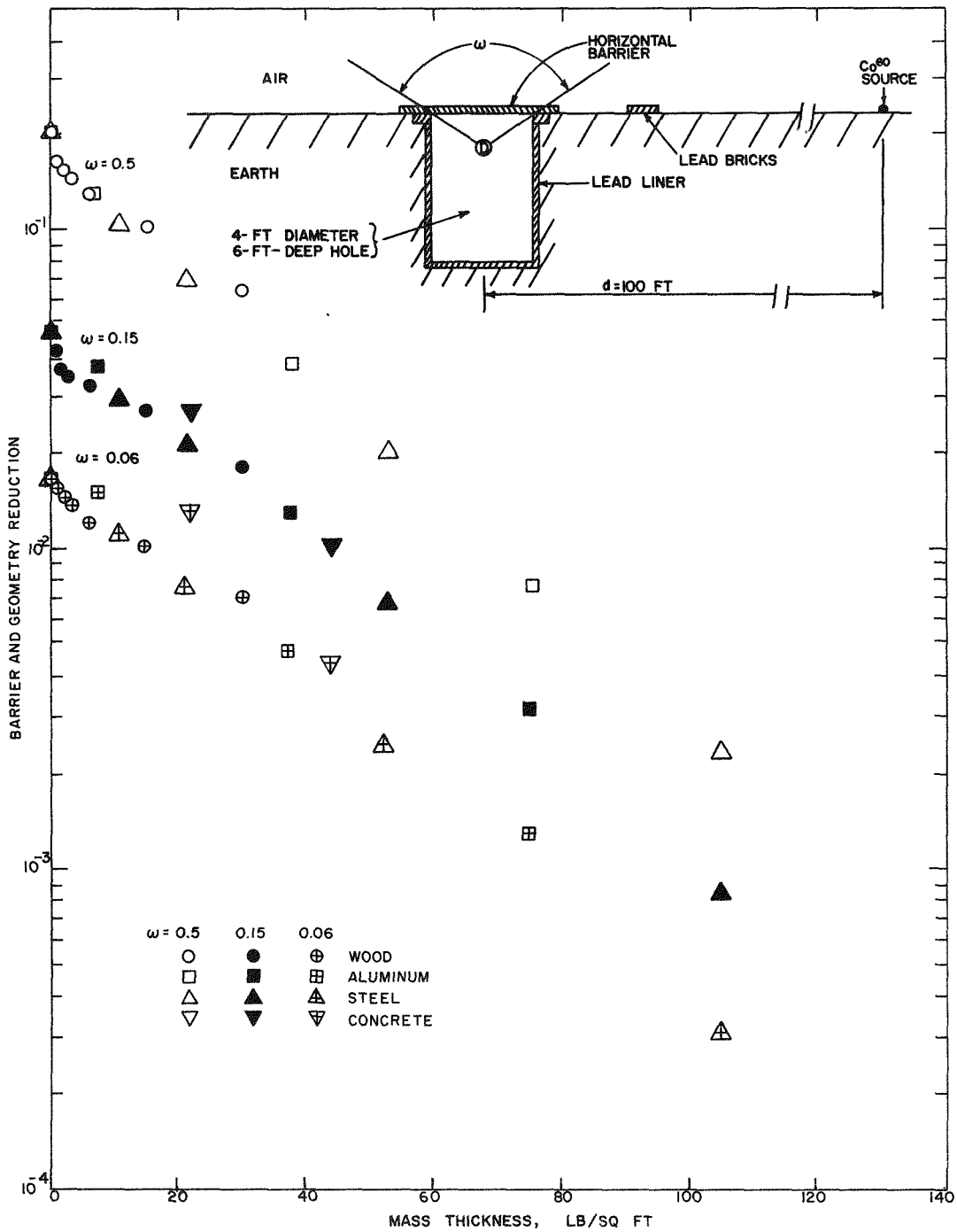

Fig. 4.23 - Barrier-and-geometry reduction provided by a horizontal shield against skyshine radiation originating from cobalt-60.

Chapter 5
SUMMARY AND CONCLUSIONS

Calculations assuming a uniform infinite medium must be corrected for the air-ground interface to predict the dose rate in an open hole from sources on the ground. These correction factors were found experimentally to vary from 1.5 to 0.7 for source-to-detector distances in air from 53 to 1325 ft respectively for cobalt-60 on smooth, dry ground.

Experimental data in Nevada indicate that the skyshine dose rate at the top of a foxhole is about 10% of the total dose rate 3 ft above ground from an infinite, smooth plane of cobalt-60. This compares with 8.8% calculated by Spencer[1] for standard temperature and pressure from infinite medium theory.

With a cobalt-60 source at 100 ft the relative dose rate of skyshine radiation versus solid angle fractions (geometry reduction) measured in an open hole is in excellent agreement with that calculated by Spencer[1]. The presence of the ground does not appear to greatly perturb the geometry reduction.

Lip scatter and wall backscatter appear to be negligible compared to the skyshine dose rate in an open hole. Exact experimental arrangements are important for skyshine radiation studies.

The attenuation provided by a vertical barrier exposed only to skyshine radiation from ring sources of cobalt-60 and cesium-137 was measured. Barrier reduction is greater at positions immediately behind the shield than at positions further in the bunker. This is because a greater percentage of radiation arriving at these positions has penetrated the shield in a more nearly normal direction. A steel shield is more efficient than an equal weight of concrete or aluminum, and these in turn are better than wood. This is presumably because a large portion of radiation reaching the detector is from low-energy photons. The shields provide greater attenuation to skyshine originating from cesium-137 than from cobalt-60 except for very small mass thicknesses.

The attenuation provided by a horizontal barrier exposed only to skyshine radiation from a cobalt-60 source at 100 ft was measured.

In this source-shield-detector configuration, a small amount of shielding material provides a large amount of protection for the detector immediately under the shield. Two inches of concrete reduces the dose rate by almost a factor of 10. At lower depths in the hole the shield is less effective, however. At a depth of 5 ft below the 2-in. concrete shield the dose rate is reduced by only a factor of 2. The dose is, of course, much less because of the small solid angle subtended by a detector at the bottom of the hole. (The attenuation refers to a ratio with and without the shield).

The type of shield material used resulted in very little difference in attenuation (on a weight basis) at the top position. A greater difference is noted at other positions, especially for small shield thicknesses.

Data points are in excellent agreement with calculations by Spencer[1] when consideration is given to the slight difference in angular distribution of the skyshine from a point source at 100 ft and from an infinite-plane source.

A slight change of the angular distribution of the radiation striking the horizontal barrier appears to have a stronger influence on the barrier or geometry reduction than either a slight change in energy or in the atomic number of the shield material.

Cobalt-60 has been widely used in radiation shielding studies. The extent to which results obtained by using cobalt-60 can be applied to idealized fallout radiation has been discussed by Eisenhauer[2] and implied by Spencer's extensive calculations[1]. For two source configurations cited[2], it requires about 10% more mass thickness to produce a given attenuation for one-hour fission-product radiation than it does for cobalt-60 radiation. Spencer's calculations[1] for horizontal-barrier attenuation from skyshine radiation indicate about the same difference. This is understandable when one notes that the angular distributions are essentially the same (except for small solid angles) and that the barrier reduction is more dependent upon the angular distribution than on source spectrum.

It is implied by the above discussion then that the data from cobalt-60 can be applied to one-hour fission spectrum by adding 10% to the mass thickness to obtain the same barrier reduction for the same source configuration. For a realistic fallout situation, however, the source configuration would more probably be infinite in extent and contain a degree of ground roughness or terrain effects.

The experimental data confirm the calculations of angular distribution of the skyshine component and confirm the horizontal barrier calculations for a detector immediately below the slab. Therefore, to apply the data to a realistic fallout situation, the data should be adjusted by consulting the theoretical calculations. This

detailed application is beyond the scope of this report.

In summary, the experimental data are consistent within themselves and compare well with other experimental data and with calculations. The results are applicable to a variety of shielding problems. Specifically, with appropriate adjustment, the results provide shielding information for basement roofs and exposed basement walls from skyshine radiation originating from fallout. The objectives were met and the experiment was conducted safely within the criteria established for the project.

REFERENCES

1. L. V. Spencer, Structure Shielding Against Fallout Radiation from Nuclear Weapons, NBS Monograph 42, National Bureau of Standards, U. S. Dept. of Commerce, June 1, 1962.
2. C. E. Eisenhauer, Analysis of Experiments on Light Residential Structures with Distributed Cobalt-60 Sources, Report NBS-6539, National Bureau of Standards, October, 1959.

CIVIL EFFECTS TEST OPERATIONS REPORT SERIES (CEX)

Through its Division of Biology and Medicine and Civil Effects Test Operations Office, the Atomic Energy Commission conducts certain technical tests, exercises, surveys, and research directed primarily toward practical applications of nuclear effects information and toward encouraging better technical, professional, and public understanding and utilization of the vast body of facts useful in the design of countermeasures against weapons effects The activities carried out in these studies do not require nuclear detonations

A complete listing of all the studies now underway is impossible in the space available here However, the following is a list of all reports available from studies that have been completed All reports listed are available at the prices indicated, from the Clearinghouse for Federal Scientific and Technical Information U S Department of Commerce, Springfield, Va

CEX-57 1, The Radiological Assessment and Recovery of Contaminated Areas, C F Miller, 1960, $0 75

CEX-58 1, Experimental Evaluation of the Radiation Protection Afforded by Residential Structures Against Distributed Sources, J A Auxier, J O Buchanan, C Eisenhauer and H E Menker, 1959, $2 75

CEX-58 2, The Scattering of Thermal Radiation into Open Underground Shelters, T P Davis, N D Miller T S Ely, J A Basso, and H E Pearse, 1959 $0 75

CEX-58 7, AEC Group Shelter AEC Facilities Division, Holmes & Narver, Inc , 1960, $0 50

CEX-58 8, Comparative Nuclear Effects of Biomedical Interest, C S White, I G Bowen, D R Richmond, and R L Corsbie, 1961, $1 00

CEX-58 9, A Model Designed to Predict the Motion of Objects Translated by Classical Blast Waves, I G Bowen, R W Albright E R Fletcher and C S White 1961, $1 25

CEX-59 1, An Experimental Evaluation of the Radiation Protection Afforded by a Large Modern Concrete Office Building, J F Batter, Jr , A L Kaplan, and E T Clarke, 1960, $0 60

CEX-59 4, Aerial Radiological Monitoring System I Theoretical Analysis, Design, and Operation of a Revised System, R F Merian, J G Lackey, and J E Hand, 1961, $1 25

CEX-59 4 (Pt II), Aerial Radiological Monitoring System Part II Performance, Calibration, and Operational Check-out of the EG&G Arms-II Revised System, J E Hand, R B Guillou, and H M Borella, 1962, $1 50

CEX-59 7B (Pt II), Experimental Radiation Measurements in Conventional Structures Part II Comparison of Measurements in Above-ground and Below-ground structures from Simulated and Actual Fallout Radiation, Z G Burson, 1964, $1 50

CEX-59 7C, Methods and Techniques of Fallout Studies Using a Particulate Simulant, W Lee and H Borella, 1962, $0 50

CEX-59 13, Experimental Evaluation of the Radiation Protection Afforded by Typical Oak Ridge Homes Against Distributed Sources, T D Strickler and J A Auxier, 1960, $0 50

CEX-59 14, Determinations of Aerodynamic-drag Parameters of Small Irregular Objects by Means of Drop Tests, E P Fletcher, R W Albright, V C Goldizen, and I G Bowen, 1961, $1 75

CEX-60 1, Evaluation of the Fallout Protection Afforded by Brookhaven National Laboratory Medical Research Center, H Borella, Z Burson, and J Jacovitch, 1961, $1 75

CEX-60 3, Extended- and Point-source Radiometric Program, F J Davis and P W Reinhardt 1962, $1 50

CEX-60 5, Experimental Evaluation of the Fallout-radiation Protection Afforded by a Southwestern Residence, Z Burson, D Parry, and H Borella, 1962, $0 50

CEX-60 6, Experimental Evaluation of the Radiation Protection Provided by an Earth-covered Shelter, Z Burson and H Borella, 1962, $1 00

CEX-61 1 (Prelim), Gamma Radiation at the Air–Ground Interface, K O'Brien and J E McLaughlin, Jr , 1963

CEX-61 4, Experimental Evaluation of the Fallout-radiation Protection Provided by Selected Structures in the Los Angeles Area, Z G Burson, 1963, $2 25

CEX-62 01, Technical Concept — Operation BREN, J A Auxier, F W Sanders, F F Haywood, J H Thorngate, and J S Cheka 1962, $0 50

CEX-62 02, Operation Plan and Hazards Report — Operation BREN, F W Sanders, F F Haywood, M I Lundin, L W Gilley, J S Cheka, and D R Ward, 1962, $2 25

CEX-62 03, General Correlative Studies — Operation BREN, J A Auxier, F F Haywood, and L W Gilley, 1963, $1 00

CEX-62 2, Nuclear Bomb Effects Computer (Including Slide-rule Design and Curve Fits for Weapons Effects), E R Fletcher, R W Albright, R F D Perret, Mary E Franklin, I G Bowen, and C S White, 1963, $1 00

CEX-62 14, An Experimental Investigation of the Spatial Distribution of Dose in an Air-over-Ground Geometry, F F Haywood, J A Auxier, and E T Loy, 1964, $4 00

CEX-62 81 (Prelim), Ground Roughness Effects on the Energy and Angular Distribution of Gamma Radiation from Fallout, C M Huddleston, Z G Burson, R M Kinkaid, and Q G Klinger, 1963 $1 25

CEX-63 7, A Comparative Analysis of Some of the Immediate Environmental Effects at Hiroshima and Nagasaki, C S White, I G Bowen, and D R Richmond, 1964 $2 00

CEX-63 11, Mobile Radiological Measuring Unit Description and Operating Information Z G Burson, R L Summers and J T Brashears, 1965 $1 00

CEX-64 3, Ichiban The Dosimetry Program for Nuclear Bomb Survivors of Hiroshima and Nagasaki — A Status Report as of April 1, 1964, J A Auxier, 1964, $0 50

CEX-65 02, Technical Concept — Operation HENRE, S. F Haywood and J A. Auxier, 1965, $1 00.